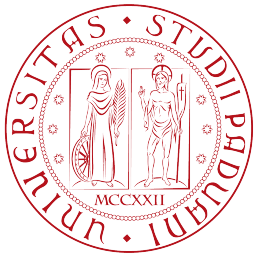

UNIVERSITÀ DEGLI STUDI DI PADOVA

Dipartimento di Fisica e Astronomia "Galileo Galilei"

Master Degree in Physics

Final Dissertation

The evolution of spherically symmetric configurations in the Schrödinger equation approach to cosmic structure formation

Thesis supervisor

Prof. Sabino Matarrese

Thesis co-supervisor

Dr. Daniele Bertacca

Candidate

Francesco Marzolla

Academic Year 2019/2020

Abstract

The evolution of spherically symmetric cold dark matter overdensities in an expanding Universe is studied using Schrödinger-Newton (SN) equations, which model self-gravitating collisionless matter.

For doing so, the density profiles of the perturbations are ideally divided into shells, for which an explicit SN solution for a $\Lambda = 0$ background can be found. Then, supposing absence of shell crossing during the whole evolution of the overdensity, the free-particle approximation is applied to each shell. This approximation, under appropriate limits, which are separately discussed, reduces either to the Zel'dovich approximation or to the adhesion one.
Then the evolution of the overdensity is treated with SN equations in Zel'dovich approximation as a whole, without dividing the system into shells, obtaining results that perfectly overlap with the ones held by the shell by shell study in the Zel'dovich limit.
Eventually, for a specific density profile, time dependent perturbation theory is used to refine the evolution of its shells computed in the free-particle approximation.

Then it is studied the evolution of a density profile coherent with the initial conditions of the Universe which are described in literature. For this system, it is explicitly found the shell by shell exact SN solution, the SN solution in Zel'dovich approximation, and it is discussed the evolution of a mini halo placed inside it.

Independently on the specific density profile considered, the exact solution prescribes that the shells of the overdensity initially expand at a slower rate than the background, then they turn around and collapse.
The free-particle approximation similarly predicts that regions of the overdensity for which the density is below a critical value initially expand, then turn around and collapse; but differently, if they exist, regions whose density exceeds, at the initial time, the critical density, directly contract.
In both treatments, eventually the density diverges: in the centre of symmetry of the perturbation if it is spherically symmetric, or possibly elsewhere if a test halo is added to the system.

Finally, the effect on the system of a non-null cosmological constant is studied, by deriving its effect on the solution which describes a shell. For low enough cosmological constants, the evolution quantitatively resembles the one computed for the $\Lambda = 0$ case.

Contents

Chapter 1

Introduction

1.1 Cosmology: what it studies, an historical excursus and its main achievements

Cosmology studies the Universe on large scales: both in time, therefore its history and destiny, and in space, hence the so-called Large Scale Structure of the Universe (LSS). In other words, its aim is the understanding of the origin of the Universe, its evolution, and its characteristics on a "large scale". How should this recurring expression be intended? Planets, stars, and planetary systems for example are too microscopical to be object of the study of cosmology. The typical length-scales of this subject are the ones of clusters of galaxies, which are gravitationally bound systems of *some* galaxies, ranging from a few, as the few tens of the Local Group (the cluster containing the Milky Way), to the thousands of galaxies contained in the Coma cluster, which is depicted in *figure 1.1* [18]. To set an order of magnitude, the Local Group has a diameter of roughly 3 Mpc [60].

The length-scales of interest for cosmology range from the ones typical of single galaxies (at least 50 kpc for the Milky Way [86]), to the Hubble horizon $d_H := c/H$ where H is the Hubble parameter. A sphere of radius $\sim d_H$ centred on us is the portion of the Universe causally connected with us, and therefore the unique one from which we can collect data (in principle, except for technical limits). Substituting into the expression for d_H the value given by the Plank 2018 data release [66] for the Hubble parameter, $H = (67.66 \pm 0.42)$ $\text{km}^{-1}\ \text{s}^{-1}\ \text{Mpc}^{-1}$, one finds

$$d_H = (4.434 \pm 0.028)\ \text{Gpc}\,.$$

An interest in the Cosmos seems to be a constitutive trait of humankind, because it is so widespread to be relevant even in cultures which never talked to each other, like the Maya and the Sumer[1] just to make an example. In Western culture, the argument of the history and destiny of the Universe had been addressed by philosophers since the Presocratics. Among them, I find particularly interesting Empedocles, because he had some particularly modern intuitions. In the appendix (in section A.1) I briefly present his cosmology and its actuality.

[1] One of the most important traces left by Sumer are the Ziqqurats, which for the historian of religions Mircea Eliade are "a symbolic image of the Cosmos" [26], and because of their orientation they were probably also sites where to perform astronomical observations [54].

Figure 1.1: The Coma cluster of galaxies observed in optical light. Only the central region is shown; the cluster contains more than a thousand galaxies, most of which are elliptical. Picture from [18].

While physics and philosophy were not separated, cosmology remained a very speculative subject, relying as much on metaphysics as on physics. Nevertheless, some ideas pointed out in this phase are still believed to be true: Kant's "island universes" resemble very closely modern galaxies, and the idea of Democritus that the Earth does not occupy a special ("privileged") position in the Universe is taken as an axiom to formulate the modern *cosmological principle*, which states that every comoving observer sees the Universe around him, at a fixed time in his own reference frame, as homogeneous and isotropic. An observer is *comoving* when she is at rest with respect to the CMB radiation.

At the beginning of the XX century, the perspective changed: the development in 1915 of the theory of General Relativity allowed cosmology to become a purely scientific subject. In 1924 the first cosmological models grounded within General Relativity were formulated [64]. Such models of the Universe, whose main characteristic is to be expanding, correctly predicted the recession of galaxies, observed by Edwin Hubble. Taking this expansion seriously and deriving its consequences, in 1948, the hot Big Bang model was proposed [64]. The success of this model is mainly due to two correct predictions of its: the abundances of light nuclei formed during the first minutes after the Big Bang, and the existence of a background radiation in the microwave region of the electromagnetic spectrum, the CMB ("Cosmic Microwave Background"). The model predicts that the CMB generated at the so-called "recombination", which is the formation of neutral atoms from free nuclei and electrons. These predictions only rely on the hypothesis that General Relativity is a valid description of the dynamics of the Universe and on the validity of ordinary physics. No other alternative model has to date been able to reproduce these observations, especially not with so few ingredients [64].

The hot Big Bang model envisages the existence of an initial state of the Universe in which the spatial distance between every two points[2] is null, time has no meaning and the energy density is infinite (that is why it is called "hot"). The concept of spacetime

[2]If one can say so, since their distance is zero.

becomes meaningful when this initial configuration starts to expand, allowing the existence of nonzero distances. As the Universe expands it cools down. Initially, the Universe is populated by all the elementary particles of the standard model. As the temperature decreases, the quarks segregate into hadrons, and heavy particles start to decade in lighter ones. Eventually, the only standard model particles left in the Universe end up being photons, neutrinos, electrons, protons, and neutrons. Then protons and neutrons assemble into light nuclei, and nuclei and electrons recombine into atoms. At recombination matter and radiation decouple, and the latter still travels in a transparent Universe and forms the Cosmic Microwave Background, which we detect since 1965.

According to the ΛCDM model (the standard model of cosmology), the particles predicted by the standard model of particle physics constitute only a tiny fraction of the content of the Universe, nowadays close to the 5% [66], while the biggest fraction of matter is "dark": it interacts significantly with ordinary standard model matter only gravitationally, therefore it is "dark" both because it does not emit light, since it does not interact electromagnetically, and because its components are still unknown. Several particles which are possible candidates for constituting dark matter have been hypothesized (e.g. WIMPs and sterile neutrinos [22]); among them, axions and Axion-Like Particles (ALPs) are especially interesting in the framework of this thesis, since we will use a tool particularly appropriated to treat axion dark matter. We will deepen the subject in a few pages.
Moreover, only 31% [66] of the energy density of the present-day Universe is due to matter, the remaining 69% [66] is represented by dark energy. In the ΛCDM model this energy is described by a cosmological constant Λ and its energy density is constant over time and space. It can be thought of as an energy associated with empty space.

Despite correctly predicting the existence of the CMB and the abundances of light elements, the hot Big Bang model, as exposed until now, presents some defects: let us mention the most relevant.

From observations, held among others by COBE, WMAP, and Planck, we know that the temperature of the CMB radiation is the same in all directions to an accuracy of better than one part in 10^5. The problem lays in the fact that the standard model predicts that regions of the sky at an angular distance of more than about 1.8 degrees, were causally disconnected at recombination, when the CMB "formed" [50]. How all these causally disconnected regions can have extremely similar temperatures? This problem is known as the *horizon problem* of the standard model.

The second major difficulty of the model is the *flatness problem*. A universe in which the cosmological principle holds is described by the solution of Einstein equations defined by the line element

$$ds^2 = -dt^2 + a^2(t)\left[\frac{1}{1-kr^2}dr^2 + r^2 d\Omega^2\right], \tag{1.1}$$

called Friedmann-Lemaître-Robertson-Walker metric. (x, y, z, t) are coordinates on the spacetime, $d\Omega := \sin\theta d\theta\, d\phi$, a is a function of time only called *scale factor* which allows contractions and expansions of the Universe, the parameter k can take three different values, which set the spatial curvature of the universe described by the solution: if $k = +1$ the universe has positive curvature, thus is closed, if $k = -1$ it has negative curvature and it is open, while if $k = 0$ it is flat. The curvature of our Universe can be deduced by estimating the value of the parameter [50]

$$\Omega_k := -\frac{k\,c^2}{H^2\,a^2}\ , \tag{1.2}$$

where H is the Hubble parameter, defined as

$$H(t) := \frac{\dot{a}}{a}\,,$$

with $\dot{a}$ the time derivative of a. The value of the parameter (1.2) today was estimated in 2018 from the Planck collaboration [66] to be

$$\Omega_k(t_0) := 0.0007 \pm 0.0019\,;$$

t_0 indicates the present time. In the standard hot Big Bang model, the value of $\Omega_k(t_0)$ descends uniquely from an initial condition, set at the Planck time, when the Universe emerged from the quantum gravity epoch. The problem arises because in the standard model Ω_k was about 60 orders of magnitude closer to 0 at Plank time than nowadays [50]. This constitutes a fine-tuning problem on the initial conditions of the Universe needed to explain the actual curvature of it.

These and other problems of the hot Big Bang model were solved if the Universe went through a period of rapid, exponential expansion, called inflation [50]. In this hypothesis, the material content of the Universe before inflation would have been washed out by the extreme dilution due to the enormous expansion which characterizes this period. The actual energy content of the Universe would have been generated at the end of inflation, during a period called reheating, by the decay of the inflaton, the yet unknown (scalar, if it is a single one) field which determined inflation.

Inflation is an appealing theory also because it would naturally explain the existence of tiny inhomogeneities in the density of the Universe after reheating. These are crucial, because if the distribution of matter in the primordial Universe were perfectly homogeneous and isotropic, the Robertson-Walker metric (1.1) would be an exact description of the entire spacetime of the Universe: no structures at all would be present at any time, including Earth and humans today.
Since instead the latter exist, the cosmological principle does not hold perfectly: in the primordial Universe, there must have been some deviations from perfect uniformity [50]. These inhomogeneities are the seeds of the actual distribution of matter on large scales, the so-called Large Scale Structure, LSS.

1.2 The Large Scale Structure of the Universe

Our actual knowledge on the LSS is inferred from observations of a sufficiently large number of galaxies, the results of which are collected in large galaxy catalogues. *Figure 1.2* shows the distribution in the sky of 1 million celestial objects mapped in one of these catalogues, the SDSS (Sloan Digital Sky Survey) [70]; in particular the SDSS covers around a quarter of the sky and measures the position and absolute brightness of around 100 million celestial objects and the distance of more than one million galaxies [64]. Looking at *figure 1.2* we clearly see that the distribution of galaxies in space is not random, but it shows a variety of structures[3] [50]. However, galaxy distribution on large scales can be different form the one of matter [50], because of phenomena which interest solely baryonic matter, like hydrodynamical effects (e.g. shocks), star formation and heating and cooling of gas [19]. As far as we know, dark matter interacts only gravitationally, therefore in order to measure the whole matter distribution, we must rely on gravity. It is because of this fact

[3] A deeper insight on how a slice of the Universe look like is conveyed by the video [3], where the positions in space of the galaxies identified by the VIPERS survey are represented on a 3D grid.

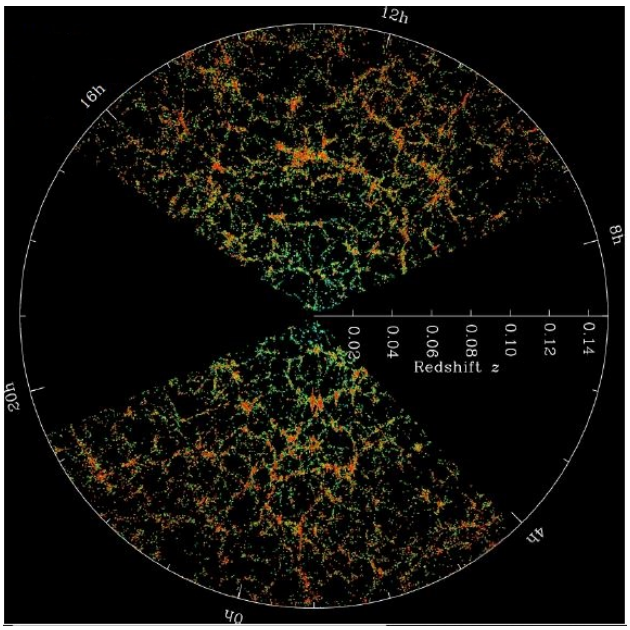

Figure 1.2: Imaging of the distribution of 100 million celestial objects in the sky as a function of redshift z. From the catalogue SDSS [70].

that gravitational lensing is a very promising way to probe the mass distribution in the Universe [50]. The phenomenon exploited by this technique is the deviation from straight lines of the geodesics in a spacetime curved by matter. Light coming from distant sources is therefore deflected when it passes by a massive object. The cumulative gravitational lensing effect due to the inhomogeneous mass distribution between source and observer is called cosmic shear [50]. Potentially it holds informations on the matter density in the vicinity of all the geodesic travelled by the light, but two problems arise: unless the light beam passes very close to a particular overdensity (i.e. a galaxy or cluster), the cosmic shear is very weak; and moreover a distortion is by definition only appreciable by referring to the original, undistorted, image. But we clearly do not have images of distant quasars taken far enough from Earth to make a comparison. Therefore we can only search for images of objects close the one from the other (therefore whose light beams travelled on close paths, in a similarly deformed spacetime), and evaluate the correlation of their distortions (i.e. image ellipticities) [50].
Studying weak gravitational lensing on the SDSS data, Mandelbaum et al. in [44] demonstrate that galaxies are surrounded by extended dark matter halos, from 10 to 100 times more massive than the galaxies themselves.

From the study of galaxy distribution, the statistical properties of matter distribution measured via gravitational lensing, and numerical simulations, we know that the Large Scale Structure of the Universe is the so called cosmic web [64]. To understand what it looks like one could imagine to tessellate the Universe with irregular polyhedra [19], with diameters[4] up to $\sim$ 100 Mpc [50]; inside each polyhedron there are underdense regions which contain very few, or no, galaxies; matter is placed on the edges of such figures, therefore it forms filaments. Where two edges cross, a knot forms, i.e. a dark matter halo likely to host a cluster of galaxies. The whole structure is continuously evolving, under the effect of gravity: structures merge and disrupt each other through tidal forces [19] and matter flows from underdense regions to overdense ones and from filaments to knots[5]. The

[4]To be technical, I am here referring to the caliper diameter of the polyhedron.
[5]Once again, this evolution in time can be seen in a video, [37], which represents the result of an N-

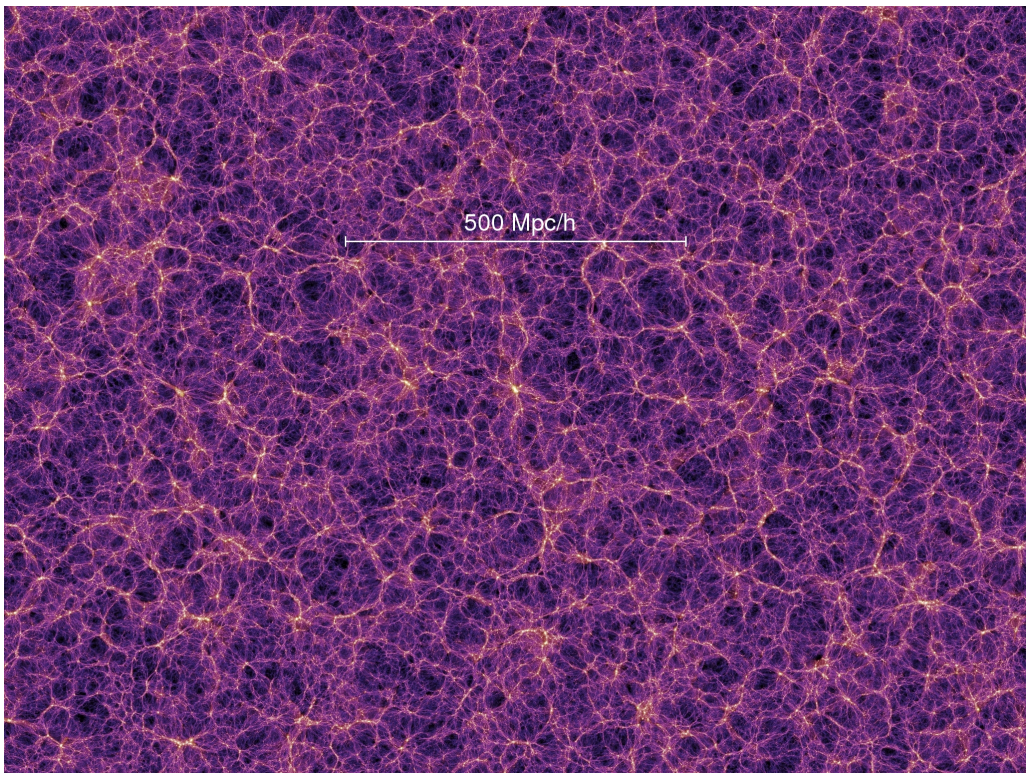

Figure 1.3: Present-day ($z = 0$), 15 Mpc/h thick slice of the large-scale distribution of cold dark matter in the Universe, as computed by Millennium simulation (2005) [73]. The parameter h is defined as $H_0 := (100\,\mathrm{h})\,\mathrm{km/s/Mpc}$, where H_0 is the Hubble constant $H_0 := H(t_0)$, with t_0 the present time.

result of a numerical simulation of the present-day cosmic web is depicted in *figure 1.3*.

To characterize the cosmic web an useful quantity is the two-point correlation function, defined as "the excess number of galaxy pairs of a given separation, r, relative to that expected for a random distribution" [50]; in formula [50]

$$\xi(r) = \frac{DD(r)\Delta r}{RR(r)\Delta r} - 1\,,$$

where $DD(r)\Delta r$ is the number of galaxy pairs with separations in the range $r \pm \Delta r/2$, and $RR(r)\Delta r$ is the number that would be expected if galaxies were randomly distributed in space. Galaxies are said to be positively correlated on scale r if $\xi(r) > 0$, to be anticorrelated if $\xi(r) < 0$, and to be uncorrelated if $\xi(r) = 0$ [50]. On scales smaller than about $10\,\mathrm{h}^{-1}$ Mpc, the real-space correlation function can be approximated by the following power law [50]:

$$\xi(r) = \left(\frac{r}{r_0}\right)^{-\gamma}\,,$$

with $\gamma \approx 1.8$ and a correlation length $r_0 \approx 5\,\mathrm{h}^{-1}$ Mpc. This shows that galaxies are strongly clustered on scales shorter than $\sim 5\,\mathrm{h}^{-1}$ Mpc, and the clustering strength becomes weak on scales much larger than $10\,\mathrm{h}^{-1}$ Mpc [50].
However the sole two-point correlation function does not specify completely a precise CDM

body simulation of the formation and evolution of Large Scale Structure of the Universe. The number of simulated particles is 512^3 and the size of the simulation box is ~ 100 Mpc. The simulation was carried on Cray XT4 at Center for Computational Astrophysics, CfCA, of National Astronomical Observatory of Japan.

distribution [68]: to do so, higher-order correlation functions are needed. Their definition is analogous to the one of ξ: e.g. the three-point correlation function $\zeta(\mathbf{x}_1, \mathbf{x}_2, \mathbf{x}_3)$ measures the joint probability of the existence of three objects (galaxies) located in the 3 infinitesimal volume elements δV_1, δV_2 and δV_3, centred on $\mathbf{x}_1$, $\mathbf{x}_2$, $\mathbf{x}_3$ respectively [42].

The current best explanation of how this large scale structure originated is that it results from the growth of the mentioned primordial, small, seed fluctuations on an otherwise homogeneous universe amplified by gravitational instability [8]. We refer to gravitational instability as the process, driven by gravity, which allows perturbations to grow with time. It works in an intuitive way: a region whose initial density is slightly higher than the mean will attract its surroundings slightly more strongly than average. Consequently, over-dense regions pull matter towards them and become even more over-dense. On the other hand, under-dense regions become even more rarefied as matter flows away from them [50].
Overdense regions of an expanding universe initially expand, but at a rate slower than the one of the background. Then, when the overdensity reaches [50]

$$\frac{\delta\rho}{\bar{\rho}} := \frac{\rho - \bar{\rho}}{\bar{\rho}} \sim 1$$

(where $\bar{\rho}$ is the mean density of the universe and ρ is the density of the perturbation), *turn-around* takes place: the overdensity reaches its maximum expansion and starts to contract. Since as said the dominant component of matter is dark, the system relaxes to a quasi-equilibrium state through violent relaxation, a process which will be discussed in detail in chapter 3. The final object which forms at the end of this process is a dark matter halo, as the ones detectable with weak gravitational lensing techniques.

While dark matter violently relaxes, the small fraction of baryonic matter (in the form of gas) which constituted the initial perturbation develops shocks, which raise the entropy of the gas [50]. If radiative cooling is inefficient, the system relaxes to hydrostatic equilibrium [50], a state in which the inward pull due to gravity is balanced by a pressure gradient which develops an outward directed force. The gas sets in the potential well of the dark matter halos: because of that, galaxy distribution bears information on the cosmic web.

1.3 Cold Dark Matter evolution as a way to explain the formation of the Large Scale Structure

As said, inflationary models are able to predict the seeds which probably originated the large scale structure, and from the analysis of the CMB power spectrum, which is influenced by those fluctuations, we can have some information on them. And then we have data on the large scale distribution of matter. One of the aims of cosmology is the explanation of the latter in terms of the evolution of the former: to build the bridge between those small seeds and the cosmic web.
To do so we need to model matter, and in particular dark matter, because trivially it is the dominant component of matter in the Universe, but also because it is dark matter the first to undergo clustering, and therefore to form the structures in which baryons, gravitationally attracted, fall giving rise to stars and galaxies [18].

In order to perform this modelling, one possibility is to follow the proposal of Widrow and Kaiser [81]: describe and study the cosmological behaviour of Cold Dark Matter with a Schrödinger equation coupled to a Poisson one.
Indeed, Madelung [43] in 1927 showed that the modulus of a wavefunction which obeys

Schrödinger equation can be interpreted as (the square root of) the density of a fluid, and its phase as (proportional to) a velocity potential, both of them satisfying fluid equations: continuity and Bernoulli ones. Madelung intended to propose a fluidodinamical interpretation of Quantum Mechanics, but his discovery was reinterpreted by Widrow and Kaiser [81]: they argued that if a wavefunction can be interpreted as a fluid, a fluid can be described by a wavefunction. This point of view opens to the possibility of using techniques specific of Quantum Mechanics to achieve results valid for collisionless self-gravitating matter [29].

In particular, in this thesis, I will concentrate on the study of spherically symmetric CDM distributions, with the just exposed technique. This assumption on the symmetry of the system, on one side, simplifies the study, and on the other one, it does not detach it too much from real objects present in our Universe, since the Local Group in which we live, is one of the knots of the cosmic web, and these, with a sufficient degree of idealization [39], can be thought to be spherically symmetric.

Therefore the approach to the study of CDM taken in this thesis is quantum mechanical. Despite being generally valid, regardless of the specific particles constituting dark matter, this nature of the treatment would be specially adequate for a dark matter candidate which could display quantum mechanical behaviours on cosmological scales, such as axions do. Let us therefore make a parenthesis on what axions are and why they display their quantum mechanical nature on such large scales.

1.4 A CDM candidate with special properties: the axion

The existence of axions was first proposed by Peccei and Quinn in the late 1970s, as a solution to the so-called strong CP problem. This one arises from the fact that to the standard QCD Lagrangian [22]

$$L_{QCD} = -\frac{1}{4}G^{\mu\nu}G_{\mu\nu} + \bar{q}i\not{D}q - [\bar{q}_R m_q q_L + \text{h.c.}] \tag{1.3}$$

it is possible to add a term ΔL_{QCD} which is consistent with the gauge symmetry of the SM [22]:

$$\Delta L_{QCD} = \theta\frac{\alpha_s}{8\pi}G^{\mu\nu}\tilde{G}_{\mu\nu}\,. \tag{1.4}$$

In the two expressions above $-\frac{1}{4}G^{\mu\nu}G_{\mu\nu}$ is the gluons kinetic term, and therefore $G_{\mu\nu}$ is the field strength; it is constructed from the gluon field A^I_μ in the following way [22]:

$$G_{\mu\nu} := \partial_\mu A^I_\nu - \partial_\nu A^I_\mu + g\mathtt{f}^{IJK}A^J_\mu A^K_\nu\ ,$$

where g is the gauge coupling constant and $\mathtt{f}^{IJK}$ is the commutator between the matrices t^I, which are the $SU(3)_c$ generators for the spinorial representation of the group. q is the quark array

$$q = \begin{pmatrix} u \\ d \end{pmatrix}\ ,$$

where each field, u and d, is a Dirac fermion; $\bar{q}$ is a shortage for $q^\dagger\gamma^0$, where in turn the γ^μ are the Dirac matrices. $\not{D}$ is a compact notation for the contraction between the covariant derivative D_μ and the Dirac matrices γ^μ; the covariant derivative is defined as [22]

$$D_\mu := \partial_\mu - igA^I_\mu t^I\ .$$

m_q denotes the masses of the quarks; the subscript R and L mean respectively "right-handed" and "left-handed"; "h.c." stands for "hermitian conjugate", therefore it is a shortage for the hermitian conjugate for the other term in the brackets.

The term (1.4) is absent in the standard QCD Lagrangian because it implies CP violation, which is not seen experimentally for strong interactions to a very high degree of accuracy. For example the existence of the ΔL_{QCD} term implies a non-vanishing electric dipole moment for the neutron [22]

$$d_n \simeq \theta \times 10^{-16} e\ cm\,.$$

Experiments gave the bound $d_n < 10^{-26} e\ cm$ [2], which implies

$$\theta < 10^{-10} e\ cm\,.$$

This extreme smallness of the coupling is seen as a fine tuning problem, and axions give an explanation to it.

The proposal of Peccei and Quinn is to promote the θ parameter to a dynamical field. Its smallness is thus no more a matter of fine tuning, but it arises naturally by the evolution of the field in the expanding Universe.
The SM has so to be extended with a new U(1) global symmetry, known as PQ symmetry, which is spontaneously broken at some large energy scale f_a. From Goldstone theorem, there must be a so-called "(pseudo-)Goldstone boson" associated with this spontaneous breaking of symmetry. This is the axion [22].
The Lagrangian of the new theory is the usual QCD one (1.3), plus the ΔL_{QCD} term (1.4) with the substitution [22]

$$\theta = \frac{\phi_a}{f_a}\,, \tag{1.5}$$

where ϕ_a is the axion field.
Axions would have no electric charge, most likely a very small mass and very low interaction cross-sections for strong and weak forces [22]. The axion mass, in particular, is expected to be a function of temperature; nonetheless it is approximately constant in the range $0 \leq T \leq \Lambda_{QCD}$ with $\Lambda_{QCD} \simeq 200\,\mathrm{MeV}$ the basic QCD scale [22]. Axions constituting dark matter would be born in a zero-momentum Bose condensate [81], therefore this range is the one of interest for the study of the LSS. In such a range the axion mass would take the following expression [22]

$$m_a = 0.62 \frac{10^7 GeV}{f_a} eV \tag{1.6}$$

as a function of the Peccei-Quinn scale f_a, whose value is to determine experimentally.

Axions can be produced by the Primakoff process $\gamma + Ze \leftrightarrow Ze + a$ [46]. In words in the presence of an external electric or magnetic field, photons can transform into axions and axions into photons. Because of this process the Universe would look more transparent to radiation if axions were there [36]: light can transform into axions, which, since they do not interact, can traverse cosmological distances unaffected by the extragalactic background light till they transform back into photons, thanks to the magnetic field of the Milky Way [27].
Primakoff process, allowing the transformation of axions into photons, justifies the possibility of indirect detection of axions via γ ray astronomy.

Axions may also be produced by the reaction $NN \rightarrow NNa$, where N is a nucleon, via nucleon-nucleon bremsstrahlung. This process can take place in neutron stars. In [7] Berenji et al. analyse data taken by Fermi LAT in 5 years, in the gamma-ray band (between 60 MeV and 200 MeV), for a sample of 4 nearby neutron stars. No evidence for

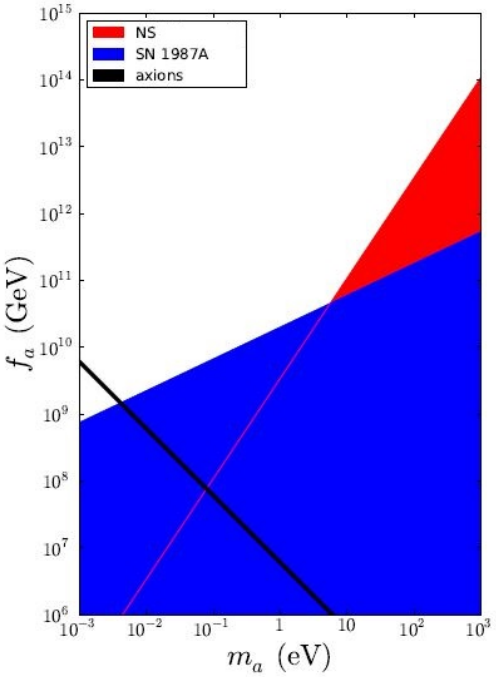

Figure 1.4: Exclusion plot for the (m_a, f_a) parameter space for ALPs at 95% CL. In red it is shown the region excluded by [7], by the study of neutron stars. In blue the bound from Fermi LAT analysis of SN 1987A [31]. The axion line (black) shows the parameters allowed by PQ axions. From [7].

an axion or axion-like particle[6] signal is there found, thus it's stated a 95% confidence level upper limit on the axion mass of $m_a = 7.9\ 10^{-2}\ eV$, which corresponds to a lower limit for the Peccei-Quinn scale f of $7.6\ 10^7\ GeV$, in the hypothesis of relativistic axions, which holds till $m_a \simeq 1keV$.

Instead, an event in which we do expect a strong occurrence of the Primakoff process is the core-collapse supernova. In [31] Giannotti et al. derive an upper bound for the axion mass (and thus a lower one on the Peccei-Quinn scale), from the lack of a gamma-ray signal in the Fermi Large Area Telescope in coincidence with the observation of the neutrinos emitted from the supernova SN1987A.

The two upper bounds mentioned, derived respectively from the observation of neutron stars and a supernova, are shown in *figure 1.4* [7].

From these bounds, we see that the axion mass should be less than a few meV, with no lower bound (axions and ALPs with $m_a \lesssim 10^{-9}$ eV are called ultralight [57]). Compton wavelength, defined as [34]

$$\lambda_c := \frac{h}{mc}\ ,$$

is the length under which a particle of mass m displays quantum mechanical effects. The constraint $m_a \lesssim 1$ meV for the axion mass translates into the constraint $\lambda_c \gtrsim (6 \times 10^{-5})$ pc.
In [57] it is experimentally found a constraint on the coupling between photons and axions in the Lagrangian which allows Primakoff process; this constraint is valid for axions with mass $m_a < 4.4 \times 10^{-10}$ eV. Such axions would have a Compton wavelength $\lambda_c > 1.5 \times 10^2$

[6]The Axion-Like Particles (ALPs) are pseudo-scalar bosons similar in properties to standard QCD axions. They are predicted by several extensions of the Standard Model.

pc.
Axions with a Compton wavelength of the order of the diameter of the Milky Way would have a mass of the order of 10^{-12}eV, which is a still plausible value.

Because of this fact, the behaviour of a Cold Dark Matter made of axions or ALPs would be powerfully described with a quantum mechanical technique, as the one adopted in this thesis. I will deepen the way to treat axions after presenting the quantum mechanical equations I will use to model CDM: the already cited Schrödinger-Newton equations.

1.5 The fluid treatment of CDM

Our aim is the study of the behaviour on cosmological scales of Cold Dark Matter. Since it does not interact if not gravitationally (or if it does, it interacts in such a feeble way that the effect of such interaction is negligible on the scales of interest) [19], its particles move under the sole influence of the mean gravitational potential generated by all of the other particles. The state of such a collisionless system is specified by a distribution function $f = f(\mathbf{r}, \mathbf{v}, t)$, which gives the density of particles in phase space as a function of time. In phase space we are using here the system of coordinates given by the physical position $\mathbf{r}$ and velocity $\mathbf{v} := \frac{d\mathbf{r}}{dt}$; f is a distribution function and therefore has to be non-negative everywhere and normalized to $\int f\, d^3r\, d^3v = 1$. The evolution of f is predicted by a Boltzmann equation in which the collision operator is identically null, which takes the name of Vlasov equation, [81]

$$\frac{\partial f}{\partial t} = \sum_{i=1}^{3} \left(\frac{\partial V}{\partial r_i} \frac{\partial f}{\partial v_i} - v_i \frac{\partial f}{\partial r_i} \right) , \tag{1.7}$$

coupled to a Poisson one for the Newtonian potential V [21]

$$\nabla^2 V = 4\pi G \int f d^3v \, . \tag{1.8}$$

One possibility is to solve the Vlasov-Poisson pair numerically, in order to evolve f and have at any time a full description of the CDM distribution. Unfortunately, efforts along this line have had limited success because f presents a too much complicated evolution to be followed, primarily because of the large number of phase-space dimensions typically involved [19] and also because distribution functions, in general, develop fine-grained structures, which are difficult to follow numerically [81].

One alternative is represented by N-body simulations, in which one discretizes the problem considering a finite number of particles, many orders of magnitude less than the actual number of particles in the physical system, distributed following the phase space distribution of interest. The discrepancy in the number of particles in the model and in reality can lead to unphysical effects due to "particle noise" such as two-body relaxation [25]. Smoothing techniques alleviate this problem but at the cost of losing spatial resolution [21]. For the same reason N-body techniques sample regions of high matter density very precisely, while underdense regions are sampled less accurately [29], for a certain number of particles considered; increasing the number of particles, one can increase the definition in underdense regions, at the cost of increasing also the time required for the computation.

Another alternative tool to study CDM behaviour is the fluid approximation; it holds every time velocity dispersion (i.e. the second moment of the velocity $\mathbf{v}$) is negligible compared to bulk velocity (the first moment of $\mathbf{v}$) [17].

Velocity dispersion is actually negligible compared to bulk speed at scales of interest in cosmology for Cold Dark Matter (CDM). Our study will be entirely focused on this type of dark matter candidate. The behaviour of a self-gravitating fluid without viscosity, as CDM is in the fluid approximation, is governed by a system of three coupled equations: the continuity one, expressing conservation of mass, Euler equation, expressing momentum conservation, and Poisson equation, for the gravitational potential. In formulae they are [19]

$$\frac{\partial \rho}{\partial t} + \nabla \cdot (\rho \mathbf{v}) = 0\,, \tag{1.9}$$

$$\frac{\partial \mathbf{v}}{\partial t} + (\mathbf{v} \cdot \nabla)\mathbf{v} = -\frac{1}{\rho}\nabla P - \nabla V\,, \tag{1.10}$$

$$\nabla^2 V = 4\pi G \rho\,. \tag{1.11}$$

For the case of CDM, we can set the pressure P identically equal to 0, so its gradient vanishes. The use of the gravitational potential, and therefore of Newtonian gravity instead of General Relativity, is accurate for scales much smaller than the Hubble horizon $d_H := c/H(t)$ [56]. The expansion of the Universe makes the vorticity of the velocity field $\mathbf{v}$ rapidly negligible [18], and the motion generated by gravity is irrotational because of Kelvin circulation theorem [17]. So, since $\nabla \times \mathbf{v} = 0$, we can define a scalar potential ϕ such that [19]

$$\mathbf{v} := \nabla \phi\,.$$

Furthermore we can exploit the following identity [45]:

$$\nabla(\frac{1}{2}\mathbf{v}^2) = \mathbf{v} \times (\nabla \times \mathbf{v}) + (\mathbf{v} \cdot \nabla)\mathbf{v}\,. \tag{1.12}$$

For what just said, the first term on the right hand side of (1.12), in our treatment is zero. Having written $\mathbf{v}$ as a gradient of a potential, we can express conservation of momentum in terms of the potentials, arriving at the so called Bernoulli equation, which implies Euler equation. With our assumptions, Bernoulli equation reads [19]

$$\frac{\partial \phi}{\partial t} + \frac{1}{2}(\nabla \phi)^2 = -V\,. \tag{1.13}$$

1.6 The wave-mechanical description of a fluid: Schrödinger-Newton equations

The possible approaches exposed in the last section, to model and study the evolution of the distribution of collisionless matter on large scales, have been successful in describing the basic features of large-scale structure [19]. Nonetheless they can be improved, since they present some weaknesses; in particular three of the latter, pointed out by Coles and Spencer in [19], are solved, at least partially, adopting a wave-mechanical approach to the study of CDM. The mentioned three weaknesses of standard techniques are [19]:

- standard perturbation methods do not guarantee a density field that is everywhere positive. This problem arises for example supposing a Gaussian distribution of initial fluctuations.
- Some analytic approximations (Zel'dovich approximation and its variations, see section 2.3) and treatments (see 2.1) break down at shell crossing.
- Analytical techniques for modelling the effects of gas pressure are scarce.

These difficulties are overcome in the approach suggested by Widrow and Kaiser in 1993 [81]. It involves re-writing the fluid equations given in the last section in the form of a non-linear Schrödinger equation.

The solution of such a Schrödinger equation is a wavefunction whose modulus squared represents the density of the fluid, and its phase is proportional to its velocity potential. In this way, we are encoding phase-space information in a continuous function defined in position space only [29].
This approach, which I will illustrate in detail in a few lines, solves the three difficulties highlighted before:

- first, the construction requires that the density field is everywhere non-negative, since it is a modulus squared [19].
- Secondly, particles are not treated as point-like entities with definite trajectories, as we will see later in the thesis is done in Zel'dovich approximation. Therefore shell-crossing does not have the catastrophic form in the wave-mechanical approach that it does in the Zel'dovich approximation [19].
- As we will soon see in detail, Schrödinger equation is equivalent to a continuity equation for the density of the fluid, and a Bernoulli equation with an additional term with respect to the standard one (1.13). Either we can get rid of this term using a trick which we will see in a few lines, making its effect vanish to model a pressureless fluid, or we can leave it, and use it to model pressure of baryonic fluids [19], or similar repulsive effects on small scales [72].

Let us now approach quantitatively this quantomechanical description of a fluid. In the previous section, we stated the equations governing a CDM pressureless fluid. If we define the following quantities

$$\psi(\mathbf{r},t) := R(\mathbf{r},t)\, e^{\frac{i}{\nu}\phi(\mathbf{r},t)} \tag{1.14}$$

$$\rho(\mathbf{r},t) := |\psi|^2 = \psi^*\psi = R^2(\mathbf{r},t)\,, \tag{1.15}$$

after some algebra continuity (1.9) and Bernoulli equation (1.13) can be re-written in one equation of the form [19] [81] [17]

$$i\nu\frac{\partial\psi}{\partial t} = -\frac{\nu^2}{2}\nabla^2\psi + V\psi + \frac{\nu^2}{2}\frac{\nabla^2 R}{R}\psi\,. \tag{1.16}$$

This equation resembles very much Schrödinger's one. Indeed making the substitution $\nu = \hbar/m$ [19] we recover Schrödinger equation plus an extra term: the last on the right hand side in (1.16).

To have a look on what this extra term describes, let's invert the path: let's start with Schrödinger equation, written in terms of ν, and find which continuity and Bernoulli equations are equivalent to it. This is, by the way, the path followed by Madelung in proposing his hydrodynamical approach to Quantum Mechanics. It turns out [72] that the fluid equations equivalent to the Schrödinger one, making the ansatz (1.14) and (1.15) are a standard continuity equation, in the form (1.9), and the following modified Bernoulli equation

$$\frac{\partial\phi}{\partial t} + \frac{1}{2}(\nabla\phi)^2 = -(V+Q)\,, \tag{1.17}$$

where

$$Q = -\frac{\nu^2}{2}\frac{\nabla^2 R}{R} \tag{1.18}$$

is the extra term appearing in Schrödinger equation, and it is called "Bohm quantum potential" [**?**] or "quantum pressure term" [19], because it has an effect on the dynamic of a collisionless fluid, similar to the one pressure has on baryonic fluids. It is the term useful to model pressure anticipated in treating the advantages of the wave-mechanical approach [19].
This implies that we are free to drop the quantum pressure term from the non-linear Schrödinger equation (1.16) and include it in the Bernoulli equation instead [72].

Notice that by taking the limit for $\nu \to 0$ of equation (1.17) we recover the usual Bernoulli equation (1.13), and so the right fluid equations for the situation we aim to describe. We can ask ourselves what is, on the quantum mechanical side, the effect of taking this limit. Since as said $\nu = \hbar/m$, we can allow variations of ν interpreting the constant $\hbar$ as an adjustable parameter [17]. Sending it to 0 gives in general the classical limit of a quantum theory, hence also in the context of SN equations, in literature they often refer to this limit as the classical one. If $\hbar$ is no more fixed, it controls the spatial resolution λ through the de Broglie relation $\lambda = \hbar/p$ [17].
As we will see, the limit $\nu \to 0$ is not compulsory even for pressureless fluids while using approximations; indeed the quantum pressure term, despite being in some sense a by-product of the Madelung transformation [29] which translates fluid equations in Schrödinger one, can be left to model effects for which the approximation is not able to account [19].

The following two coupled equations, mathematically equivalent to fluid equations with the extra quantum pressure term, are called in literature Schrödinger-Newton (SN) or Schrödinger-Poisson (SP) equations [17]

$$i\nu\frac{\partial\psi}{\partial t} = -\frac{\nu^2}{2}\nabla^2\psi + V\psi\,, \tag{1.19}$$

$$\nabla^2 V = 4\pi G|\psi|^2\,. \tag{1.20}$$

Garny et al. in [29] claim that the Schrödinger-Poisson equations should not be perceived as a generalization of the fluid model with quantum pressure, but rather as one way of sampling the phase space of the exact Vlasov-Poisson system, just as N-body simulations. This in fact was the approach followed by Widrow and Kaiser [81] in proposing SN equations to simulate collisionless matter for the first time. In particular, no information about moments of the DM distribution higher than the first, such as the velocity power spectrum, could be computed in the fluid treatment, while in [29] Garny et al. explicitly find the second moment of the velocity for numerical simulations of halos, computed using the wave-mechanical approach, and Davies and Widrow in [21] compute expressions for the velocity moment of order n in terms of the solution ψ of SN equations.

This seems to be a paradox: how could the Schrödinger-Newton system encode more information than the mathematically equivalent fluid treatment? Garny et al. [29] answer that this additional information arises by averaging the phase space distribution function one can compute with the wave-mechanical approach, to obtain the coarse-grained distribution function. Indeed if one sets the parameter ν at a low enough value that the associated De Broglie wavelength is significantly smaller than the scale one is smoothing/coarse-graining over, each coarse-grained cell contains a significant number of wave packets, making the prediction of higher order cumulants viable, just as for N-body simulations.

Since moreover a computation done with a wave mechanical simulation of a certain CDM distribution needs on average the same computational power as the same calculation performed with an N-body simulation (see [81] and [21]), the Schrödinger-Newton approach

happens to be a promising one, which can give insights where N-body simulations or analytical techniques, such as Zel'dovich and adhesion approximation, fail.
In particular in [81] Widrow and Kaiser simulate the evolution until present time of an overdensity with a density contrast $\delta\rho(t_i)/\rho(t_i) \simeq 0.1$ at an initial time t_i such that $a(t_i)/a_0 = 0.04$, in a two-dimensional cold dark matter universe. They performed the simulation both using a code based on the Schrödinger-Newton approach discussed till now and with a PM code (Kate et al. 1991). They found comparable results in a similar computation time, with the Scrödinger method being slightly faster [81].
In [21] Davies and Widrow find that the CPU time/time step required by both a code based on Schrödinger method and an N-body simulation, scales as $N \ln N$, where N is the number of test particle considered, in the N-body simulation, and its analogue in the quantum mechanical approach: the number of single coherent-state wavepacket centred at some chosen point in phase space. Moreover, the wave-mechanical approach can give predictions even in the mildly non-linear regime [72], which is achieved by a perturbation after trajectories of individual particles cross, a phenomenon that makes Zel'dovich approximation breaking down. Indeed the density forecasted by SN equations does not necessarily diverge when shell crossing happens [19]; for example the simulation performed by Widrow and Kaiser in [81] extends after trajectories cross.

As anticipated, Schrödinger-Newton equations are also particularly appropriate to model axions. Let us see in detail how.

1.7 Schrödinger-Newton equations for modelling axions

Axions are described by the scalar field ϕ_a (1.5). A classical scalar field obeys the coupled Klein-Gordon and Einstein equations [81]:

$$\left(\Box + m^2\right)\phi_a = 0 \tag{1.21}$$

$$G_{\mu\nu} = 8\pi G\, T_{\mu\nu}\,, \tag{1.22}$$

where [81]

$$T_{\mu\nu} = \partial_\mu\phi_a\partial_\nu\phi_a - \frac{1}{4}g_{\mu\nu}\left[\partial_k\phi_a\partial^k\phi_a - m^2\phi_a^2\right]\,.$$

For nonrelativistic fields ($|\Delta\psi/\dot{\psi}| \ll 1$) we can write [81]

$$\phi_a = \frac{1}{\sqrt{2}m}(\psi e^{-imt} + \psi^* e^{imt})\,, \tag{1.23}$$

where ψ is a slowly varying function of time in the sense that $|m\psi| \gg |\partial\psi/\partial t|$. This is an excellent approximation for dark matter axions since they are born in a Bose condensate. Then Schrödinger and Poisson equations follow by direct substitution of (1.23) into (1.21) and (1.22) once two assumptions are made: that the gravitational field generated by ϕ_a is weak (therefore only the Newtonian potential enters into the metric) and that we can neglect $\ddot{\psi}$ terms [81]. In all this treatment were used units in which $\hbar = 1$.

The Klein-Gordon equation (1.21) was first proposed as a relativistic extension for spin-zero particles of Schrödinger equation; therefore ϕ_a was intended as a wavefunction. However such a theory would predict some unreal phenomena, like superluminal propagation and particle number conservation even at high energies. To get rid of these erroneous predictions, ϕ_a has to be intended as a field operator, with appropriate commutation rules [63]. However, in the limit of very large occupation numbers, the Klein-Gordon equation can

be interpreted as a wave equation [81]. This is the case for axions, since they form a Bose-Einstein condensate and therefore they all occupy a single state of zero momentum.

As said treating the $\nu \to 0$ limit, the de Broglie wavelength controls the spatial resolution of an LSS study held with SN equations. When treating axions, the $\nu \to 0$ limit is no more justified, because h is no more a simple adjustable parameter coming out from a mathematical trick, but it is precisely the Plank constant. Therefore the value of $\nu = \hbar/m_a$ is set. For axion masses low enough, the de Broglie wavelength of the axions moving in the gravitational field of a galaxy would be large enough to perform simulations, but as the mass increase, the resolution of the simulation increase too, making it more demanding in terms of computational power (or equivalently time). For example axions with mass $m_a = 10^5$ eV would have a de Broglie wavelength of $\sim 10\,\mathrm{m}$, which makes it unreasonable to follow them if we are interested in galaxies and clusters [81].
Therefore, if axions exist, either they have low enough masses to make the Schrödinger-Newton approach exact for treating the evolution of their distribution on cosmic scales, or they are too massive to be handled by numerical simulations with this technique, and in this case we can consider fictitious lighter particles to derive approximate results. In N-body simulations one considers too few superheavy particles, in this case we would consider too many superlight particles [81].

Despite being able to model CDM and to describe almost exactly axion CDM, Schrödinger-Newton equations are not only useful in cosmology, or anyway to model a pressureless self-gravitating fluid: they were proposed in the context of the measurement problem in quantum mechanics and arise very naturally in quantum gravity, either as part of an effective theory or of a possible fundamental one. In the next section I would like to give a brief recap of the physical domains in which SN equations appear, in order to broaden our view on the subject.

1.8 Schrödinger-Newton equations in other fields of physics

Schrödinger-Newton equations were proposed for the first time by L. Diósi in a paper [23] dated 1985 to solve the following problem. According to classical physics, in the absence of external forces, the centre of mass of a given macroscopic object either moves uniformly along a straight line or, in a particular frame, rests at a certain point. Unfortunately, the Schrödinger equation of a free particle does not have localized stationary solutions. Wave-packet solutions, which are possibly the best representation for the free motion of a macroscopic body, are not stationary. When such wave-packets evolve as prescribed by the usual Schrödinger equation they widen, and thus the position of the centre of mass becomes more and more uncertain as time flows. At the same time, experience seems to show that a macroscopic object always has a well-defined position. As one could imagine given that such a problem is not yet solved and scientists do not seem to urge for a conclusion of it, the effects of the cited spread are extremely difficult to measure. Let us for example consider a body of several grams localized (i.e. with its centre of mass localized) within the typical atomic size, i.e. in a cube of side $10^{-8}cm$. Then the initial position displays no change for thousands of years [5]. Therefore we still do not know if we have to adapt our intuition to another unexpected reality predicted by quantum mechanics, or we have to modify the theory in order to make it agree with our intuition deduced by common experience. Diósi goes in the latter direction and proposes that the wavefunction gravitationally self-interacts, giving rise to a force which acts against dispersion. This behaviour is encoded in Schrödinger-Newton equations (1.19) (1.20).

It is interesting to note that such an interaction can be conceived only intending the wavefunction ψ as a physical object, as Schrödinger and de Broglie thought it was; if on the other hand ψ was a *probability wave*, i.e. a theoretical tool useful to compute values of observables of the particle it describes, like it was intended by Bohr, Heisenberg, Pauli and the school of Copenhagen, it could not interact with anything, even less with itself. Indeed every detector works assuming that if something interacts, then it exists (there)[7].

More recently, in 2011, D. Giulini et al. tested with numerical simulations the effectiveness of the gravitational self-interaction proposed by Diósi in inhibiting dispersion of wave-packets [32]. They started with a spherically symmetric Gaussian wave-packet and they found that independently of its width, for masses $m \leq 6 \times 10^9$ u, the wave-packet spreads, but slower than what the free solution without self-interaction would do. The larger the mass, the slower the spreading becomes compared to the free solution, until for masses $m \geq 7 \times 10^9$ u, simulations showed the wave-packet to collapse.

Ten years later the work of Diósi, R. Penrose proposed Schrödinger-Newton equations in a different context: to provide a dynamical, unitary, description of the collapse of the wavefunction [59]. He indeed examined a quantum superposition of two different stationary mass distributions, and computed the perturbing effect of each distribution on the space-time structure, in accordance with the principles of general relativity. He then supposed that these perturbed spacetimes coexisted in a quantum superposition; he therefore assumed that gravity has a quantum nature, as the other fundamental forces have, indeed Wheeler *defines* quantum gravity as the possibility for different spacetime geometries to be in superposition. Penrose showed that in this superposition of space-times, time translations are ill-defined, and, using Noether theorem, that therefore the energy of the superposed state has an uncertainty which, in the Newtonian limit, is proportional to the gravitational self-energy E_Δ of the difference between the two mass distributions. He then argued that this is consistent with a finite lifetime of the order of $\hbar/E_\Delta$ for the superposed state. After this time interval, the superposed state would collapse to a stationary solution of SN equations. I used the word "collapse" because with such a mechanism Penrose aimed at describing unitarily the process of quantum state reduction, making it a spontaneous, gravitationally induced, process.

In a later work [5] Bahrami et al. argued however that if the only correction brought to quantum mechanics is the gravitational self-interaction prescribed by SN equations, it is easy to show that the "collapse" prescribed by the new theory is not equivalent to the one we know it takes place. If we indeed consider a wavefunction peaked at $x = 0$ and $x = 2$, it would evolve in the modified theory towards a single peak at $x = 1$, differently from what would occur during a measurement. Moreover, the normal collapse postulate, together with the dynamics prescribed by SN equations, generates superluminal propagation of information. One can avoid this effect by introducing ad hoc prescriptions on the mechanism of collapse, but this surely implies that SN equations are not able alone to explain unitarily the wavefunction collapse after a measurement.

The third and last context in which Schrödinger-Newton equations arise is quantum gravity. They could be the nonrelativistic limit either of a fundamental theory of gravity or of an effective classical limit of a quantum gravity theory. The latter case arises when one follows the proposal of Møller and Rosenfeld that only matter fields are quantized, while

[7] Plato too would agree with this assumption: he writes in Sophist, 247d-f (English translation from [62])

> I suggest that everything which possesses any power of any kind, either to produce a change in anything of any nature or to be affected even in the least degree by the slightest cause, though it be only on one occasion, has real existence.

Therefore he defines as existing whatever interacts.

the gravitational field remains classical even at the fundamental level. This theory is often called semi-classical gravity. In this theory the Einstein tensor G_{ab} remains classical as it is in general relativity: it is not promoted to an operator [5]; Einstein equation equate therefore G_{ab} to the expectation value of the stress energy tensor operator in a given quantum state ψ, i.e. $\langle\psi|\,\hat{T}_{ab}\,|\psi\rangle$. The nonrelativistic limit of this equation, in which the energy density ρ dominates in $\langle\psi|\,\hat{T}_{ab}\,|\psi\rangle$ and the Newtonian potential in G_{ab}, is the Schrödinger-Newton system [5]. If instead gravity has a quantum nature, G_{ab} must be promoted to an operator, and SN equations arise as an effective theory, describing the mean field generated by many particles [5]. SN equations nonetheless are not the only nonrelativistic limit of a quantum theory of gravitation: as said, SN equations suppose a realistic interpretation of the wavefunction; Bernstein et al. in [9] write a different classical limit of quantum gravity, which is linear, and assumes, in accordance with Copenhagen interpretation, that $|\psi(\mathbf{r})|^2$ describes nothing more than the probability density for finding the mass it describes at the location $\mathbf{r}$.

In the next few years we could assess the nature of SN equations by discovering if gravity has to be quantized (recall moreover that if it has a classical nature, the argument of Penrose exposed above becomes inconsistent). Indeed an experiment aimed at measuring a quantum gravitational effect in the lab has been recently proposed by Bose et al. [13] and by Marletto and Vedral [47]. This experiment would try to entangle two masses through a gravitational interaction. Indeed a general argument based on information theory (see [47] and [15]) ensure that if a physical entity can entangle two systems while complying with locality, then it must be non-classical (i.e. it has to be described by at least two non-commuting variables). Therefore detection of the Bose-Marletto-Vedral (often referred to as BMV) effect, which is due to an entanglement, would count as evidence that gravity is quantised.

1.9 Properties of Schrödinger-Newton equations

To conclude our overview on Schrödinger-Newton equations, let us point out their symmetries. Some of them are enjoyed also by the action from which equations (1.19) and (1.20) can be derived. That action reads [32]

$$S[\psi,\psi^*] = \int dt \left\{ \frac{i\nu}{2} \int (\psi^*(\mathbf{r},t)\dot{\psi}(\mathbf{r},t) - \psi(\mathbf{r},t)\dot{\psi}^*(\mathbf{r},t))\, d^3r + \right.$$
$$- \frac{\nu^2}{2} \int \nabla\psi(\mathbf{r},t)\cdot\nabla\psi^*(\mathbf{r},t)\, d^3r +$$
$$\left. + \frac{G}{2} \int d^3r \int \frac{|\psi(\mathbf{r},t)|^2 |\psi(\mathbf{s},t)|^2}{||\mathbf{r}-\mathbf{s}||}\, d^3s \right\}. \quad (1.24)$$

As D. Giulini et al. in [32] show, S is left invariant by the action of the following transformations:

- constant phase shifts:

  $$\psi \mapsto \psi' = e^{i\beta}\psi \qquad \text{with constant } \beta \in \mathbb{R}\,.$$

  Noether theorem for this symmetry implies that the space integral of $|\psi|^2$ is time independent;

- proper orthochronous Galilei transformations. Hence linear and angular momentum, as well as energy, are conserved.

The equations instead are left invariant also by:

- space (P) and time (T) inversions which together with the proper orthochronous Galilei transformations close the Galilei group; these symmetries are enjoyed by SN equations in the sense that if ψ solves the equations, then $P\psi$ and $T\psi$ also solve it;
- the action of the group $\mathbb{R}_+$ of positive real numbers with multiplication: if $\psi(\mathbf{r}, t)$ is a solution of

$$-\frac{\hbar^2}{2m}\nabla^2\psi + V\psi = i\hbar\frac{\partial\psi}{\partial t} \tag{1.25}$$

$$\nabla^2 V = 4\pi G m^2 |\psi|^2 \tag{1.26}$$

  then $\mu^{9/2}\psi(\mu^3\mathbf{r}, \mu^5 t)$ satisfies the same equations for mass $m_\mu = \mu m$. This scaling preserves normalization.

Another important feature of Schrödinger-Newton equations is the fact that, unlike ordinary Schrödinger equation, they are non-linear, because of the gravitational self-interaction of the wavefunction. In particular when one performs the transformation $\psi \mapsto a\psi$ with $a \in \mathbb{C}$, the term $V\psi$ of (1.19) is mapped in $a^3 V\psi$. This non-linearity has important consequences; the superposition principle is not valid anymore: a linear combination of solutions of SN equations is not necessarily solution in turn. Because of that, states in a theory in which SN equations are valid are not elements of a Hilbert space, since they are not vectors because their set is not closed with respect to summation.

After this general discussion of Schrödinger-Newton equations, the next step will be to recall techniques that are useful to study, with SN equations, the kind of system this thesis aims at describing: spherically symmetric density perturbations. But before, let us briefly point out the plan of the thesis.

1.10 Plan of the thesis

The plan of the rest of the thesis is as follows.

In chapter 2, I will recall some treatments and tools which are useful to study a spherically symmetric overdensity with the approach presented until now. In particular I will expose the treatment of spherical collapse, a re-writing of SN equations in an expanding background, as our Universe is, Zel'dovich and adhesion approximations, which are realized in the SN approach by the *free particle approximation*, and a solution of Schrödinger-Newton equations, found by Johnston et al. [38], for a matter distribution similar to a top-hat.

In chapter 3, I will then make use of those tools to study the evolution of a spherically symmetric density profile. I will decompose the profile in shells and write for it a solution using the top-hat one just mentioned. Then I will implement the free-particle approximation proposed by Short and Coles in [72]. Finally I will specify a particular spherically symmetric profile, work out the previous general predictions for it, and refine those results with time dependent perturbation theory.

In chapter 4 the tools of chapter 2 will be applied to predict the evolution of an overdensity coherent with the initial conditions of our Universe, the ones determined by inflation. In particular, an exact solution is found and the free-particle approximation is implemented,

as before. The effect of the additional presence of a mini sub-halo is briefly discussed. Stationary solutions, describing virialized halos, are finally presented.

Finally, in chapter 5 the top-hat solution considered in chapter 2 will be generalized to Universes with non-null cosmological constant.

Chapter 2

Theoretical tools

Let us here start to focus on spherically symmetric cold dark matter configurations.
In particular if the configuration is an overdensity, it will eventually collapse. Let us hence recall in the following section the theory of spherical collapse. The treatment will be taken and readapted from [50] and [56].

2.1 Spherical Collapse in a spatially flat $\Lambda = 0$ Universe

Expansion of the overdensity In the absence of a cosmological constant, the radius r of a mass shell in a spherically symmetric density perturbation evolves according to the Newtonian equation [50]

$$\frac{d^2r}{dt^2} = -\frac{Gm}{r^2}\,, \tag{2.1}$$

where m is the mass within the mass shell. Before shell crossing, m is independent of t for a given mass shell, and so eq. (2.1) can be integrated once to give [50]

$$\frac{1}{2}\left(\frac{dr}{dt}\right)^2 - \frac{Gm}{r} = \mathcal{E}\,, \tag{2.2}$$

where $\mathcal{E}$ is the specific energy of the mass shell. For $\mathcal{E} < 0$ the mass shell eventually contracts, while for $\mathcal{E} \geq 0$ it expands forever (the same behaviour is predicted by SN equations for their solutions with positive energy: they expand indefinitely; for the demonstration see [4]). Since we are interested in spherical *collapse*, let us focus on the first case: for an $\mathcal{E} < 0$ mass shell, one can write the following explicit parametric solutions of the E.O.M. [50]

$$r = A(1 - \cos\eta)\,, \qquad\qquad t = B\,(\eta - \sin\eta)\,, \tag{2.3}$$

where A and B are two constants, which can be determined knowing the initial (i.e. computed at a reference initial time t_i) radius of the mass shell, r_i, and the initial mean overdensity within it. A way to express the latter is through the dimensionless density contrast δ, defined as [50]

$$\delta = \frac{\rho - \bar{\rho}}{\bar{\rho}}\,, \tag{2.4}$$

where $\bar{\rho}$ is some background density. If we use as ρ the mean overdensity inside the shell of radius r_i, defined as

$$\bar{\rho}_i = \frac{3\,m}{4\pi r_i^3}\,, \tag{2.5}$$

we recover the mean density contrast $\bar{\delta}_i$. This quantity will be of crucial importance in the following; let us therefore define here, generally, the mean overdensity of a spherical region with radius r; let us call it $\bar{\delta}(r, a)$:

$$\bar{\delta}(r,a) := \frac{\frac{4\pi}{V}\int_0^r \rho\, r'^2\, dr' \;-\; \bar{\rho}}{\bar{\rho}} = \frac{4\pi}{V}\int_0^r \frac{\rho(r',a)-\bar{\rho}}{\bar{\rho}}\, r'^2\, dr' = \frac{4\pi}{V}\int_0^r \delta(r',a)\, r'^2\, dr'\,, \quad (2.6)$$

where V represents the volume of a sphere of radius r.

In terms of the mean density contrast $\bar{\delta}_i$, the constants A and B, in a spatially flat background, read [50]

$$A = \frac{3}{10}\frac{r_i}{\bar{\delta}_i}\,, \qquad\qquad B = \frac{9}{20}\frac{t_i}{\bar{\delta}_i}\,. \quad (2.7)$$

The evolution of a shell in the overdensity is therefore as follows: it expands, till at [50]

$$t = t_{\rm ta} := \pi B \quad (2.8)$$

it reaches its maximum expansion with [50]

$$r = r_{\rm max} := 2A\,, \quad (2.9)$$

and then it starts collapsing. Eq. (2.7) states that the turnaround time $t_{\rm ta}$ of a given shell depends on the initial overdensity enclosed by it.

All this treatment has been carried in the assumption that the mass m enclosed by a shell was constant in time. As soon the first shell starts to contract, this assumption could be violated because of *shell crossing*: particles in the contracting mass shell can cross the mass shells that were originally inside it, and consequently m is no longer constant [50]. What happens indeed after the turnaround is the setting up of a process called violent relaxation, which drive the system towards a virialized final state [56].

Violent relaxation Every time a mixing such as the one caused by shell crossing, coexists with a variation in time of the gravitational potential, violent relaxation occurs.

Let $\epsilon = (1/2)\mathbf{v}^2 + V$ be the specific energy for a given particle of the considered overdensity. Then (from [50])

$$\frac{d\epsilon}{dt} = \frac{\partial\epsilon}{\partial\mathbf{v}}\frac{d\mathbf{v}}{dt} + \frac{\partial\epsilon}{\partial V}\frac{dV}{dt} = -\mathbf{v}\cdot\nabla V + \frac{dV}{dt} = -\mathbf{v}\cdot\nabla V + \frac{\partial V}{\partial t} + \mathbf{v}\cdot\nabla V = \frac{\partial V}{\partial t}\,.$$

Thus, a time-dependent gravitational potential of a collisionless system can induce a change in the energies of the particles involved (i.e. in a time-varying potential, energy is no longer an integral of motion). Therefore, in such a time varying potential, particles can both gain or lose energy, and some particles can even become unbound. Overall, the effect is to broaden the range of energies [50].

After turnaround, a shell starts collapsing, therefore in this phase too the density is a function of time, and it is easy to see, from Poisson equation, that this means that the gravitational potential is also time dependent. In particular, during collapse the gravitational potential experiences fluctuations on large scales [56]. If moreover the shells constituting the spherical overdensity cross, this provides mixing and the process the whole overdensity undergoes in these conditions is called *relaxation*, because it drives the system towards a virialized state of equilibrium, and *violent*, because the timescale for the process to occur can be defined as [50]

$$t_{\rm vr} = \left\langle \frac{\epsilon^2}{\dot{\epsilon}^2} \right\rangle^{1/2} = \left\langle \frac{1}{\epsilon^2}\left(\frac{\partial V}{\partial t}\right)^2 \right\rangle^{-1/2}\,, \quad (2.10)$$

where the average $\langle ... \rangle$ is over all particles that make up the collective potential. As shown by Lynden-Bell (1967), this is approximately equal to the free fall time of the system $t_{\rm ff} = [3\pi/(32G\bar{\rho})]^{1/2}$, with $\bar{\rho}$ the average density; therefore the process is fast (hence "violent").

Violent relaxation is self-limiting, because as soon as a system approaches any equilibrium state, the variations in time of the potential, which drive the evolution, vanish [50]. The ending point of this process is indeed a virialized configuration [56] with radius $r_{\rm vir}$, velocity dispersion $v_{\rm vir}$ and density $\rho_{\rm vir}$. For a spherically symmetric system with constant density, numerical simulations [69] show that this configuration is achieved by the time $t_{\rm vir} = 2t_{\rm max}$, where $t_{\rm max}$ is its turnaround time. Still in the constant density case, we can compute $r_{\rm vir}$, $v_{\rm vir}$ and $\rho_{\rm vir}$ following [56] and hence exploiting the fact that in a virialized system the potential energy U and the kinetic one T are related by $|U| = 2T$. The total energy is therefore $E = U + T = -T$. At $t = t_{\rm max}$ all the energy is in the potential form and it is [56]

$$E = -\frac{3}{5}\frac{GM^2}{r_{\rm max}}\,,$$

where M is the mass of the overdensity. Then using [56]

$$T := \frac{Mv_{\rm vir}^2}{2} = -E$$

we get [56]

$$v_{\rm vir} = \sqrt{\frac{6GM}{5r_{\rm max}}}\,; \tag{2.11}$$

and using [56]

$$|U| = \frac{3GM^2}{5r_{\rm vir}} = 2T := Mv_{\rm vir}$$

we get [56]

$$r_{\rm vir} = \frac{r_{\rm max}}{2}\,. \tag{2.12}$$

$\rho_{\rm vir}$ is finally easily obtained as

$$\rho_{\rm vir} = \frac{M}{\frac{4}{3}\pi\, r_{\rm vir}^3} \tag{2.13}$$

and therefore $\rho_{\rm vir} = 8\,\rho_{\rm max}$ where $\rho_{\rm max}$ is the density at the turning point.

For some specific density profiles, however, shell crossing at turnaround does not take place; therefore the analytic solution remains valid and, since there is no mixing, violent relaxation does not take place. In this thesis we will study this kind of profiles, which avoid shell crossing.

In order to study the evolution of these profiles in our Universe, it is necessary to place the system, described by the Schrödinger-Newton equations, in an expanding background. In the next section we will recall a re-writing of Schrödinger-Newton equations in terms of quantities which are particularly useful in an expanding background.

2.2 Schrödinger-Newton equations in a spatially flat expanding background

Let us assume an Einstein-de Sitter Universe as such a background, and call $\bar{\rho}$ its uniform energy density.

We will make use of comoving coordinates, as it is customary in cosmology:

$$\mathbf{r} = a\mathbf{x}$$

with $\mathbf{r}$ the physical coordinate, $a(t)$ the scale factor and $\mathbf{x}$ the comoving coordinate. In the same outlook, let us define the following scaled quantities [**?**]

$$\begin{aligned} \delta &= \frac{\rho - \bar{\rho}}{\bar{\rho}}\,, \\ \chi &= \frac{\rho}{\bar{\rho}} = 1 + \delta\,, \\ \mathbf{u} &= \frac{d\mathbf{x}}{da}\,; \end{aligned} \tag{2.14}$$

let us moreover define Φ as the potential of the comoving peculiar velocity field $\mathbf{u}$, just like we did with the physical velocity one $\mathbf{v}$ [**?**]:

$$\mathbf{u} = \nabla_x \Phi\,. \tag{2.15}$$

In order to rewrite fluid equations (1.9) (1.13) and (1.11) in terms of the above defined quantities, let us compute some derivatives of them [48].

$$\frac{d\chi(x,t)}{dt} = \left.\frac{\partial \chi}{\partial t}\right|_x + \nabla_x \chi \cdot \dot{a}\mathbf{u}\,,$$

but because of the definition of χ, it is also true that

$$\frac{d\chi}{dt} = \frac{\dot{\rho}}{\bar{\rho}} - \frac{\rho\dot{\bar{\rho}}}{\bar{\rho}^2} \tag{2.16}$$

and by definition of total derivative we can moreover write [48]

$$\frac{d\rho(x,t)}{dt} = \left.\frac{\partial \rho}{\partial t}\right|_x + \nabla_x \rho \cdot \dot{a}\mathbf{u}\,.$$

Hence we can rewrite (2.16) as

$$\frac{\partial \chi}{\partial a}\dot{a} + \nabla_x \chi \cdot \dot{a}\mathbf{u} = \frac{1}{\bar{\rho}}\left(\left.\frac{\partial \rho}{\partial t}\right|_x + \nabla_x \rho \cdot \dot{a}\mathbf{u}\right) - \frac{\rho\dot{\bar{\rho}}}{\bar{\rho}^2}\,,$$

which simplified reads

$$\left.\frac{\partial \rho}{\partial t}\right|_x = \frac{\rho\dot{\bar{\rho}}}{\bar{\rho}} + \frac{\partial \chi}{\partial a}\dot{a}\bar{\rho}\,.$$

Le us moreover calculate the relation between $\mathbf{u}$ (2.14) and $\mathbf{v} := d\mathbf{r}/dt$

$$\mathbf{v} := \frac{d\mathbf{r}}{dt} = \frac{d(a\mathbf{x})}{dt} = \dot{a}(\mathbf{x} + a\mathbf{u})\,.$$

Considering now ρ as a function of $\mathbf{r}$ and t we can write [48]

$$\begin{aligned} \frac{D\rho(\mathbf{r},t)}{Dt} &= \left.\frac{\partial \rho}{\partial t}\right|_r + \frac{\partial \rho}{\partial \mathbf{r}} \cdot \dot{\mathbf{r}} = \\ &= \left.\frac{\partial \rho}{\partial t}\right|_r + H(\mathbf{r} \cdot \nabla_r)\rho + (a\dot{\mathbf{x}} \cdot \nabla_r)\rho\,, \end{aligned}$$

meanwhile considering it as a function of $\mathbf{x}$ and t we can write [48]

$$\frac{D\rho(\mathbf{x},t)}{Dt} = \left.\frac{\partial\rho}{\partial t}\right|_x + \frac{\partial\rho}{\partial\mathbf{x}}\cdot\dot{\mathbf{x}}\,,$$

but [48]

$$\frac{D\rho(\mathbf{r},t)}{Dt} = \frac{D\rho(\mathbf{x},t)}{Dt}$$

so, exploiting the relation [48]

$$\nabla_r = \frac{1}{a}\nabla_x\,, \tag{2.17}$$

one obtains the following equation [48]

$$\left.\frac{\partial\rho}{\partial t}\right|_r = \left.\frac{\partial\rho}{\partial t}\right|_x - H(\mathbf{r}\cdot\nabla_r\rho)\,.$$

The above found expressions can be plugged into the continuity equation (1.9)

$$\left.\frac{\partial\rho}{\partial t}\right|_r + \nabla_r\cdot(\rho\mathbf{v}) = 0$$

to obtain

$$\frac{\rho\dot{\bar{\rho}}}{\bar{\rho}} + \frac{\partial\chi}{\partial a}\dot{a}\bar{\rho} - H(\mathbf{r}\cdot\nabla_r\rho) + \bar{\rho}\dot{a}\left[\nabla_r\cdot(\chi\mathbf{x}) + \nabla_r\cdot(\chi a\nabla_x\Phi)\right] = 0\,; \tag{2.18}$$

supposing as a background a matter dominated Universe in which the cosmological principle holds, (2.18) becomes[1] [17]

$$\frac{\partial\chi}{\partial a} + \nabla_x\cdot(\chi\nabla_x\Phi) = 0\,. \tag{2.19}$$

In an expanding background it is useful to define, following [55], the peculiar velocity field $\mathbf{b}$ as

$$\mathbf{v} = \dot{\mathbf{r}} = \frac{\dot{a}}{a}\mathbf{r} + a\dot{\mathbf{x}} = H\mathbf{r} + \mathbf{b} \tag{2.20}$$

and the peculiar gravitational potential $\mathcal{V}$ as [55]

$$V = \bar{V} + \mathcal{V}\,,$$

where V is the usual Newtonian potential defined by

$$\nabla_r^2 V = 4\pi G\rho$$

and $\bar{V}$ is the background gravitational potential defined to obey [55]

$$\nabla_r^2\bar{V} = 4\pi G\bar{\rho}\,,$$

which in an Einstein de Sitter Universe is solved by [55]

$$\bar{V} = \frac{2\pi G}{3}\bar{\rho}|\mathbf{x}|^2\,;$$

[1] See the appendix for the derivation

consequently, $\mathcal{V}$ obeys the following Poisson equation [55]

$$\nabla_x^2 \mathcal{V} = 4\pi G a^2(\rho - \bar{\rho}) = 4\pi G a^2 \bar{\rho}\delta\,.$$

With these variables, in an Universe where Friedmann equations are valid, Euler equation becomes [55]

$$\left.\frac{\partial \mathbf{b}}{\partial t}\right|_x + (\mathbf{b}\cdot\nabla_r)\mathbf{b} + H\mathbf{b} = -\frac{1}{a}\nabla_x \mathcal{V}\,.$$

Let us compute the relation connecting $\mathbf{b}$ (2.20) and $\mathbf{u}$ (2.14)

$$\mathbf{b} := a\frac{d\mathbf{x}}{dt} = a\frac{d\mathbf{x}}{da}\frac{da}{dt} := a\dot{a}\mathbf{u} := a\dot{a}\nabla_x\Phi$$

and plug this expression into Euler equation (1.10)

$$\left.\frac{\partial\left(a\dot{a}\nabla_x\Phi\right)}{\partial t}\right|_x + (a\dot{a}\nabla_x\Phi\cdot\nabla_r)a\dot{a}\nabla_x\Phi + Ha\dot{a}\nabla_x\Phi = -\frac{1}{a}\nabla_x\mathcal{V}\,;$$

the equation above is then equivalent to

$$\dot{a}^2\nabla_x\Phi + a\ddot{a}\nabla_x\Phi + a\dot{a}\nabla_x\dot{\Phi} + a\dot{a}^2\nabla_x\left[\frac{1}{2}(\nabla_x\Phi)^2\right] + \dot{a}^2\nabla_x\Phi = -\frac{1}{a}\nabla_x\mathcal{V}\,. \tag{2.21}$$

If the following equation is satisfied, so it is also (2.21)

$$2H^2\Phi + \frac{\ddot{a}}{a}\Phi + \frac{\dot{a}^2}{a}\frac{\partial\Phi}{\partial a} + \frac{\dot{a}^2}{a}\left[\frac{1}{2}(\nabla_x\Phi)^2\right] = -\frac{1}{a^3}\mathcal{V}\,. \tag{2.22}$$

(2.22) is then equivalent to

$$2\frac{8\pi G}{3}\bar{\rho}\Phi - \frac{4\pi G}{3}\bar{\rho}\Phi + \frac{\dot{a}^2}{a}\frac{\partial\Phi}{\partial a} + \frac{\dot{a}^2}{a}\left[\frac{1}{2}(\nabla_x\Phi)^2\right] = -\frac{1}{a^3}\mathcal{V}\,,$$

and to

$$\frac{3}{2}H^2\Phi + \frac{\dot{a}^2}{a}\frac{\partial\Phi}{\partial a} + \frac{\dot{a}^2}{a}\left[\frac{1}{2}(\nabla_x\Phi)^2\right] = -\frac{1}{a^3}\mathcal{V}\,,$$

and to

$$\frac{\partial\Phi}{\partial a} + \left[\frac{1}{2}(\nabla_x\Phi)^2\right] = -\frac{3}{2a}\left(\Phi + \frac{2}{3\dot{a}^2 a}\mathcal{V}\right)\,. \tag{2.23}$$

The last written equation can be rewritten as [**?**]

$$\frac{\partial\Phi}{\partial a} + \frac{1}{2}(\nabla_x\Phi)^2 = -\tilde{V} \tag{2.24}$$

providing that the effective potential $\tilde{V}$ is defined as the following sum of the velocity potential Φ and a slightly modified Newtonian potential φ [17]

$$\tilde{V} = \frac{3}{2a}(\Phi + \varphi)\,, \tag{2.25}$$

where φ is [17]

$$\varphi := \frac{2\mathcal{V}}{3a^3H^2}\,. \tag{2.26}$$

Starting from (2.23) one can compute the equivalent of Poisson equation for the effective potential

$$\nabla_x^2\tilde{V} = \frac{3}{2a}\nabla_x^2\Phi + \frac{1}{\dot{a}^2a^2}\nabla_x^2\mathcal{V} = \frac{3}{2a}\nabla_x^2\Phi + \frac{1}{\dot{a}^2}4\pi G\bar{\rho}\delta = \frac{3}{2a}\nabla_x^2\Phi + \frac{1}{\dot{a}^2}4\pi G\bar{\rho}(\chi-1) =$$
$$= \frac{3}{2a}\nabla_x^2\Phi + \frac{3}{2\dot{a}^2}H^2(\chi-1) = \frac{3}{2a}\nabla_x^2\Phi + \frac{3}{2a^2}(\chi-1)\,.$$

Because of this expression it is easy to check that the following relation holds [**?**]

$$\nabla_x^2\varphi = \frac{\delta}{a}\,.$$

We are then left with the following system of equations, in which every quantity should be thought as function of $(\mathbf{x}, a)$ [**?**]

$$\frac{\partial\chi}{\partial a} + \nabla_x\cdot(\chi\nabla_x\Phi) = 0 \tag{2.27}$$
$$\frac{\partial\Phi}{\partial a} + \frac{1}{2}(\nabla_x\Phi)^2 = -\tilde{V} \tag{2.28}$$
$$\nabla_x^2\tilde{V} = \frac{3}{2a}\nabla_x^2\Phi + \frac{3}{2a^2}(\chi-1)\,. \tag{2.29}$$

Following Madelung procedure (i.e. substitution (1.14)) and interpreting this time the squared modulus of Ψ as χ [17]:

$$|\Psi|^2 = R^2(\mathbf{x}, a) := \chi\,, \tag{2.30}$$

one can obtain (1.16), with the only difference that the derivative in t is now replaced by one in the scale factor a, and $\tilde{V}$ is now the quantity defined in (2.25), [17]:

$$i\nu\frac{\partial\Psi}{\partial a} = -\frac{\nu^2}{2}\nabla_x^2\Psi + \tilde{V}\psi + \frac{\nu^2}{2}\frac{\nabla_x^2R}{R}\,, \tag{2.31}$$

coupled to the following modified Poisson equation [**?**]

$$\nabla_x^2\left[\tilde{V} + \frac{3i\nu}{4a}\ln\left(\frac{\Psi}{\Psi^*}\right)\right] = \frac{3}{2a^2}(|\Psi|^2-1)\,. \tag{2.32}$$

The just written system of equations is usually difficult to solve; therefore let us introduce some approximations, which lower the complexity of the study.

2.3 Zel'dovich and adhesion approximations

An useful tool to study the overdensities which lead to the LSS is the approximation proposed by Zel'dovich in [87] (see also [56] and [67]). Zel'dovich starts form the following result of linear theory for the growth of perturbations. In a uniform Universe with energy density $\bar{\rho}(t)$, the actual position of any particle $\mathbf{r}(t)$ is related to its initial (Lagrangian) location $\mathbf{q}$ by a very simple expression [56]:

$$\mathbf{r}(t) = a(t)\mathbf{q}\,.$$

This result is no more valid in presence of density perturbations; but in the linear regime, valid for perturbations with contrast $\delta < 1$, a similar relation holds (readapted from [56]):

$$\mathbf{r}(t) = a(t)[\mathbf{q} + D_+(t)\mathbf{p}(\mathbf{q})] := a(t)\mathbf{x}(t)\,, \tag{2.33}$$

where $D_+(t)$ is the growing mode of the linear density contrast and $\mathbf{x}(t)$ is by definition the usual comoving Eulerian coordinate. In an Einstein-de Sitter Universe $D_+(t) \propto a(t)$ [14], but since the actual value of the scale factor is non physical, we can set the proportionality constant between D_+ and a equal to 1.

Then, using (2.33), we can compute

$$\mathbf{u} := \frac{d\mathbf{x}}{da} = \mathbf{p}(\mathbf{q}) \tag{2.34}$$

and therefore (2.33) can be rewritten as

$$\mathbf{r}(t) = a(t)[\mathbf{q} + a(t)\mathbf{u}(\mathbf{q})]\,.$$

This equation shows that particles in the Zel'dovich approximation execute a kind of inertial motion on straight line trajectories [17].

Let us now calculate how the perturbed density evolves when the individual particles move according to (2.33). If the initial, unperturbed, homogeneous density is ρ_q, then conservation of mass implies the following relation for the perturbed density $\rho(\mathbf{r}, t)$ [56]

$$\rho(\mathbf{r}, t)d^3r = \rho_q d^3q\,. \tag{2.35}$$

Therefore [56]

$$\rho(\mathbf{r}, t) = \rho_q \det\left(\frac{\partial q_i}{\partial r_j}\right) = \frac{\rho_q/a^3}{\det\left(\frac{\partial x_j}{\partial q_i}\right)} = \frac{\bar{\rho}(t)}{\det\left(\delta_{ij} + a(t)\left(\frac{\partial u_j}{\partial q_i}\right)\right)}\,; \tag{2.36}$$

$\rho(\mathbf{r}, t)$ is known as *continuity* density.

Since in (2.15) we defined Φ as

$$\mathbf{u}(\mathbf{x}) = \nabla_x \Phi(\mathbf{x})\,,$$

the Jacobian $\partial u_j/\partial q_i$ appearing in (2.36) can be written as the following tensor, called *deformation tensor* [67]

$$d_{ij} := \frac{\partial u_j}{\partial q_i} = \frac{\partial^2 \Phi}{\partial q_i \partial q_j}\,. \tag{2.37}$$

Expanding the determinant of (2.36) to the first order in the perturbation $D_+(t)\mathbf{p}(\mathbf{q})$, the expression for the density distribution is therefore [67]

$$\begin{aligned}\rho(\mathbf{r}, t) &= \frac{\bar{\rho}(t)}{(1 - D_+(t)\lambda_1(\mathbf{q}))(1 - D_+(t)\lambda_2(\mathbf{q}))(1 - D_+(t)\lambda_3(\mathbf{q}))} = \\ &= \frac{\bar{\rho}(t)}{(1 - D_+ I_1 + D_+^2 I_2 - D_+^3 I_3)}\end{aligned} \tag{2.38}$$

where λ_1, λ_2, λ_3 are the eigenvalues of the deformation tensor and $I_1 = \lambda_1 + \lambda_2 + \lambda_3$, $I_2 = \lambda_1\lambda_2 + \lambda_2\lambda_3 + \lambda_1\lambda_3$, $I_3 = \lambda_1\lambda_2\lambda_3$ are its invariants. Since D_+ grows with time, a positive eigenvalue denotes collapse and a negative one signals expansion. If at least one of the eigenvalues is positive, at the time $t_{\rm sc}$ for which $D_+(t_{\rm sc}) = 1/\max\{\lambda_j\}$ with $j = 1, 2, 3$, the overdensity becomes formally infinite and Zel'dovich approximation breaks down. When the density diverge, the material contained initially in a cube in $\mathbf{q}$ space gets

compressed to a sheet in the **r** space, perpendicular to the direction of the eigenspace of the bigger eigenvalue [67]. Unavoidably different particle trajectories cross, therefore shell crossing occurs. The structures formed, because of their flatness, are called "pancakes". Numerical simulations have been employed to test how well Zel'dovich approximation works [56]. It was found that it reproduces in an excellent fashion the formation, appearance and location of the pancakes. Once the pancake is formed however, particles in the Zel'dovich approximation go on in their travel without having a feedback from the formation of an highly dense region, called caustic; therefore this caustic blur and the pancake thickens. What on the contrary simulations show is that particles falling into pancakes oscillate about the central region in the collapsed direction, and flow freely in the "plane" in which the pancake lays; at the intersection of different pancakes then they can form filaments and finally clumps at the intersection of filaments, and all this structure is not smeared out with time as Zel'dovich approximation would forecast [55]. To overcome this problem we have to switch to the so called adhesion approximation, but first let us deepen a bit the study of Zel'dovich approximation.

The internal consistency of Zel'dovich approximation can be assessed by means of the following argument [67]. Differentiating equation (2.33) twice with respect to time allows us to determine the acceleration of the fluid element. A dynamical estimate of the density $\rho_{\rm dyn}$ is then provided by Euler equation: for a pressureless fluid it reads

$$\begin{aligned} \frac{\partial \mathbf{v}}{\partial t} + (\mathbf{v}\cdot\nabla_r)\mathbf{v} &= -\nabla_r V \\ \frac{D\mathbf{v}}{Dt} &= -\nabla_r V \\ \nabla_r \ddot{\mathbf{r}} &= -\nabla_r^2 V \\ \nabla_r \ddot{\mathbf{r}} &= -4\pi G\, \rho_{\rm dyn}\,, \end{aligned} \tag{2.39}$$

where in the first passage I used the definition of convective derivative [55]

$$\frac{D}{Dt} := \frac{\partial}{\partial t} + \mathbf{v}\cdot\nabla_r$$

and in the the last one Poisson equation (1.11).
If the Zel'dovich approximation were exact, the values of the just determined $\rho_{\rm dyn}$ and of the continuity density of eq. (2.36) would coincide. The fractional difference [67]

$$\tilde{\delta} := \frac{\rho_{\rm dyn} - \rho}{\rho}$$

therefore provides a measure of the accuracy of the Zel'dovich approximation. Sahni and Coles in [67] find

$$\tilde{\delta} = -D_+^2 I_2 + 2D_+^3 I_3\,; \tag{2.40}$$

from this expression we can see that $\tilde{\delta} = 0$ if $\lambda_2 = \lambda_3 = 0$. This means that the Zel'dovich approximation is an exact solution of the fluid equations for a system with planar symmetry, as long as there is no shell-crossing [67] [55].

The Zel'dovich approximation can also be formulated in Eulerian space by noting that (2.33) implies $d\mathbf{u}/da = 0$ along a particle trajectory, provided particle trajectories do not intersect [67]. Since we are following a fluid element in its evolution, the correct notion of total derivative is the one provided by the convective derivative, defined in the variables introduced in the last section as

$$\frac{D}{Da} := \frac{\partial}{\partial a} + \mathbf{u}\cdot\nabla_x\,.$$

It follows that the Zel'dovich approximation corresponds to

$$\frac{\partial \mathbf{u}}{\partial a} + \mathbf{u} \cdot \nabla_x \mathbf{u} = \frac{D\mathbf{u}}{Da} = \frac{d\mathbf{u}}{da} = 0\,. \tag{2.41}$$

We can then integrate the equation formed by the first and the last member of (2.41) to obtain the so-called Zel'dovich–Bernoulli equation [67]:

$$\frac{\partial \Phi}{\partial a} - \frac{1}{2}\left|\nabla_x \Phi\right|^2 = 0\,. \tag{2.42}$$

Comparing this equation to the Bernoulli equation in an expanding background (2.28), we see that the latter turns into (2.42) in the case $\tilde{V} = 0$.

Since the starting point of Zel'dovich approximation is a result of linear theory, one could argue what is the difference between the two, and why the former fairly predicts density distributions even in the non-linear regime where the latter fails. The key [56] lays in the fact that Zel'dovich approximation linearises the temporal evolution of particles, and with their trajectories describes perturbations, while linear theory linearises the evolution of the density contrast. Another way of understanding this fact is by realizing that Zel'dovich approximation uses the Newtonian potential extrapolated from linear theory, instead of the density; this has advantages since potentials are much smoother functions than densities [56].

As anticipated, in order to predict the stability of caustics, we need to improve our model: in the so called adhesion approximation [72], particles follow Zel'dovich trajectories until shell-crossing occurs. However, when particle trajectories cross, the particles are assumed to stick to each other. As a result, the singularities predicted by the Zel'dovich approximation are frozen rather than being washed out, and stable structures form. Mathematically, the adhesion model is obtained from the Zel'dovich approximation by including an artificial viscosity term in (2.42) [55] [72]:

$$\frac{\partial \Phi}{\partial a} - \frac{1}{2}\left|\nabla_x \Phi\right|^2 = \mu \nabla_x^2 \Phi\,. \tag{2.43}$$

The constant $\mu > 0$ has dimensions of L^2 and can be thought as a viscosity coefficient. In the inviscid limit $\mu \to 0$ the structures formed in the adhesion model are infinitely thin and the adhesion approximation reduces exactly to the Zel'dovich approximation outside of mass concentrations [67]. For finite values of μ, the viscosity term causes density perturbations to be suppressed on scales $\lesssim \mu^{1/2}$ [55].

In [72], Short and Coles consider the following free-particle Schrödinger equation in the coordinates $(\mathbf{x}, a)$

$$i\nu \frac{\partial \Psi}{\partial a} = -\frac{\nu^2}{2}\nabla_x^2 \Psi\,; \tag{2.44}$$

it is mathematically equivalent, via Madelung transformation, to the usual continuity equation (1.9) and the following modified Bernoulli equation [72]

$$\frac{\partial \Phi}{\partial a} - \frac{1}{2}\left|\nabla_x \Phi\right|^2 = -\frac{\nu^2}{2}\frac{\nabla_x^2 |\Psi|}{|\Psi|}\,. \tag{2.45}$$

Short and Coles then define the approximation scheme called *free-particle approximation* by the one which uses eq. (2.44) and gives rise to the Bernoulli equation (2.45). In this approximation the Poisson equation (2.29) decouples from the Schrödinger one and provides the following relationship between the amplitude and phase of the wavefunction [72]:

$$\nu \nabla_x^2 [\arg(\Psi)] + \frac{1}{a}(|\Psi|^2 - 1) = 0\,. \tag{2.46}$$

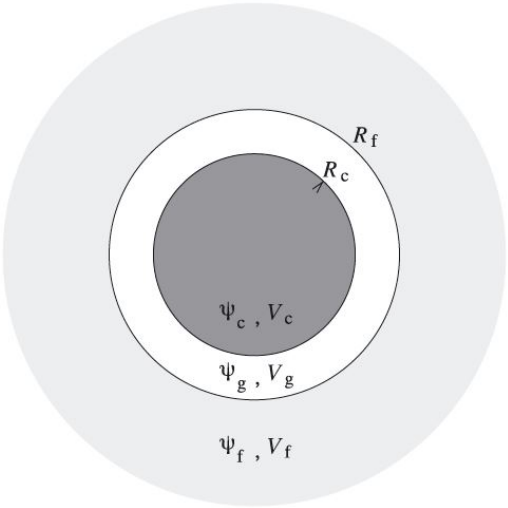

Figure 2.1: Illustration of the spherical overdensity. The wavefunction and gravitational potential that solve the SP system in the inner, vacuum and outer regions, respectively, are (ψ_c, V_c), (ψ_g, V_g) and (ψ_f, V_f). The radii R_c and R_f label the boundaries of the vacuum region. (From [38]

Equations (2.43) and (2.45) resemble each other: in the inviscid limit $\mu \to 0$ for the first one, and in the classical one $\nu \to 0$ for the second, they both give Zel'dovich-Bernoulli equation. Moreover the viscous term of the former and the quantum pressure term of the latter present phenomenological similarities: the quantum pressure term prohibits the formation of structures below the de Broglie wavelength [29]; therefore, recalling that $\nu = \hbar/m$, in the limit $\nu \to 0$, as well as in the $\mu \to 0$ one, thin structures can form, while for bigger values of the two parameters, only thicker ones are allowed. In [72] numerical simulations are performed which show that, in the limit $\nu \to 0$, the free-particle approximation reduces to the Zel'dovich approximation prior to shell-crossing. They also argue that in that limit[2] the quantum pressure term will only become important in regions where particle trajectories intersect. They then propose to study a modification of adhesion approximation in which the viscous term $\mu\nabla_x^2\Phi$ is replaced by the quantum pressure term, which has moreover a similar mathematical expression, in addition to a similar phenomenology.

2.4 Schrödinger-Newton solution for a top-hat compensated overdensity

Let us now discuss a solution of Schrödinger-Newton equations that will be of very useful for our later work. It is found by Johnston et al. in [38] and it describes a matter overdensity similar to a top-hat one. The physical system described is the one represented in *figure 2.1.* It is made up of three parts: an infinite outer fluid region of homogenous density; an inner fluid sphere, also of homogenous density and overdense relative to the outer region; and a spherical shell of vacuum which separates the two fluids. The inner fluid sphere is 'compensated', that is, we can imagine forming the inner fluid region by removing the mass from the vacuum (gap) region and adding it (homogeneously) to the mass within the inner radius of the gap [38].

[2]more precisely, in the limit of small yet finite ν, since predictions in the actual $\nu \to 0$ limit cannot be computed explicitly by a simulation, because they would need either an infinite computational power or an infinite time.

Because of Birkhoff's theorem the evolution of the inner overdensity is independent from the one of the external region, at $r > R_f$ [18]. Exploiting this property, Johnston et al. find a solution of the SP system for this matter configuration by simply attaching to each other three different solutions: one describing a closed Universe, to model the inner overdensity, one for the void region and a third piece describing a flat Universe to model the external region [38]. Let us see the three of them in more details.

Flat Universe Johnston et al. in the cited paper [38] start by recalling that in a spatially flat Universe in which the cosmological principle holds, the density evolves in terms of a globally defined cosmic time t according to the following law

$$\rho(t) := |\psi|^2 = \frac{\Lambda c^2}{8\pi G} \operatorname{cosech}^2\left(\frac{3}{2}\sqrt{\frac{\Lambda c^2}{3}}t\right) . \tag{2.47}$$

This expression is then substituted into the following modified version of Poisson equation (1.11) which enables the existence of a non-zero cosmological constant Λ [38]

$$\begin{aligned} \nabla^2 V &= 4\pi G|\psi|^2 - \Lambda c^2 \\ &= \Lambda c^2 \left[\frac{1}{2}\operatorname{cosech}^2\left(\frac{3}{2}\sqrt{\frac{\Lambda c^2}{3}}t\right) - 1\right] . \end{aligned} \tag{2.48}$$

If we then define for notational convenience

$$\lambda := \frac{3}{2}\sqrt{\frac{\Lambda c^2}{3}} ,$$

the root of such equation can be written as [38]

$$V = \frac{\Lambda c^2}{12}\left[\coth^2(\lambda t) - 3\right] r^2 , \tag{2.49}$$

as it is now proven. Because of spherical symmetry, the Laplacian takes the form [38]

$$\nabla^2 = \frac{\partial^2}{\partial r^2} + \frac{2}{r}\frac{\partial}{\partial r} ; \tag{2.50}$$

thus let us compute

$$\begin{aligned} \frac{\partial V}{\partial r} &= \frac{\Lambda c^2}{6}\left[\coth^2(\lambda t) - 3\right] r , \\ \frac{\partial^2 V}{\partial r^2} &= \frac{\Lambda c^2}{6}\left[\coth^2(\lambda t) - 3\right] . \end{aligned}$$

To check (2.48) we have therefore to prove

$$\frac{\Lambda c^2}{6}\left[\coth^2(\lambda t) - 3\right] + \frac{2\Lambda c^2}{6}\left[\coth^2(\lambda t) - 3\right] = \Lambda c^2\left(\frac{1}{2}\operatorname{cosech}^2(\lambda t) - 1\right) ,$$

which, using the relation $\cosh^2(x) - \sinh^2(x) = 1$, turns out to be equivalent to

$$\frac{\Lambda c^2}{2}\left[\coth^2(\lambda t) - 3\right] = \Lambda c^2 \frac{1}{2}\frac{\cosh^2(\lambda t) - \sinh^2(\lambda t) - 2\sinh^2(\lambda t)}{\sinh^2(\lambda t)} ,$$

and thus to

$$\frac{\Lambda c^2}{2}\left[\coth^2(\lambda t) - 3\right] = \frac{\Lambda c^2}{2}\left[\coth^2(\lambda t) - 3\right] .$$

Substituting then the expression for V (2.49) in the Schrödinger equation (1.16), Johnston and al. find an expression for the potential ϕ which allows to compute the following final wavefunction [38]

$$\psi = \sqrt{\frac{\Lambda c^2}{8\pi G}}\,\mathrm{cosech}\,(\lambda t)\exp\left[\frac{i}{\nu}\sqrt{\frac{\Lambda c^2}{12}}\coth(\lambda t)r^2\right]. \tag{2.51}$$

In order to check that (2.51) was indeed a solution of (1.16) for the gravitational potential (2.49) we need to calculate

$$\begin{aligned}
\frac{\partial\psi}{\partial t} &= -\sqrt{\frac{\Lambda c^2}{8\pi G}}\exp\left(\frac{i}{\nu}\frac{\lambda}{3}\coth(\lambda t)r^2\right)\mathrm{cosech}^2(\lambda t)\lambda\left[\cosh(\lambda t)+\frac{i}{\nu}\frac{\lambda}{3}\,\mathrm{cosech}(\lambda t)r^2\right],\\
\frac{\partial\psi}{\partial r} &= 2\frac{i}{\nu}\frac{\lambda}{3}\sqrt{\frac{\Lambda c^2}{8\pi G}}\exp\left(\frac{i}{\nu}\frac{\lambda}{3}\coth(\lambda t)r^2\right)\mathrm{cosech}(\lambda t)\coth(\lambda t)r\,,\\
\frac{\partial^2\psi}{\partial r^2} &= 2\frac{i}{\nu}\frac{\lambda}{3}\sqrt{\frac{\Lambda c^2}{8\pi G}}\exp\left(\frac{i}{\nu}\frac{\lambda}{3}\coth(\lambda t)r^2\right)\mathrm{cosech}(\lambda t)\coth(\lambda t)\left(2\frac{i}{\nu}\frac{\lambda}{3}\coth(\lambda t)r+1\right).
\end{aligned}$$

Defining

$$\sqrt{\frac{\Lambda c^2}{8\pi G}} := A\,,$$

equation (1.16) becomes

$$\begin{aligned}
&-i\nu A\frac{\lambda}{\sinh(\lambda t)}\cosh(\lambda t)+A\frac{\lambda}{3}r^2\frac{\lambda}{\sinh^2(\lambda t)}+\\
&+\frac{\nu^2}{2}A\left[-\frac{\lambda^2}{\nu^2 9}\coth^2(\lambda t)4r^2+\frac{2i}{\nu}\frac{\lambda}{3}\coth(\lambda t)+\frac{4i}{\nu}\frac{\lambda}{3}\coth(\lambda t)\right]-\frac{\lambda^2}{9}\left[\coth^2(\lambda t)-3\right]r^2A=0\,,
\end{aligned}$$

which is equivalent to

$$\begin{aligned}
&-i\nu\lambda\coth(\lambda t)+\frac{\lambda^2}{3}r^2\,\mathrm{cosech}^2(\lambda t)+\\
&\qquad+\left[-2\frac{\lambda^2}{9}\coth^2(\lambda t)r^2+i\nu\lambda\coth(\lambda t)\right]-\frac{\lambda^2}{9}\left[\coth^2(\lambda t)-3\right]r^2=0\,,
\end{aligned}$$

and thus to

$$\frac{\lambda^2}{3}r^2\,\mathrm{cosech}^2(\lambda t)-2\frac{\lambda^2}{9}\coth^2(\lambda t)r^2-\frac{\lambda^2}{9}\coth^2(\lambda t)r^2+\frac{\lambda^2}{3}r^2=0\,,$$

which can be simplified to

$$\mathrm{cosech}^2(\lambda t)-\coth^2(\lambda t)+1=0\,,$$

which is an identity.

The solutions in the special case of a spatially flat universe with zero cosmological constant can be obtained by taking the $\Lambda\to 0$ limit of (2.51) and (2.49), which yields [38]

$$\psi = \frac{1}{\sqrt{6\pi G t^2}}\exp\left(\frac{ir^2}{3t\nu}\right), \tag{2.52}$$

$$V = \frac{r^2}{9t^2}\,. \tag{2.53}$$

In a spatially flat, matter dominated Universe the following two relations hold [18]

$$H^2 = \frac{8\pi G}{3}\rho\,, \tag{2.54}$$

$$H = \frac{2}{3t}\,; \tag{2.55}$$

from these it is easy to find a law[3] for the temporal variation of ρ

$$\rho(t) = \frac{1}{6\pi G t^2}\,. \tag{2.56}$$

Closed Universe In order to write a solution of the SP system for a closed Universe, it is convenient to define the following dimensionless conformal time [38]

$$\eta = a\left(\frac{3M}{4\pi}\right)^{-1/3}\int \alpha^{2/3}dt\,, \tag{2.57}$$

where a is a constant with dimensions of velocity, whose explicit expression we will find afterwards; $M := (4/3)\pi\rho R^3$, with R being the scale factor of such a Universe; $\alpha := |\psi| = \sqrt{\rho}$.

Johnston and al. then assume the well-known form of the density evolution in a closed FRW model with $\Lambda = 0$ [38]

$$\rho = \alpha^2 = \frac{A^2}{\sin^6(\eta/2)}\,, \tag{2.58}$$

where A is a constant; then following the same procedure explained for the spatially flat case, they find the following solutions of the SP system

$$\psi = \frac{A}{\sin^3(\eta/2)}\exp\left[\frac{ia\mu^{-1/3}A^{2/3}\cos(\eta/2)}{\nu 2\sin^3(\eta/2)}r^2\right]\,, \tag{2.59}$$

$$V = \frac{a^2\mu^{-2/3}A^{4/3}}{4\sin^6(\eta/2)}r^2\,, \tag{2.60}$$

where we defined for notational convenience $\mu := 3M/(4\pi)$ and the value of A is now set by the following condition [38]

$$\frac{a}{(\mu A)^{1/3}} = \sqrt{\frac{8\pi G}{3}}\,.$$

What we have written till now implies the following well-known results [38]

$$R = \frac{2GM}{a^2}\sin^2(\eta/2)\,, \tag{2.61}$$

$$t = \frac{GM}{a^3}(\eta - \sin\eta)\,. \tag{2.62}$$

From the expression for $R(\eta)$, setting $\sin(\eta/2) = 1$ we find an expression for the velocity parameter a [38]:

$$a = \sqrt{\frac{2GM}{R_{\max}}}\,, \tag{2.63}$$

where $R_{\max}$ is the maximum value of R attained during the evolution.

[3] Which differs from the one found in [38], probably because of a typo there.

In order to check the validity of (2.59) and (2.60), let us calculate

$$\frac{\partial\psi}{\partial\eta} = A\exp\left[\frac{ia\mu^{-1/3}A^{2/3}\cos(\eta/2)}{\nu 2\sin^3(\eta/2)}r^2\right]\times$$
$$\times\left[-\frac{3}{2}\sin^{-4}(\eta/2)\cos(\eta/2) - \frac{ia\mu^{-1/3}A^{2/3}r^2}{4\nu\sin^7(\eta/2)}(\sin^2(\eta/2)+3\cos^2(\eta/2))\right],$$

$$\frac{d\eta}{dt} = a\mu^{-1/3}\frac{A^{2/3}}{\sin^2(\eta/2)},$$
$$\frac{\partial\psi}{\partial r} = \frac{A}{\sin^3(\eta/2)}\exp\left[\frac{ia\mu^{-1/3}A^{2/3}\cos(\eta/2)}{2\nu\sin^3(\eta/2)}r^2\right]\frac{ia\mu^{-1/3}A^{2/3}\cos(\eta/2)}{\nu\sin^3(\eta/2)}r,$$

$$\frac{\partial^2\psi}{\partial r^2} = \frac{A}{\sin^3(\eta/2)}\exp\left[\frac{ia\mu^{-1/3}A^{2/3}\cos(\eta/2)}{2\nu\sin^3(\eta/2)}r^2\right]\times$$
$$\times\left[\left(\frac{ia\mu^{-1/3}A^{2/3}\cos(\eta/2)}{\nu\sin^3(\eta/2)}r\right)^2 + \frac{ia\mu^{-1/3}A^{2/3}\cos(\eta/2)}{\nu\sin^3(\eta/2)}\right].$$

Thus equation (1.16) becomes

$$i\nu A\exp\left[\frac{ia\mu^{-1/3}A^{2/3}\cos(\eta/2)}{2\nu\sin^3(\eta/2)}r^2\right]\times$$
$$\times\left[-\frac{3}{2}\cos(\eta/2)\sin^{-4}(\eta/2) - \frac{ia\mu^{-1/3}A^{2/3}r^2}{4\nu\sin^7(\eta/2)}(1+2\cos^2(\eta/2))\right]\frac{a\mu^{-1/3}A^{2/3}}{\sin^2(\eta/2)} =$$
$$= -\frac{\nu^2}{2}\frac{A}{\sin^3(\eta/2)}\exp\left[\frac{ia\mu^{-1/3}A^{2/3}\cos(\eta/2)}{2\nu\sin^3(\eta/2)}r^2\right]\left[\left(\frac{ia\mu^{-1/3}A^{2/3}\cos(\eta/2)}{\nu\sin^3(\eta/2)}r\right)^2 + \frac{ia\mu^{-1/3}A^{2/3}\cos(\eta/2)}{\nu\sin^3(\eta/2)}\right] +$$
$$-\nu^2\frac{A}{\sin^3(\eta/2)}\exp\left[\frac{ia\mu^{-1/3}A^{2/3}\cos(\eta/2)}{2\nu\sin^3(\eta/2)}r^2\right]\frac{ia\mu^{-1/3}A^{2/3}\cos(\eta/2)}{\nu\sin^3(\eta/2)} +$$
$$+\frac{a^2\mu^{-2/3}A^{4/3}}{4\sin^6(\eta/2)}r^2\frac{A}{\sin^3(\eta/2)}\exp\left[\frac{ia\mu^{-1/3}A^{2/3}\cos(\eta/2)}{2\nu\sin^3(\eta/2)}r^2\right],$$

which simplified becomes

$$i\nu\left[-\frac{3}{2}\cos(\eta/2) - \frac{ia\mu^{-1/3}A^{2/3}r^2}{4\nu\sin^3(\eta/2)}(1+2\cos^2(\eta/2))\right]\frac{\mu^{-1/3}A^{2/3}}{\sin^2(\eta/2)} =$$
$$= -\frac{\nu^2}{2}\left(\frac{i\mu^{-1/3}A^{2/3}\cos(\eta/2)}{\nu\sin^2(\eta/2)}\right)\left[\frac{ia\mu^{-1/3}A^{2/3}\cos(\eta/2)}{\nu\sin^3(\eta/2)}r^2+1\right] +$$
$$-\nu\frac{i\mu^{-1/3}A^{2/3}\cos(\eta/2)}{\sin^2(\eta/2)} + \frac{a\mu^{-2/3}A^{4/3}}{4\sin^5(\eta/2)}r^2,$$

and

$$i\nu\left[-\frac{3}{2}\cos(\eta/2)-\frac{ia\mu^{-1/3}A^{2/3}r^2}{4\nu\sin^3(\eta/2)}(1+2\cos^2(\eta/2))\right]+$$
$$-\frac{1}{2}\left(\frac{a\mu^{-1/3}A^{2/3}\cos^2(\eta/2)}{\sin^3(\eta/2)}r^2\right)+\frac{3}{2}\nu i\cos(\eta/2)-\frac{a\mu^{-1/3}A^{2/3}}{4\sin^3(\eta/2)}r^2=0\,,$$

and again

$$-\frac{3}{2}i\nu\cos(\eta/2)+\frac{a\mu^{-1/3}A^{2/3}r^2}{4\sin^3(\eta/2)}(1+2\cos^2(\eta/2))+$$
$$+\frac{3}{2}\nu i\cos(\eta/2)-\frac{1}{2}\frac{a\mu^{-1/3}A^{2/3}}{\sin^3(\eta/2)}r^2\left(\frac{1}{2}+\cos^2(\eta/2)\right)=0\,,$$

which is equivalent to

$$\frac{a\mu^{-1/3}A^{2/3}r^2}{4\sin^3(\eta/2)}(1+2\cos^2(\eta/2))-\frac{1}{2}\frac{a\mu^{-1/3}A^{2/3}}{\sin^3(\eta/2)}r^2\left(\frac{1}{2}+\cos^2(\eta/2)\right)=0\,,$$

which is finally the same as

$$\frac{1}{2}r^2(1+2\cos^2(\eta/2))-r^2\left(\frac{1}{2}+\cos^2(\eta/2)\right)=0\,,$$

which is true $\forall r$ and $\forall\eta$.

For future convenience, let us calculate the following two quantities [38]:

$$H:=\frac{\dot{R}}{R}=\frac{1}{R}\frac{dR}{d\eta}\frac{d\eta}{dt}=\frac{a^3}{2GM}\frac{\cos(\eta/2)}{\sin^3(\eta/2)}\,, \tag{2.64}$$

$$\Omega:=\frac{8\pi G\rho}{3H^2}=\frac{1}{\cos^2(\eta/2)}\,. \tag{2.65}$$

Vacuum region The vacuum wavefunction is trivially [38]

$$\psi(r,t)=0\,, \tag{2.66}$$

since by construction $\rho(r,t)=0$. Because of this fact the Newtonian potential must satisfy the Laplace equation, so it takes the form [38]

$$V=C+\frac{B}{r}\,, \tag{2.67}$$

where B and C are functions of time only and must be fixed by appropriate boundary conditions.

Top-hat wavefunction Now that we have solutions for all the regions of the system we aim at describing, we are almost ready to write down the solution we are looking for.

Let us indicate with a subscript c (closed) the quantities referring to the inner overdensity, with a g (gap) the ones referred to the void region and with f (flat) the ones referred to the external part. The temporal evolution of the inner boundary R_c (see *figure 2.1*) is

described by equation (2.61), while the one of the outer boundary R_f can be computed from (2.56) using $M = (4\pi/3)\rho_c R_c^3$ and results[4]

$$R_f = \left(\frac{9GM}{2}\right)^{1/3} t^{2/3}\,. \tag{2.68}$$

Since we possess solutions for each "piece" of the system we want to describe, the only study left concerns the discontinuities at $R_c(t)$ and $R_f(t)$. Johnston et al. then write down the form of the modulus of ψ, α, in the vicinity of a boundary, let us say R_f [38]:

$$\alpha(t,r) = f(t)\,\mathrm{H}(r - R_f(t))\,, \tag{2.69}$$

where $f(t)$ describes the time evolution of α within the outer (flat) region of homogeneous fluid and $\mathrm{H}(x)$ is the Heaviside function.
The requirement they demand explicitly in the paper is that this α satisfies the following equation

$$\frac{\partial\alpha}{\partial t} = -\frac{\partial\alpha}{\partial r}\frac{\partial\phi}{\partial r} - \frac{\alpha}{r}\frac{\partial\phi}{\partial r} - \frac{\alpha}{2}\frac{\partial^2\phi}{\partial r^2}\,. \tag{2.70}$$

This equation is the continuity one in the hypothesis that α^2 and ϕ are spherically symmetric; indeed continuity equation reads

$$\frac{\partial\rho}{\partial t} + \nabla\cdot(\rho\mathbf{v}) = 0$$

and making the usual assumptions,

$$\rho = \alpha^2 \qquad\qquad \mathbf{v} = \nabla\phi\,,$$

it becomes

$$\frac{\partial\alpha^2}{\partial t} + \nabla\cdot(\alpha^2\nabla\phi) = 0\,,$$

which is

$$\frac{\partial\alpha^2}{\partial t} + \nabla\alpha^2\cdot\nabla\phi + \alpha^2\nabla^2\phi = 0\,; \tag{2.71}$$

then in the case of spherical symmetry, the Laplacian takes the form

$$\nabla^2 = \frac{\partial^2}{\partial r^2} + \frac{2}{r}\frac{\partial}{\partial r}\,; \tag{2.72}$$

therefore if spherical symmetry holds, (2.71) is equivalent to

$$2\alpha\frac{\partial\alpha}{\partial t} + 2\alpha\frac{\partial\alpha}{\partial r}\frac{\partial\phi}{\partial r} + \alpha^2\frac{\partial^2\phi}{\partial r^2} + \alpha^2\frac{2}{r}\frac{\partial\phi}{\partial r} = 0\,,$$

which is trivially equivalent to (2.70).

The solutions written in the previous paragraphs satisfy the continuity equation (2.70), thus Johnston et al. finally write the following solution for the wavefunction of the system

[4]This result differs from [38]. The $R_f(t)$ proposed there seems incoherent with an expansion in power series around $t = 0$ of the quantity R_f/R_c proposed in the same paper. Contrarily, (2.68) yields that power series.

in *figure 2.1*

$$\alpha = \begin{cases} \sqrt{\frac{3\Omega H_c^2}{8\pi G}} & r \leq R_c(t) \\ 0 & R_c(t) < r < R_f(t) \\ \sqrt{\frac{3H_f^2}{8\pi G}} & r \geq R_f(t) \end{cases} \tag{2.73}$$

$$\phi = \begin{cases} \frac{H_c r^2}{2} & r \leq R_c(t) \\ \text{undefined} & R_c(t) < r < R_f(t) \\ \frac{H_f r^2}{2} + \frac{3GM}{2}\int_0^t \left(\frac{1}{R_f} - \frac{1}{R_c}\right) dt' & r \geq R_f(t)\,. \end{cases} \tag{2.74}$$

Since the velocity potential is defined only up to the addition of an arbitrary function of time, the second term of the expression for ϕ in the $r \geq R_f(t)$ case has no physical consequence, but is useful to define a coherent smooth gravitational potential, as we will see later.

Normalization for $r \leq R_f$ Let us check that this is the solution of a compensated overdensity, i.e. let us check if the modulus squared of ψ integrated from 0 to R_f equals M:

$$\int_{r<R_f} |\psi|^2 d^3r = 4\pi \int_0^{R_f} |\psi|^2(r,t) r^2 dr = 4\pi \int_0^{R_c} \frac{3\Omega H_c^2}{8\pi G} r^2 dr = 4\pi \frac{\Omega_c H_c^2}{8\pi G} R_c^3 = M\,. \tag{2.75}$$

The last result was found simply by substituting expressions (2.65), (2.64), (2.61) for Ω_c, H_c and R_c respectively.

Top-hat gravitational potential For the gravitational potential we still have to find the coefficients $B(t)$ and $C(t)$ in (2.67); to do so we need two boundary conditions: we can use the potentials prescribed by the Bernoulli equations respectively for $r \to R_c^-$ and $r \to R_f^+$ and demand that $V(r)$ is continuous with continuous first derivative[5].

Let us take the Bernoulli equation [19]

$$V = -\frac{1}{2}\left(\frac{\partial \phi}{\partial r}\right)^2 - \frac{\partial \phi}{\partial t} \tag{2.76}$$

and let us particularize the study to $r \leq R_c$; this implies [38]

$$\phi = \frac{1}{2} H_c r^2\,,$$

and so

$$V(r) = -\frac{1}{2}\left(H_c^2 r^2 + \dot{H}_c r^2\right)\,.$$

Using

$$\dot{H}_c = \frac{\ddot{a}}{a} - H_c^2$$

we get

$$V(r) = -\frac{1}{2}\frac{\ddot{a}}{a} r^2 = \frac{1}{2}\frac{4\pi G}{3}\rho_c r^2\,,$$

[5] V has to be C^1 because at each boundary, the fluid "boundary layer" is infinitesimally thin, and effectively massless. Consequently, it cannot support a force acting on it, which implies that $\partial V/\partial r$ must be continuous at each boundary [38].

and finally

$$\lim_{r\to R_c^-} V(r) = \frac{GM}{2R_c}\,, \tag{2.77}$$

where M is as usual $M = (4/3)\pi R_c^3 \rho_c$.

Repeating the reasoning at $r \geq R_f$, because of the function of time only added to ϕ for a spatially flat Universe in (2.74), we find

$$\lim_{r\to R_f^+} V(r) = -\frac{3GM}{4R_c} - \frac{GM}{4R_f} \tag{2.78}$$

because, since the overdensity is compensated, M is also equal to $(4/3)\pi R_f^3 \rho_f$. Without the time dependent term added in ϕ for $r \geq R_f$ (2.74) [38], it would not have been possible for the gravitational potential in the void region $V_g(r)$ to match both the boundary condition at $r = R_c$ and the one at $r = R_f$.

With these conditions, requiring that V is C^1, we find the following unique solution [38]

$$V = \begin{cases} GM\frac{r^2}{2R_c^3} & r \leq R_c(t) \\ GM\left(\frac{3}{2R_c} - \frac{1}{r}\right) & R_c(t) < r < R_f(t) \\ \frac{1}{2}GM\left(\frac{r^2}{R_f^3} - \frac{3}{2R_c} - \frac{3}{2R_f}\right) & r \geq R_f(t)\,. \end{cases} \tag{2.79}$$

Until now we have shown that the above written expression is a good solution for the gravitational potential of the matter distribution taken in consideration, and that each piece of the wavefunction is a good solution separately in its domain (i.e. $r \leq R_c$, $R_c < r < R_f$ and $r \geq R_f$). In the article by Johnston et al. it is stated that the global piecewise solution defined by (2.73) and (2.74) satisfies continuity equation in the form (2.70) at the boundaries. It is not shown, on the contrary, that it satisfies also Bernoulli equation, or equivalently that it is solution of the Schrödinger equation with quantum pressure term, at the boundaries.

Notice that without performing any calculation we can assess that the wavefunction $\psi = \alpha\, e^{i\phi/\nu}$ with α given by (2.73) and ϕ by (2.74) is a solution of the standard Schrödinger equation, even at the discontinuities R_c and R_f. Indeed, once it is damped to 0 at $r > R_{\text{ext}}$ for some $R_{\text{ext}} > R_f$ to have finite norm, it can describe a particle which we know, for example after a measurement, it does not occupy positions at radii $R_c < r < R_f$, and has a greater probability of being found at radii $r \leq R_c$ than $r \geq R_f$. Moreover Schrödinger-Newton equations without quantum pressure term are a possible extension of Schrödinger equation, as exposed in section 1.8. Then every quantum system described by a wavefunction solution of Schrödinger equation is described by the same wavefunction with SN equations. Different is the case of a classical system, as the one considered here, described by a solution of Schrödinger-Newton equations *with the quantum pressure term*, which derives from the classical nature of the system studied, which is simply a fluid. No a priori arguments seem to hold for ψ to be solution of the SN pair with Bohm quantum potential. In the appendix it is therefore checked that it actually is. In particular, at the discontinuities R_c and R_f the quantum potential is nonzero, and it contains terms proportional to the Dirac delta function and its first derivative. Because of this fact I got inspiration for my calculation from an article [33] of Griffiths, where he considers the boundary conditions on a time-independent wavefunction in the presence of a potential possessing a discontinuity (modelled as a Heaviside function). As stated by Johnston et al. [38], in the time dependent case we are studying Griffiths' solutions can't be used.

In A.2 I then referred to the calculation of Griffiths to perform a new and different one, adapted to our case.

In the following section we will use the top-hat solution of Johnston et al. to predict the evolution of a spherically symmetric primordial overdensity.

Chapter 3

Evolution of spherically symmetric compensated overdensities

Let us consider, like in the paper of Johnston et al., a spatially flat background Universe, with null cosmological constant. For $r > R_f$ let the solution $(\psi(r), V(r))$ remain the Johnston et al. one. No matter the exact density profile of a spherically symmetric compensated overdensity at $r < R_f$, it is known in literature its evolution towards a spherical collapse, as it was recalled in section 2.1. Let us here study the evolution of such an overdensity with various techniques in the Schrödinger equation approach to CDM modelling.

3.1 SN solution for a spherically symmetric compensated overdensity which does not undergo shell crossing

Let us consider as initial condition at a reference time t_i the dark matter distribution described by a spherically symmetric density profile of the form

$$\rho(r, \theta, \phi, t_i) = \begin{cases} \rho(r) & r \leq R_f(t_i) \\ \rho_f & r > R_f(t_i) \end{cases} \tag{3.1}$$

satisfying the following three requirements:

- being compensated, i.e.

$$\int_{r<R_f(t_i)} \rho(r) d^3r = \frac{4}{3}\pi \left[R_f(t_i)\right]^3 \rho_f := M \ ;$$

- being continuous in the region $r < R_f(t_i)$;
- not giving rise to shell crossing. In order to state a criterion for this requirement, let us define the quantity $m_i(r)$ to be the mass enclosed by a spherical shell of radius r at $t = t_i$

$$m_i(r) := 4\pi \int_0^r \rho(r)\, r'^2 dr' \,. \tag{3.2}$$

From equations (2.3) and (2.7), we can see that the evolution of a shell of initial radius r_i is completely specified, in absence of shell crossing, once we know the initial

mean overdensity inside it, $\bar{\rho}_i(r_i)$, from which one can easily deduce the parameter $\bar{\delta}_i$ appearing in (2.7). For our density profile

$$\bar{\rho}_i(r_i) = \frac{3\, m_i(r_i)}{4\pi r_i^3}\,. \tag{3.3}$$

As said in the last section, the turnaround of a shell takes place at [50]

$$t_{\max} = \frac{9\pi}{20}\frac{t_i}{\bar{\delta}_i}\,, \qquad\qquad r_{\max} = \frac{3}{5}\frac{r_i}{\bar{\delta}_i}\,.$$

Therefore mass shells which enclose an higher density experience turnaround before and at an inner radius than shells which enclose a lower density. In other words, shell crossing does not take place $\iff \bar{\delta}_i(r_1) \geq \bar{\delta}_i(r_2) \quad \forall\, r_1 \leq r_2$, or equivalently

$$\frac{m_i(r_1)}{r_1^3} \geq \frac{m_i(r_2)}{r_2^3} \qquad \forall\, r_1 < r_2\,. \tag{3.4}$$

If (3.4) holds, every shell starts to collapse before and at a lower radius than every external one; this fact ensures the absence of shell crossing.

In the last section we saw how the evolution of a shell is completely determined, by equation (2.1), once we know the radius of the shell and the mass m within it. In absence of shell crossing this mass is independent of time. Since the parameter appearing is the mass m and not the density ρ, the evolution of a shell is insensible of the actual shape of the density profile inside it [56]. This fact ensures that, when we consider the behaviour of a certain shell, if we suppose that, inside it, the matter m was distributed homogeneously, we obtain the same temporal evolution that we would have recalled considering the actual density profile. In other words, the evolution of a shell of radius r is influenced solely by the mean density within it, which is [56]

$$\bar{\rho} = \frac{3\, m}{4\pi r^3} = \frac{3\, m}{4\pi A^3 (1-\cos\eta)^3}\,. \tag{3.5}$$

The special case in which the average density calculated above is also the actual density is called top-hat profile. Therefore in order to compute the temporal evolution of a shell we can use the top-hat solution exposed in last section; let us see how.

Let us consider n initial radii $r_j(t_i) := r_{i,j}$, with $j = 1...n$, in the range $(0, R_f(t_i)]$. Let us choose the indices such that $r_{i,j} \leq r_{i,k} \iff j < k$. Let us moreover call for notational convenience $m_j := m_i(r_{i,j})$, i.e. the mass enclosed by the $j-$th considered shell. We know the temporal evolution of each $r_{i,j}$, which is predicted by eq. (2.3). For what just said, every shell at $r(t_i) = r_j$ behaves like a top-hat and we can use the solution exposed in last chapter to build the following SN solution ψ for a discretized version of the density profile (3.1)

$$\psi(r,t) = \alpha(r,t)\, e^{\frac{i}{\nu}\phi(r,t)}\,, \tag{3.6}$$

with

$$\alpha(r,t) = \begin{cases} \sqrt{\frac{3\Omega_1(t)H_1^2(t)}{8\pi G}} & r < r_1(t) \\ \sqrt{\frac{3\Omega_2(t)H_2^2(t)}{8\pi G}} & r_1(t) \le r < r_2(t) \\ \dots & \dots \\ \sqrt{\frac{3H_f^2(t)}{8\pi G}} & r \ge r_n(t) \end{cases} \tag{3.7}$$

$$\phi(r,t) = \begin{cases} \frac{H_1(t)r^2}{2} & r < r_1(t) \\ \frac{H_2(t)r^2}{2} - \frac{G}{2}\int_0^t \left(\frac{m_1}{r_1(t)} - \frac{m_2\, r_1^2(t)}{r_2^3(t)}\right) dt' & r_1(t) \le r < r_2(t) \\ \dots & \dots \\ \frac{H_f(t)r^2}{2} - \frac{G}{2}\int_0^t \left(\frac{m_1}{r_1(t)} + \dots + \frac{m_n}{r_n(t)} - \frac{m_2\, r_1^2(t)}{r_2^3(t)} - \frac{m_3\, r_2^2(t)}{r_3^3(t)} - \dots - \frac{M\, r_n^2(t)}{R_f^3(t)}\right) dt' & r \ge r_n(t) \end{cases} \tag{3.8}$$

$$V(r,t) = \begin{cases} Gm_1\, \frac{r^2}{2r_1^3(t)} & r \le r_1(t) \\ Gm_2\, \frac{r^2}{2r_2^3(t)} + \frac{G}{2}\left(\frac{m_1}{r_1(t)} - \frac{m_2\, r_1^2(t)}{r_2^3(t)}\right) & r_1(t) < r \le r_2(t) \\ \dots & \dots \\ GM\, \frac{r^2}{2R_f^3(t)} + \frac{G}{2}\left(\frac{m_1}{r_1(t)} + \dots + \frac{m_n}{r_n(t)} - \frac{m_2\, r_1^2(t)}{r_2^3(t)} - \frac{m_3\, r_2^2(t)}{r_3^3(t)} - \dots - \frac{M\, r_n^2(t)}{R_f^3(t)}\right) & r > r_n(t) \end{cases} \tag{3.9}$$

where

$$H_j = \frac{a_j^3}{2Gm_i(r_j)} \frac{\cos(\eta/2)}{\sin^3(\eta/2)}\,, \tag{3.10}$$

$$\Omega_j = \frac{1}{\cos^2(\eta/2)}\,, \tag{3.11}$$

$$H_f = \frac{2}{3t}\,, \tag{3.12}$$

where in turn

$$t = \frac{Gm_i(r_j)}{a_j^3}(\eta - \sin\eta)\,, \tag{3.13}$$

$$a_j = \sqrt{\frac{2Gm_i(r_j)}{r_{\max,j}}}\,, \tag{3.14}$$

$$r_{\max,j} = \frac{3r_j}{5\bar{\delta}_i(r_j)}\,. \tag{3.15}$$

In the limit $n \to \infty$ this solution describes exactly the density profile (3.1). Let us note that the conversion between η and t (3.13), depends on the shell considered, therefore for example Ω is function of r too, differently from last chapter. The integrals over time present in the expression of ϕ, which are not functions of r and therefore do not contribute to the definition of the velocity field, are added to ensure that ϕ and V satisfy Bernoulli equation. Similarly the time dependent coefficients appearing in the expression of V do not have any physical counterpart, but ensure continuity of the gravitational potential. It is important to note that the Newtonian potential proposed here is only continuous and differentiable, and not C^1 as it was required by Johnston et al.; we relaxed this requirement because in the top-hat case there are only two huge discontinuities, where the separation surface is two-dimensional and therefore effectively massless, and hence unable

to support a force acting just on it, as it would happen if $\partial V/\partial r$ were discontinuous at the boundary. In the case of a tessellation of a continuous profile as the one considered here for $r < R_f(t_i)$, this requirement can be neglected, since in the limit of large n, which we consider, the discontinuities of $\partial V/\partial r$ at the boundaries become tiny, and go to zero in the limit $n \to \infty$.

From what said in chapter 2.4, we know that the radius of each mass shell obey eq. (2.61) [38]:

$$r_j(t) = \frac{2Gm_i(r_{i,j})}{a^2} \sin^2(\eta/2)\,, \tag{3.16}$$

which, using the trigonometric identity

$$\sin^2(\eta/2) = \frac{1-\cos\eta}{2}$$

and substituting expression (3.14) for a and (3.15) for $r_{\max}$, turns out to be exactly what predicted in last section, i.e. equation (2.3).

The time conversion $t(\eta)$ happens to be the same in the two treatments too, provided that we use as reference initial time

$$t_i = \frac{2\, r_i^{3/2}}{\sqrt{30\,\delta_i\, G\, m_i(r_i)}} = \frac{H_f r_i^3}{G\sqrt{15\, m_i[m(r_i) - M]}}\,. \tag{3.17}$$

Therefore the Schrödinger-Newton approach yields the exact same result of the usual analytical treatment discussed in section 2.1: they both forecast the formation of a black hole. In literature it is well known that this is not the reality: numerical simulations [69] show that at $t \simeq 2t_{\max}$ a collapsing overdensity reaches a virialized state of equilibrium instead of forming the singularity predicted by (2.3). The reason of this discrepancy lays in fact that the just exposed treatment steams from a too strongly idealized model for the system. Indeed with a more realistic density profile, shell crossing would eventually occur, producing mixing, and therefore allowing violent relaxation to take place. The study held until now is therefore not completely satisfactory. But in order to make other predictions, the solution (3.7) (3.8) (3.9) is too analytically involved; let us therefore simplify our treatment using the free-particle approximation.

3.2 Evolution of the shells of the overdensity in the free-particle approximation

In the last section, we found expressions for the physical velocity potential $\phi(r,t)$ and the Newtonian potential $V(r,t)$ of a compensated spherically symmetric overdensity divided in shells which do not cross each other. Let us now recast the same solution in terms of comoving coordinates, and the potentials Φ and φ introduced in section 2.2.

The potential φ (defined by (2.26)) in the region $r_{j-1} < r < r_j$ with $j = 1 \dots n$ (where in the case $j = 1$, $r_0 := 0$) is

$$\varphi_j := \frac{2\mathcal{V}_j}{3a^3H_f^2} = \frac{2}{3a^3H_f^2}(V_j - V_f)\,, \tag{3.18}$$

where V_j is the Newtonian potential in the region $r_{j-1} < r < r_j$ and V_f is the one valid for $r > r_n(t)$.

The velocity potential Φ, for what stated in chapter 2, is defined as follows

$$\nabla_x \Phi := \mathbf{u} := \frac{1}{a}\left(\frac{\mathbf{v}}{\dot{a}} - \mathbf{x}\right) := \frac{1}{a}\left(\frac{\nabla_r \phi}{\dot{a}} - \mathbf{x}\right) . \tag{3.19}$$

Supposing spherical symmetry, both $\mathbf{u}$ and $\mathbf{v}$ have to be radial, therefore $\mathbf{x}$ is like that too, thus eq. (3.19) is nothing more than its projection onto the radial direction

$$\frac{\partial \Phi}{\partial r_x} = \frac{1}{a}\left(\frac{1}{\dot{a}}\frac{\partial \phi}{\partial r} - r_x\right) , \tag{3.20}$$

where r_x is the radial coordinate of a system of comoving spherical coordinates (r_x, θ_x, ϕ_x). Equation (3.20) is solved by the following potential, as always defined up to the addition of a function of time only

$$\phi = H_f \frac{r^2}{2} + a^2 \dot{a} \Phi \, . \tag{3.21}$$

Let us now study the evolution of the shells in which we divided the profile (3.1) in the free particle approximation. Let us start form the matter distribution (3.7):

$$\alpha(r_x, a) = \begin{cases} \sqrt{\frac{3\Omega_1(a) H_1^2(a)}{8\pi G}} & r_x < r_{x,1}(a) \\ \sqrt{\frac{3\Omega_2(a) H_2^2(a)}{8\pi G}} & r_{x,1}(a) \leq r_x < r_{x,2}(a) \\ \dots & \\ \sqrt{\frac{3H_f^2(a)}{8\pi G}} & r_x \geq r_{x,n}(a) \, , \end{cases} \tag{3.22}$$

where $r_{x,j} = r_j/a$. Using the notation introduced in section 2.2, the free-particle approximation prescribes $\tilde{V} = 0$ and therefore, as we saw, Poisson equation provides the relationship (2.46) between the amplitude and phase of the wavefunction $\Psi := \chi \exp(i\Phi/\nu)$ [72]:

$$\nu \nabla_x^2 [\arg(\Psi)] + \frac{1}{a}(|\Psi|^2 - 1) = 0 \, .$$

In the j-th shell this equation prescribes

$$\nabla_x^2 \Phi_j = -\frac{\bar{\delta}_j(a)}{a} = -\frac{3\Omega_j H_j^2 - 8\pi G \rho_f}{8\pi G a \, \rho_f} \, , \tag{3.23}$$

where the mean density contrast $\bar{\delta}_i$ is defined by (2.6). Since the Laplacian of Φ_j is a function of the time coordinate only, in our spherically symmetric system the velocity potential becomes

$$\Phi_j(r_x, a) = -\frac{\bar{\delta}_j(a)}{a} \, \frac{r_x^2}{6} \, . \tag{3.24}$$

Let us now address the question: what gravitational potential are we considering is acting on the j-th shell when we perform the free particle approximation? We know that, to realize $\tilde{V} = 0$, the following relation must hold

$$\varphi_j = -\Phi_j \, ; \tag{3.25}$$

which is, plugging expressions (3.24) and (3.23) for Φ_j and (3.18) for φ_j,

$$\frac{2}{3a^3 H_f^2}(V_j - V_f) = \frac{3\Omega_1 H_1^2 - 8\pi G \rho_f}{48\pi G a \, \rho_f} r_x^2 \, ,$$

which gives for the gravitational potential of the j-th shell

$$V_j = \frac{3\Omega_1 H_1^2 - 8\pi G\rho_f}{12} r^2 + V_f \,.$$

Making use of (3.9) and getting rid of additive factors functions of time only, we can write the Newtonian potential V_j in the following more transparent form

$$\begin{aligned} V_j &= \left(\frac{3\Omega_1 H_1^2 - 8\pi G\rho_f}{12} + \frac{GM}{2R_f^3(t)} \right) r^2 = \\ &= \left(\frac{\Omega_1 H_1^2}{4} - \frac{2\pi G\rho_f}{3} + \frac{2\pi G\rho_f}{3} \right) r^2 = \\ &= \frac{\Omega_1 H_1^2}{4}\, r^2 = \\ &= \frac{2\pi G}{3}\rho_j r^2 \,. \end{aligned}$$

This potential should be confronted with the exact gravitational potential acting on the shell, as prescribed by (3.9):

$$V_{j,\text{exact}} = G m_j \frac{r^2}{2r_j^3(a)} = \frac{2\pi G}{3}\rho_j r^2 \,. \tag{3.26}$$

Therefore the gravitational potential considered by the free particle approximation to act on the j-th shell is the exact one.
The difference of the approximated approach respect to the exact one, lays in the velocity potential Φ. We will deepen the study of this diversity later (in section 3.5), by considering, for a specific density profile, the difference between the two potentials as a perturbation to the study held here.

With (3.22) and (3.24) we can write the wavefunction describing the j-th shell in the free-particle approximation at some initial reference time a_i

$$\Psi_j(r_x, a_i) = \frac{\alpha_j(a_i)}{\sqrt{\rho_f(a_i)}}\, e^{\frac{i}{\nu}\Phi_j(r_x, a_i)} \,. \tag{3.27}$$

Let us now compute its temporal evolution, as it is prescribed by the free-particle Schrödinger equation [72]

$$i\nu \frac{\partial \Psi_j}{\partial a} = -\frac{\nu^2}{2}\nabla_x^2 \Psi_j \,, \tag{3.28}$$

the solution of which can be written as [**?**]

$$\Psi_j(r_x, a) = \int G(r_x, a|q, a_i)\, \Psi_j(q, a_i)\, dq \,, \tag{3.29}$$

where G is the free particle propagator, given by [**?**] [61]

$$G(r_x, a|q, a(t_i)) = [2\pi i\nu\Delta a]^{-1/2} e^{\frac{i}{\nu}\frac{(r_x - q)^2}{2\Delta a}} \,, \tag{3.30}$$

where we defined $\Delta a := a - a(t_i)$. Therefore

$$\Psi_j(r_x, a) = \int_{r_{i,j-1}/a}^{r_{i,j}/a} [2\pi i\nu\Delta a]^{-1/2} e^{\frac{i}{\nu}\frac{(r_x - q)^2}{2\Delta a}}\, \frac{\alpha_j(a_i)}{\sqrt{\rho_f(a_i)}}\, e^{\frac{i}{\nu}\Phi_j(q, a_i)}\, dq \,, \tag{3.31}$$

where $r_{i,j-1}$ and $r_{i,j}$ are the radii which delimit the shell at the initial time a_i.

Plugging (3.24), (3.31) is equivalent to

$$\begin{aligned}\Psi_j(r_x,a) &= \frac{1}{\sqrt{2\pi i\nu\Delta a}}\frac{\sqrt{\rho_j(a_i)}}{\sqrt{\rho_f(a_i)}}\int_{r_{i,j-1}/a}^{r_{i,j}/a} e^{\frac{i}{\nu}\left[\frac{(r_x-q)^2}{2\Delta a}+\Phi_j(q,a_i)\right]}\,dq \\ &= \frac{\sqrt{\chi_j(a_i)}}{\sqrt{2\pi i\nu\Delta a}}\int_{r_{i,j-1}/a}^{r_{i,j}/a} e^{\frac{i}{\nu}\left[\frac{(r_x-q)^2}{2\Delta a}-\frac{\bar\delta_j(a_i)}{6a_i}\,q^2\right]}\,dq\,. \end{aligned} \tag{3.32}$$

In the case of thin shell, in particular in the limit $n\to\infty$ where n is the number of shells in which we divided our profile (3.1), the amplitude of the shell becomes infinitesimal and the integral in (3.32) can be computed by its integrand multiplied by the infinitesimal thickness of the shell $r_{i,j}/a - r_{i,j-1}/a = dr_{x,i}$. In a more realistic case in which n is large but finite, we can take this passage as an approximation and define $\delta r_{x,i} := r_{i,j}/a - r_{i,j-1}/a$. The result is as follows

$$\Psi_j(r_x,a) = \frac{\sqrt{\chi_j(a_i)}}{\sqrt{2\pi i\nu\Delta a}}\,\delta r_{x,i}\,e^{\frac{i}{\nu}\left[\frac{(r_x-r_{x,i})^2}{2\Delta a}-\frac{\bar\delta_j(a_i)}{6a_i}\,r_{x,i}^2\right]}\,. \tag{3.33}$$

In order to understand the physics of this solution, let us rewrite it by completing the square at the exponential. The calculation reported in the appendix leads to the following, more transparent, result:

$$\Psi_j(r_x,a) = \delta r_{x,i}\,\frac{\sqrt{\chi_j(a_i)}}{\sqrt{2\pi i\nu\Delta a}}\,e^{\frac{i}{\nu}\frac{\bar\delta_j(a_i)}{2\,\Delta a\,\bar\delta_j(a_i)-6a_i}r_x^2}e^{\frac{i}{2}\left(\frac{r_x-\mu}{\sigma}\right)^2} \tag{3.34}$$

if one defines

$$\mu(r_{x,i},\Delta a) = r_{x,i}\left(1-\frac{\Delta a}{a_i}\,\frac{\bar\delta_j(a_i)}{3}\right)\,, \tag{3.35}$$

$$\sigma(\Delta a) = \sqrt{\nu\left[\Delta a-\frac{(\Delta a)^2}{a_i}\,\frac{\bar\delta_j(a_i)}{3}\right]}\,. \tag{3.36}$$

This is the result for the evolution of a shell of a spherically symmetric matter configuration in the free-particle approximation of the Schrödinger equation approach to cosmic structure formation.

Let us now interpret it. Looking at (3.36) we find that for $a\to a_i^+$, $\sigma\to 0^+$ and eq. (3.53) tells us that $\Psi_j(r_x,a_i)$ in the thin shell case (3.34) becomes, as it should, proportional to a Dirac delta peaked at $\mu(r_{x,i},\Delta a=0) = r_{x,i}$ where $r_{x,i}$ in the thin shell case represents the initial position of the shell.

The evolution, for $\Delta a>0$, is more complicated to study, since $\Psi_j(r_x,a)$ has an oscillating behaviour, and is different in the Zel'dovich approximation, which is recovered in the $\nu\to 0$ limit of free-particle approximation, and in the adhesion one, realized by a finite value of ν. For $\Delta a>0$, we can map the regions in which the matter density is important and those in which it is negligible: the latter are those in which the wavefunction is rapidly oscillating. Indeed since the first work proposing to use SN equations to model collisionless self gravitating dark matter by Widrow and Kaiser [81], and also later in many other papers, like [21] and [29], the density in phase space $f(\mathbf{r},\mathbf{p},t)$ is not obtained by simply taking the modulus squared of the solution ψ of SN equations, but it is defined as

$$f(\mathbf{r},\mathbf{p},t) := |\psi_H(\mathbf{r},\mathbf{p},t)|^2 \tag{3.37}$$

where $\psi_H(\mathbf{r}, \mathbf{p}, t)$ is a coarse-grained wavefunction, which can be obtained by using for smoothing the Husimi representation, which is a windowed Fourier transform. In one dimension ψ_H reads

$$\psi_H(r, p, t) = \int dy\, K_H(r, y, p)\psi(y)\,, \tag{3.38}$$

with the Husimi kernel

$$K_H(r, y, p) = \frac{\exp\left[-\frac{(r-y)^2}{4\epsilon^2} - \frac{i}{\hbar}py\right]}{(2\pi\hbar)^{1/2}(2\pi\epsilon^2)^{1/4}}\,, \tag{3.39}$$

where ϵ has units of length and roughly gives the resolution in position space. As it is clear from simulations performed for example in [29], the matter density in regions in which ψ is rapidly oscillating is the modulus squared of the average of ψ in the region. Since the complex exponentials in (3.34) can be seen as complex superpositions of sines and cosines, their average on a length ϵ significantly greater than their wavelength λ is zero, therefore matter density is negligible in areas in which $\lambda \ll \epsilon$.

Another way, less rigorous but more fundamental, to approach the fact that regions in which Ψ_j is oscillating on smaller length scales are those in which matter density is closer to zero, is the following. Consider a particle in a position eigenstate $|x_i\rangle = \delta(x - x_i)$ and compute its temporal evolution by means of eq. (3.29). It is easy to deduce that the wavefunction at generic time t is nothing more than the propagator. As it is well known in literature, regions in which the propagator oscillates with higher frequencies are less likely to be crossed by the particle[1] in its evolution than regions in which it has a lower frequency of oscillation; the classical path is indeed given by the stationary points of the phase [61]. For our particle initially in a position eigenstate, asking what is the probability that it passes in its evolution by position $\mathbf{x}$ at time t, happens to be the same as asking what is the probability to find the particle at $\mathbf{x}$ at time t if a measure is performed. Therefore we expect the probability amplitude to be negligible in highly oscillating areas, and vice versa to be important near the stationary points of the phase of the propagator.

In (3.34) in particular there are two complex exponentials to consider, in order to study where in spacetime the wavefunction is rapidly or slowly oscillating. In the first one

$$e^{\frac{i}{\nu}\frac{\bar{\delta}_j(a_i)}{2\,\Delta a\,\bar{\delta}_j(a_i) - 6a_i} r_x^2} \tag{3.40}$$

the term r_x^2, and therefore the spatial dependence of the factor, has no physical meaning. It indeed tells us that the frequency of oscillation of $\Psi(r_x, a)$ increases proportionally to r_x^2, but the volume element to which a certain coordinate r_x refers to is

$$dV = r_x^2 \sin\theta_x\, d\theta_x\, d\phi_x\, dr_x$$

and therefore it scales as r_x^2; thus it has only a geometrical meaning: it would ensure, in absence of other terms, a constant wavelength throughout all space. The effects of the factor (3.40) are therefore homogeneous in space, but they depend on time:, in a way that depends on the sign of

$$\bar{\delta}_j(a_i) = \frac{2G}{H_f^2(a_i)}\left(\frac{m_j}{r_j^3(a_i)} - \frac{M}{R_f^3(a_i)}\right)\,.$$

[1] In saying so rigorously I would implicitly suppose that quantum particles possess trajectories in their evolution; this is never true for example in some versions of Copenhagen interpretation of quantum mechanics, and in the modal one it is only true if the position is part of the complete set of commuting observables simultaneously defined. In truth I am not supposing one particular interpretation, I am only using what an Fraassen calls *the scientific image*: I am writing *as if* particles would have trajectories, in order to think, and convey to the reader an image which leads to correct results.

If the region enclosed by the shell is initially overdense respect to the background, then $m_j/r_j^3(a_i) > M/R_f^3(a_i)$ and $\bar{\delta}_j(a_i) > 0$. In this case, as time flows, initially the factor (3.40) decreases the wavelength of the oscillations, and therefore the areas in which $\lambda \ll \epsilon$ grow, for a fixed ϵ in the Husimi transform. In other words in this case the factor reduces, over time, the area in comoving coordinates occupied by the matter distribution.

In the case of an underdense region, vice versa, $m_j/r_j^3(a_i) < M/R_f^3(a_i)$ and $\bar{\delta}_j(a_i) < 0$. As time flows the factor (3.40) increases the wavelength of the oscillations, enlarging the area in comoving coordinates occupied by the matter distribution.

The second complex exponential appearing in (3.34) is

$$e^{\frac{i}{2}\left(\frac{r_x-\mu}{\sigma}\right)^2} \tag{3.41}$$

with

$$\mu(r_{x,i}, \Delta a) = r_{x,i}\left(1 - \frac{\Delta a}{a_i}\frac{\bar{\delta}_j(a_i)}{3}\right), \tag{3.42}$$

$$\sigma(\Delta a) = \sqrt{\nu\left[\Delta a - \frac{(\Delta a)^2}{a_i}\frac{\bar{\delta}_j(a_i)}{3}\right]}. \tag{3.43}$$

This factor tells us that the regions in which the oscillations have a lower frequency, hence the matter density is higher, are the ones near $\mu(\Delta a)$, in a range defined by $\sigma(\Delta a)$. At $a = a_i$ (i.e. $\Delta a = 0$), we already saw that the shell is peaked at $r_x = r_{x,i}$, as it should. When times flows, i.e. for $\Delta a > 0$, the shell migrates towards $r_x = 0$, determining a spherical collapse, if (and only if) $\bar{\delta}_j(a_i)$ is positive, i.e. if the shell encloses initially a region overdense respect to the background. On the contrary, μ moves in the direction of growing r_x if the inner region is initially underdense respect to the background, making matter dispersing away. Overdense regions therefore collapse and underdense ones become more and more void. Posing $\mu(\Delta a) = 0$ we can figure out that perturbations collapse at a time coordinate

$$\frac{\Delta a_{\text{coll}}}{a_i} = \frac{3}{\bar{\delta}_j(a_i)}, \tag{3.44}$$

which is positive for an overdensity and negative for an underdensity. Indeed a spherical expansion can be seen as a time reversed collapse. Expression (3.44) shows also that slighter overdensities collapse later than denser ones. As a consistency check, this value (3.44) can be confronted with the value of the scale factor at shell crossing prescribed by Zel'dovich approximation [17]:

$$a_{\text{sc}} = -\frac{1}{\lambda_{e_i}} \tag{3.45}$$

where λ_{e_i} is the eigenvalue relative to the eigenvector which generate the direction e_i which is collapsing.

For the case we are studying, the deformation tensor for the j-th shell is (for the calculation see the appendix)

$$d_{kl} = \frac{\partial^2 \Phi_j}{\partial q_k \partial q_l} = -\frac{\bar{\delta}_j(a_i)}{3a_i}\,\mathbb{I}_{3\times 3} \tag{3.46}$$

where $\mathbb{I}_{3\times 3}$ denotes the three-dimensional identity matrix. Therefore collapse happens at the same instant in all the three spatial directions, as it is required by spherical symmetry, and equation (3.45) prescribes that shell crossing happens at time coordinate

$$a_{\text{sc}} = -1/\left[-\frac{\bar{\delta}_j(a_i)}{3a_i}\right],$$

but since shell crossing happens exactly at the collapse for our distribution, this is precisely the same result stated in (3.44).
The form (3.46) for the deformation tensor implies also that Zel'dovich approximation is not exact, since $\lambda_2 \neq 0 \wedge \lambda_3 \neq 0$ and the quantity (2.40) reads (for the calculation see the appendix)

$$\tilde{\delta} = -\frac{a^2}{a_i^2}\frac{\bar{\delta}_j^2(a_i)}{3} - \frac{2}{27}\frac{a^3}{a_i^3}\bar{\delta}_j^3(a_i)\,.$$

The evolution computed until now is in comoving coordinate space: in physical ones the peak of the matter distribution of the j-th shell has the following evolution in time

$$\begin{aligned} r_{\text{peak}}(a) &= a\mu(\Delta a) = \\ &= r_{x,i}\left(a - \frac{a\Delta a}{a_i}\,\frac{\bar{\delta}_j(a_i)}{3}\right) = \\ &= r_{x,i}\left(a_i + \Delta a - (a_i+\Delta a)\Delta a\,\frac{\bar{\delta}_j(a_i)}{3a_i}\right) = \\ &= r_i + r_{x,i}\left[\Delta a\left(1 - \frac{\bar{\delta}_j(a_i)}{3}\right) - (\Delta a)^2\,\frac{\bar{\delta}_j(a_i)}{3a_i}\right]. \end{aligned} \tag{3.47}$$

Let us study the sign of the coefficient of the addendum linear in Δa:

$$\left(1 - \frac{\bar{\delta}_j(a_i)}{3}\right) > 0 \quad \Longleftrightarrow \quad \bar{\delta}_j(a_i) < 3\,. \tag{3.48}$$

Therefore the evolution of the peak of the matter distribution of a shell can be of three types depending on the initial mean value of the density contrast inside the shell $\bar{\delta}_j(a_i)$:

- $\bar{\delta}_j(a_i) < 0$
  in this case both the coefficients of the terms linear and quadratic in Δa, in (3.47), are positive, therefore the peak of the shell increase its radial coordinate indefinitely and the shell expands forever.

- $0 < \bar{\delta}_j(a_i) < 3$
  in this case the coefficient of the linear term in (3.47) is positive, while the one of the quadratic term is negative. Therefore initially, i.e. for small values of Δa, the shell expands, then it turns around and for larger values of Δa the quadratic term dominates and the shell collapses. The turn around time coordinate Δa_{ta} can be computed as follows

$$\begin{aligned} \left.\frac{dr_{\text{peak}}}{dt}\right|_{t_{\text{ta}}} &= 0 \\ \left.\frac{dr_{\text{peak}}}{d(\Delta a)}\right|_{(\Delta a)_{\text{ta}}} \left.\frac{d(\Delta a)}{dt}\right|_{t_{\text{ta}}} &= 0 \\ r_{x,i}\left[1 - \frac{\bar{\delta}_j}{3} - (\Delta a)_{\text{ta}}\,\frac{2\bar{\delta}_j}{3a_i}\right]\frac{2}{3\sqrt{a_{\text{ta}}}} &= 0 \\ 1 - \frac{\bar{\delta}_j}{3} - (\Delta a)_{\text{ta}}\,\frac{2\bar{\delta}_j}{3a_i} &= 0 \\ \frac{(\Delta a)_{\text{ta}}}{a_i} &= \frac{3 - \bar{\delta}_j(a_i)}{2\,\bar{\delta}_j(a_i)} \end{aligned} \tag{3.49}$$

  The denominator in this range of density contrast is positive, therefore the numerator needs to be positive too in order for the collapse to happen in the future; imposing this inequality we recover again the constraint $\delta_j < 3$.

The estimation (3.49) can moreover be confronted with (2.8), which gives the turnaround time of a top-hat overdensity of initial density contrast δ_i:

$$\left(\frac{t_{\rm ta}}{t_i}\right)_{\rm exact} = \frac{9\pi}{20}\frac{1}{\delta_i}\,.$$

Since in a matter dominated Universe $a \propto t^{2/3}$, the just written expression implies

$$\left(\frac{a_{\rm ta}}{a_i}\right)_{\rm exact} = \left(\frac{9\pi}{20}\frac{1}{\delta_i}\right)^{2/3}\,. \tag{3.50}$$

On the other hand, the result (3.49) of free-particle approximation implies

$$\left(\frac{a_{\rm ta}}{a_i}\right)_{\text{free-particle}} = \frac{3}{2}\frac{1}{\bar{\delta}(r_i)} + \frac{1}{2}\,. \tag{3.51}$$

Because of Birkhoff theorem, (3.50) and (3.51) are different estimations of the same quantity. The discrepancy is due to the approximation introduced to calculate (3.51). In particular (3.50) and (3.51) both tend to infinity when the density contrast tends to 0 (a region which is not overdense never collapse), but while (3.50) prescribes that every overdensity initially expands and then turns around and collapse, (3.51) forecasts this behaviour only for shells that enclose an overdensity with average density contrast inferior to 3.

After turnaround, the collapse ends in the formation of a singularity, as I will soon clarify. As previously mentioned, simulations [69] show that collapse happens at $t_{\rm coll} \simeq 2t_{\rm ta}$; with (3.44) and (3.49) we can compute the following ratio

$$\frac{t_{\rm coll}}{t_{\rm ta}} = \left(\frac{(\Delta a)_{\rm coll}}{(\Delta a)_{\rm ta}}\right)^{3/2} = \left(\frac{6}{3-\bar{\delta}_j(a_i)}\right)^{3/2} \tag{3.52}$$

where in the first step I supposed a matter dominated Universe. Hence for small values of $\bar{\delta}_j(a_i)$, as the ones which describe primordial overdensities, $t_{\rm coll}$ does not differ too much from $2t_{\rm ta}$.

- $\bar{\delta}_j(a_i) > 3$
  in this case both the coefficients in (3.47) are negative, therefore the shell directly contracts, till it forms a singularity.

While the evolution of the peak of the matter distribution of a shell is insensible of the value of the parameter ν chosen, the details on how matter is disposed around that peak differ in Zel'dovich ($\nu \to 0$ case) and adhesion approximation (finite ν case).

Zel'dovich approximation When considering smaller values for the parameter ν, the exponential (3.40) sharpens the matter distribution, making thinner the structure formed by the j-th shell. The second exponential (3.41) is affected by the limit $\nu \to 0$ by the decrease of $\sigma(\Delta a)$. In particular, recalling the following definition of the Dirac delta function as a limit of oscillating functions [82]

$$\delta(x) := \lim_{\sigma\to 0^+} \frac{1}{\sqrt{2\pi i\sigma}} e^{\frac{i}{2}\frac{x^2}{\sigma}}\,. \tag{3.53}$$

we directly see that the distribution becomes proportional to a Dirac delta peaked at $r_x = \mu(\Delta a)$.

A limit of Zel'dovich approximation is that, in the collapsing case $\bar{\delta}_j(a_i) > 0$, nothing prevents μ of eq. (3.42) to become negative. This is mathematically erroneous, but apart from that, it would mean physically that a particle coming from a certain direction (θ_x, ϕ_x), once it reaches $r_x = 0$ it continues straight in the opposite direction $(-\theta_x, -\phi_x)$. This fact could seem reasonable but we have to recall that spherical symmetry ensures that when this particle reaches $r_x = 0$, it crosses the trajectories of all the other particles forming the shell from which it comes from; this means that a shell which before occupied an extended region is now collapsed into a caustic. Adhesion approximation rightfully predicts the stability of caustics; let us study what the arbitrary ν case of free-particle approximation, which is proposed as similar to adhesion approximation in [72], forecasts.

Adhesion approximation If ν can take arbitrary high values, the first complex exponential (3.40) prescribes that the structures formed are generally thicker than in the low ν case, and the second one (3.41) predicts that matter density were non negligible in a range defined by $\sigma(\Delta a)$. This factor, (3.43), is monotonously growing with Δa, hence the shell of an overdensity, while collapsing towards lower r_x, expands in thickness. The behaviour prescribed by the second exponential (3.41) is in accordance with what stated by Garny et al. in [29], that the quantum pressure term prohibits the formation of structures on length scales shorter than

$$x \lesssim \sqrt{\frac{\nu}{H_f}}\,. \tag{3.54}$$

Indeed in an EdS matter dominated Universe, since $H_f = 2/(3t)$, x is proportional to $t^{1/2}$; therefore every shell has to spread in time, in order to avoid the formation of structures of increasing minimal length scale. This behaviour is also in accordance with the result of simulations performed in [72].
While the constraint (3.54) is respected for the evolution of an underdense region, an overdensity eventually collapses to a singularity, as we will see right after, so the constraint is eventually violated, for the compelling effect of the exponential (3.40).

To understand what finally the free-particle approximation predicts for our spherical perturbation (3.1), it is important to notice that the constraint (3.4), which ensures the absence of shell crossing, coupled to the requirement for the perturbation of being compensated, forces that perturbation to be an overdensity.
Therefore both in the small ν case as well as in the arbitrary ν one, the free-particle approximation predicts an initial expansion, followed by a turnaround and a collapse, which leads to the formation of a singularity at $r = 0$ at the time coordinate $\Delta a = 3a_i/\bar{\delta}_j(a_i)$. In the arbitrary ν case the shell spreads in space during the collapse, while in the analogous of Zel'dovich approximation it remains thinner, but the final state is identical in the two cases: the exponential (3.40) in both cases at $\Delta a = 3a_i/\bar{\delta}_j(a_i)$ makes non negligible the matter density only at the precise stationary point of the other exponential (3.41), which is

$$\mu(\Delta a_{\text{coll}}) = 0\,.$$

Neither of the two assumptions on the value of the parameter ν are unfortunately able to model the stability of caustics.

3.3 Global evolution of the overdensity in Zel'dovich approximation

Another legitimate approach to the study of the evolution of the overdensity (3.1), is the one which considers it globally, without decomposing the profile in shells.

Since the spherically symmetric overdensity (3.1) is compensated, Birkhoff theorem ensures that the evolution of the region at $r \geq R_f(t_i)$ is not affected by the region at $r < R_f(t_i)$, and therefore in the region external to $R_f(t_i)$ matter just dilutes scaling like $\rho_f \propto a^{-3} \propto t^{-2}$ (where the last passage holds in a matter dominated Universe). Therefore let us restrict our study at the region $r < R_f$; here, using the coordinates $(\mathbf{x}, a)$, we can define

$$\Psi(r_x, a) = \sqrt{\frac{\rho(r_x, a)}{\rho_f(a)}} e^{\frac{i}{\nu}\Phi(\mathbf{x},a)}\,, \tag{3.55}$$

and the evolution of the overdensity will be predicted by the Schrödinger-Newton equations (2.31) (2.32) [**?**]

$$\begin{aligned} i\nu\frac{\partial\Psi}{\partial a} &= -\frac{\nu^2}{2}\nabla_x^2\Psi + \tilde{V}\psi + \frac{\nu^2}{2}\frac{\nabla_x^2 R}{R} \\ \nabla_x^2\left[\tilde{V} + \frac{3i\nu}{4a}\ln\left(\frac{\Psi}{\Psi^*}\right)\right] &= \frac{3}{2a^2}(|\Psi|^2 - 1)\,. \end{aligned}$$

Since the potential is time dependent we are not allowed to write the time independent Scrödinger equation, and therefore the system is solvable only numerically. Let us therefore make use of approximations, and in particular of the free-particle approximation. As done in section 3.2, following [72] let us consider the quantum pressure term into Bernoulli equation and put $\tilde{V} = 0$. With this assumptions, Poisson equation provides us with an expression (2.46) for the Laplacian of the velocity potential at $a = a_i$ [72]

$$\nabla_x^2\Phi(\mathbf{x}, a_i) = -\frac{\delta(r_x, a_i)}{a_i} \tag{3.56}$$

where as usual $\delta(r_x, a) := [\rho(r_x, a) - \rho_f(a)]/\rho_f(a)$. Restricting to a zero angular momentum configuration, we can rewrite (3.56) in the following form, in order to solve it for Φ

$$\begin{aligned} \frac{1}{r_x^2}\frac{d}{dr_x}\left(r_x^2\frac{d\Phi}{dr_x}\right) &= -\frac{\delta(r_x, a_i)}{a_i} \\ r_x^2\frac{d\Phi}{dr_x} + C &= -\frac{1}{a_i}\int \delta(r'_x, a_i)\, {r'_x}^2\, dr'_x \\ \Phi + D &= -\frac{1}{a_i}\int \frac{\int \delta(r'_x, a_i)\, {r'_x}^2\, dr'_x}{r''^2_x}\, dr''_x - \int \frac{C}{{r'_x}^2} d{r'_x}^2 \\ \Phi(r_x, a_i) &= -\frac{1}{a_i}\int \frac{\int \delta(r'_x, a_i)\, {r'_x}^2\, dr'_x}{r''^2_x}\, dr''_x + \frac{C}{r_x} - D\,. \end{aligned} \tag{3.57}$$

Since D is a function of time only, it can be set to 0 without loss of generality, and C has to be set to zero too if one requires the potential not to diverge in $r_x = 0$.

With those choices of the coefficients and the definition of mean interior overdensity (2.6), Φ results

$$\Phi(r_x, a_i) = -\frac{(V/a_i^3)}{4\pi\, a_i}\int_0^{r_x} \frac{\bar{\delta}(r'_x, a_i)}{{r_x}'^2}\, dr'_x\,. \tag{3.58}$$

Let us now compute the temporal evolution of the initial configuration, described by $\Psi(r_x, a_i)$ of eq. (3.55), as it is prescribed by the free-particle Schrödinger equation (2.44), which is solved by (3.29) [**?**]:

$$\begin{aligned}\Psi(r_x, a) &= \int G(r_x, a|q, a_i)\, \Psi(q, a_i)\, dq \\ &= \int_0^{R_f/a_i} [2\pi i\nu\Delta a]^{-1/2} e^{\frac{i}{\nu}\frac{(r_x-q)^2}{2\Delta a}} \sqrt{\frac{\rho(q,a_i)}{\rho_f(a_i)}} e^{\frac{i}{\nu}\Phi(q,a_i)}\, dq \\ &= \frac{1}{\sqrt{\rho_f(a_i)\, 2\pi i\nu\Delta a}} \int_0^{R_f/a_i} \sqrt{\rho(q,a_i)}\, e^{\frac{i}{\nu}\frac{(r_x-q)^2+2\Delta a\,\Phi(q,a_i)}{2\Delta a}}\, dq\,. \end{aligned} \tag{3.59}$$

Recall that, since the profile (3.1) does not give rise to shell crossing, Zel'dovich approximation is the $\nu \to 0$ limit of the free-particle one [72]. In this limit the integral in (3.59) is dominated by the stationary points of the phase [**?**], since in all the other regions in which we are integrating, in the $\nu \to 0$ limit the phase is oscillating on a length scale $\lambda \to 0$, and therefore mediates to zero the integral. The stationary points $\bar{q}_s$ of the phase are the ones satisfying

$$\begin{aligned}\left[\frac{\partial}{\partial q}\left(\frac{(r_x-q)^2 + 2\Delta a\,\Phi\,(q,a_i)}{2\Delta a}\right)\right]_{\bar{q}_s} &= 0 \\ \left[-2(r_x-q) + 2\Delta a\,\frac{\partial}{\partial q}\Phi(q,a_i)\right]_{\bar{q}_s} &= 0 \\ r_x = \bar{q}_s + \Delta a\,\frac{\partial}{\partial q}\Phi(q,a_i)\Big|_{\bar{q}_s}&\,, \end{aligned} \tag{3.60}$$

where in the last line we solved for r_x and we recovered the Zel'dovich trajectories (2.33). This can be seen as a consistency check, that the $\nu \to 0$ limit of the free-particle approximation is effectively equal to Zel'dovich approximation. The second passage of (3.57) provides an expression for the first derivative of Φ, which can be plugged in (3.60) to obtain

$$\begin{aligned} r_x &= \bar{q}_s - \Delta a\,\frac{1}{a_i\, q^2}\int \delta(r'_x, a_i)\, {r'_x}^2\, dr'_x\Big|_{\bar{q}_s} \\ &= \bar{q}_s + \frac{1}{3}\frac{\Delta a}{a_i}\bar{q}_s - \frac{\Delta a}{a_i}\,\frac{1}{\rho_f}\,\frac{1}{\bar{q}_s^2}\int_0^{\bar{q}_s} \rho(r'_x, a_i)\, {r'_x}^2\, dr'_x\,. \end{aligned} \tag{3.61}$$

Therefore in free-particle approximation a fluid element that initially, at time coordinate a_i, occupied a position at radial comoving coordinate $\bar{q}_s$ is mapped, after a time Δa, in the position r_x prescribed by (3.61).

A particle of our matter distribution, initially in a position denoted by a physical radial coordinate $r = a_i\bar{q}_s := r_i$, evolves therefore in Zel'dovich approximation in the following way (multiple writings of the same quantity are presented, because they highlight different

aspects of the evolution):

$$
\begin{aligned}
r(r_i,a) = a r_x(\bar{q}_s,a) &= \frac{a}{a_i} r_i - a\Delta a\,\frac{1}{a_i^2 r_i^2}\int_0^{r_i} \delta(r',a_i)\, r'^2\, dr' = \\
&= \frac{a}{a_i} r_i + \frac{1}{3}\frac{a\Delta a}{a_i^2} r_i - a\,\Delta a\, a_i\,\frac{1}{\rho_f}\,\frac{1}{r_i^2}\int_0^{r_i/a_i} \rho(r'_x,a_i)\, {r'_x}^2\, dr'_x = \\
&= a\left[\frac{2}{3}\frac{1}{a_i} r_i + a_i^2\,\frac{1}{\rho_f}\,\frac{1}{r_i^2}\int_0^{r_i/a_i} \rho(r'_x,a_i)\, {r'_x}^2\, dr'_x\right] + \\
&+ a^2\left[\frac{1}{3}\frac{1}{a_i^2} r_i - a_i\,\frac{1}{\rho_f}\,\frac{1}{r_i^2}\int_0^{r_i/a_i} \rho(r'_x,a_i)\, {r'_x}^2\, dr'_x\right] = \\
&= r_i + \Delta a\left[\frac{4}{3}\frac{1}{a_i} r_i - a_i^2\,\frac{1}{\rho_f}\,\frac{1}{r_i^2}\int_0^{r_i/a_i} \rho(r'_x,a_i)\, {r'_x}^2\, dr'_x\right] + \\
&+ (\Delta a)^2\left[\frac{1}{3}\frac{1}{a_i^2} r_i - a_i\,\frac{1}{\rho_f}\,\frac{1}{r_i^2}\int_0^{r_i/a_i} \rho(r'_x,a_i)\, {r'_x}^2\, dr'_x\right] .
\end{aligned}
\tag{3.62}
$$

We can see two compelling effects taking place: for $\Delta a > 0$, the terms

$$
\frac{4}{3}\frac{\Delta a}{a_i} r_i + \frac{1}{3}\frac{(\Delta a)^2}{a_i^2} r_i \tag{3.63}
$$

make r grow and represent the effect of the expansion of the Universe, while

$$
-(a_i + \Delta a)\,\Delta a\, a_i\,\frac{1}{\rho_f}\,\frac{1}{r_i^2}\int_0^{r_i/a_i} \rho(r'_x,a_i)\, {r'_x}^2\, dr'_x \tag{3.64}
$$

makes, as time flows, r decrease, and represents the effect of the gravitational interaction of the element of the fluid considered with the rest of the matter distribution constituting the overdensity.

Initially, i.e. for small values of Δa, the leading term in (3.62) is the linear one in Δa, and therefore the behaviour of a fluid element in this period is determined by the sign of the coefficient of Δa:

$$
\begin{aligned}
\left[\frac{4}{3}\frac{1}{a_i} r_i - a_i^2\,\frac{1}{\rho_f}\,\frac{1}{r_i^2}\int_0^{r_i/a_i} \rho(r'_x,a_i)\, {r'_x}^2\, dr'_x\right] &> 0 \\
\frac{1}{3}\frac{1}{\rho_f}\frac{a_i^3}{\frac{4}{3}\pi r_i^3} 4\pi \int_0^{r_i/a_i} \rho(r'_x,a_i)\, {r'_x}^2\, dr'_x &< \frac{4}{3} \\
\frac{\bar{\rho}(r<r_i,a_i)}{\rho_f} &< 4 \\
\bar{\delta}(r_i,a_i) &< 3\,.
\end{aligned}
$$

Hence fluid elements placed at radii r_i inside which the density contrast is lower than 3 initially drift towards larger radii, while an element at a radius inside which the density contrast exceeds the critical value 3 initially decreases its radius.

Later, for larger values of Δa, the higher power of this parameter become dominant in (3.62) and therefore the behaviour of a fluid element initially at r_i is determined by the sign of the coefficient of $(\Delta a)^2$:

$$
\left[\frac{1}{3}\frac{1}{a_i^2} r_i - a_i\,\frac{1}{\rho_f}\,\frac{1}{r_i^2}\int_0^{r_i/a_i} \rho(r'_x,a_i)\, {r'_x}^2\, dr'_x\right] > 0 \iff \bar{\delta}(r_i,a_i) < 0\,.
$$

Hence a fluid element on the edge (or inside) of an underdensity will drift towards larger radii, and one placed on the edge (or inside) of an overdensity will eventually move towards smaller radii.

In summary, in perfect accordance with what previously stated in section 3.2, if it exists, the central part of the overdensity for which $\bar{\delta}(r, a_i) > 3$, just collapses; the peripheral part, on the contrary, with a density contrast $\bar{\delta}(r, a_i) < 3$ initially expands. For this region too, eventually the effect of the gravitational interaction, encoded by (3.64), grows till it becomes predominant and the fluid elements of which the region is composed turn around (each one at a different time, depending on its initial radial coordinate) and collapse.

Let us compute now the turnaround time coordinate of a fluid element initially at r_i. To do so, we have to impose the condition

$$\frac{dr}{dt}(r_i, \Delta a)\bigg|_{\Delta a=(\Delta a)_{\rm ta}} = 0\,. \tag{3.65}$$

Using (3.62) and recalling that there is no shell crossing, in the appendix the following solution of (3.65) is explicitly found

$$\frac{(\Delta a)_{\rm ta}}{a_i} = \frac{3 - \bar{\delta}(r_i, a_i)}{2\bar{\delta}(r_i, a_i)}\,. \tag{3.66}$$

This equation prescribes that $(\Delta a)_{\rm ta}/a_i > 0$ (i.e. it is physically acceptable), only for $0 < \bar{\delta}(r_i, a_i) < 3$. Indeed from our previous study we know that underdensities ($\bar{\delta}(r_i, a_i) \leq 0$) never collapse, and overdensities with $\bar{\delta}(r_i, a_i) \geq 3$ do not turn around because they directly collapse, from $a = a_i$. Expression (3.66) is precisely equal to (3.49) found applying the free-particle approximation to a single shell.

An equation for the scale factor at the instant of collapse of a fluid element initially at r_i can be found instead by imposing

$$r(r_i, a)|_{\Delta a=(\Delta a)_{\rm coll}} = 0\,,$$

which is solved by (for the calculation see the appendix)

$$\frac{(\Delta a)_{\rm coll}}{a_i} = \left\{-1,\, \frac{3}{\bar{\delta}(r_i)}\right\}\,. \tag{3.67}$$

The first solution, being negative, is unphysical, while the second one, which is acceptable, is identical to the result (3.44) found in section 3.2 while applying the free-particle approximation to a shell.

We are then finally ready to compute the temporal evolution of the whole profile (3.1) under Zel'dovich approximation: it is the $\nu \to 0$ limit of (3.59). As said, the complex exponential makes more and more negligible in the integration the regions far from $\bar{q}_s$ as ν approaches zero. Let us make more rigorous this passage by explicitly computing the limit.

If we define

$$I_\nu = \int_a^b g(t) e^{\frac{i}{\nu} h(t)}\, dt\,, \tag{3.68}$$

the stationary phase approximation consists in equating I_ν with the following expression (readapted from [85] and [12]), valid for small ν, which becomes exact in the limit $\nu \to 0$

$$I(\nu) \simeq g(\bar{q}_s)\sqrt{\frac{2\pi\nu}{|h''(\bar{q}_s)|}}\exp\left\{i\left[\frac{h(\bar{q}_s)}{\nu} + \sigma\frac{\pi}{4}\right]\right\}\,, \tag{3.69}$$

where $\sigma(a) := \mathrm{sgn}(h''(\bar{q}_s))$.

Therefore

$$\lim_{\nu\to 0}\Psi(r_x,a) := \lim_{\nu\to 0}\frac{1}{\sqrt{\rho_f(a_i)\,2\pi i\nu\Delta a}}\int_0^{R_f/a_i}\sqrt{\rho(q,a_i)}\,e^{\frac{i}{\nu}\frac{(r_x-q)^2+2\Delta a\,\Phi(q,a_i)}{2\Delta a}}\,dq = \\ = \lim_{\nu\to 0}\frac{\sqrt{\rho(\bar{q}_s,a_i)}}{\sqrt{\rho_f(a_i)\,i\Delta a}}\sqrt{\frac{1}{|\nabla_q^2 f(\bar{q}_s,\Delta a)|}}\,e^{\frac{i}{\nu}\frac{(r_x-\bar{q}_s)^2+2\Delta a\,\Phi(\bar{q}_s,a_i)}{2\Delta a}}e^{i\mu\pi/4}\,, \tag{3.70}$$

where it was defined

$$f(q,\Delta a) := \frac{(r_x-q)^2+2\Delta a\,\Phi(q,a_i)}{2\Delta a}$$

and

$$\mu(q,\Delta a) := \mathrm{sgn}(\nabla_q^2 f(\bar{q}_s))\,.$$

Let us then compute the Laplacian of the phase

$$\nabla_q^2 f(q) = \frac{1}{2\Delta a}\left[\left(\frac{\partial^2}{\partial q^2}+\frac{2}{q}\frac{\partial}{\partial q}\right)(r_x-q)^2+2\Delta a\nabla_q^2\Phi(q,a_i)\right] = \\ = \frac{1}{\Delta a}\left[1-2\frac{r_x-q}{q}-\Delta a\frac{\delta(q,a_i)}{a_i}\right].$$

From (3.61) we know

$$-r_x+\bar{q}_s = \Delta a\,\frac{1}{a_i\,q^2}\int\delta(r'_x,a_i)\,{r'_x}^2\,dr'_x\Big|_{\bar{q}_s}\,,$$

which can be plugged into the following expression

$$\nabla_q^2 f(\bar{q}_s) = \frac{1}{\Delta a}\left[1+\frac{2}{\bar{q}_s}(-r_x+\bar{q}_s)-\Delta a\frac{\delta(\bar{q}_s,a_i)}{a_i}\right] = \\ = \frac{1}{\Delta a}\left\{1+\frac{2}{\bar{q}_s}\left[\Delta a\,\frac{1}{a_i\,\bar{q}_s^2}\int_0^{\bar{q}_s}\delta(r'_x,a_i)\,{r'_x}^2\,dr'_x\right]-\Delta a\frac{\delta(\bar{q}_s,a_i)}{a_i}\right\}$$

to finally obtain the desired result

$$\nabla_q^2 f(\bar{q}_s) = \frac{1}{\Delta a}\left\{1-\frac{\Delta a}{a_i}\left[-\frac{2}{\bar{q}_s^3}\int_0^{\bar{q}_s}\delta(r'_x,a_i)\,{r'_x}^2\,dr'_x+\delta(\bar{q}_s,a_i)\right]\right\}. \tag{3.71}$$

Plugging (3.71) into (3.70) we deduce

$$\lim_{\nu\to 0}|\Psi(r_x,a)|^2 = \frac{\rho(\bar{q}_s,a_i)}{\rho_f(a_i)\,\Delta a}\,\frac{1}{|\nabla_q^2 f(\bar{q}_s,a)|} = \\ = \frac{\rho(\bar{q}_s,a_i)}{\rho_f(a_i)}\,\frac{1}{\left|1-\frac{\Delta a}{a_i}\left[-\frac{2}{\bar{q}_s^3}\int_0^{\bar{q}_s}\delta(r'_x,a_i)\,{r'_x}^2\,dr'_x+\delta(\bar{q}_s,a_i)\right]\right|}\,.$$

Therefore in Zel'dovich approximation[2]

$$\chi(r_x,a) = \frac{\rho(\bar{q}_s,a_i)}{\rho_f(a_i)}\,\frac{1}{\left|1-\frac{\Delta a}{a_i}\left[-\frac{2}{\bar{q}_s^3}\int_0^{\bar{q}_s}\delta(r'_x,a_i)\,{r'_x}^2\,dr'_x+\delta(\bar{q}_s,a_i)\right]\right|}\,,$$

[2]here we are omitting the Husimi transform of Ψ because the wavefunction, in the $\nu\to 0$ limit, is no more oscillating, and as we will see it is some continuous deformation of the initial smooth profile. Therefore it would be left unchanged by a coarse graining over some reasonably small length scale ϵ.

which implies, using physical coordinates,

$$\rho(r,a) = \frac{\rho_f(a)}{\rho_f(a_i)} \frac{1}{\left|1 - \frac{\Delta a}{a_i}\left[-\frac{2}{(a_i\bar{q}_s)^3}\int_0^{a_i\bar{q}_s}\delta(r',a_i)\,r'^2\,dr' + \delta(a_i\bar{q}_s,a_i)\right]\right|}\rho(a_i\bar{q}_s,a_i)\,,$$

and thus finally

$$\rho(r,a) = \frac{a_i^3}{a^3}\frac{1}{\left|1 - \frac{\Delta a}{a_i}\left[\delta(a_i\bar{q}_s,a_i) - \frac{2}{3}\bar{\delta}(a_i\bar{q}_s,a_i)\right]\right|}\rho(a_i\bar{q}_s,a_i)\,. \tag{3.72}$$

Equation (3.72) tells us that the initial Gaussian overdensity $\rho(a_i\bar{q}_s,a_i)$ gets deformed, as time flows, by the two factors in front of it:

- $$\frac{a_i^3}{a^3}$$
  just rescales the density by taking into account the expansion of the Universe between the initial scale factor a_i and the final one a, and the fact that the density of pressureless matter scales like a^{-3} as the Universe expands;

- $$\frac{1}{\left|1 - \frac{\Delta a}{a_i}\left[\delta(a_i\bar{q}_s,a_i) - \frac{2}{3}\bar{\delta}(a_i\bar{q}_s,a_i)\right]\right|} \tag{3.73}$$
  where recall that $\bar{\delta}(a_i\bar{q}_s,a_i)$ indicates the average of the contrast $\delta(r,a_i)$ in the region $r < a_i\bar{q}_s$. The term (3.73) expresses the effect of gravitational interaction. It is the one responsible for the stretching of the profile described until now, and eventually of the collapse. As time goes on the whole factor (3.73) increase, but non homogeneously in the initial position $a\bar{q}_s := r_i$: inner regions have a larger term in square bracket and therefore grow in density faster than external ones. When the density becomes infinite (in the first place where it happens i.e. at $r = 0$), Zel'dovich approximation breaks down, because shell crossing takes place and a caustic forms.
  It is interesting to note that (3.73) is simply 1 for $r \geq R_f$, as it should since the only evolution of the density in that area is the dilution due to the expansion of the Universe.

The instant at which $\rho(r=0)$ becomes infinite provides an estimation of the collapse time of the whole overdensity. Let us compute it. The term (3.73) is not defined in $a\bar{q}_s = 0$, but we can define it there as its limit for $a\bar{q}_s \to 0$. Let us therefore compute the following quantity.

$$\begin{aligned}
&\lim_{(a_i\bar{q}_s)\to 0}\left[-\frac{2}{(a_i\bar{q}_s)^3}\int_0^{a_i\bar{q}_s}\delta(r',a_i)\,r'^2\,dr' + \delta(a_i\bar{q}_s,a_i)\right] \overset{\text{H}}{=} \\
&\overset{\text{H}}{=} \lim_{(a_i\bar{q}_s)\to 0} -\frac{2\delta(a_i\bar{q}_s,a_i)\,(a_i\bar{q}_s)^2}{3(a_i\bar{q}_s)^2} + \delta(0,a_i) = \\
&= \frac{1}{3}\delta(0,a_i)
\end{aligned}$$

where the "H" on the top of the equal sign indicates the use of the de l'Hôpital theorem. We can hence impose the instant of collapse to be the one which makes null the denominator of (3.73) for $r = 0$:

$$\begin{aligned}
1 - \frac{\Delta a_{\text{coll}}}{a_i}\frac{1}{3}\delta(0,a_i) &= 0 \\
\frac{\Delta a_{\text{coll}}}{a_i} &= \frac{3}{\delta(0,a_i)}\ ;
\end{aligned} \tag{3.74}$$

this is the same result as (3.67), and as (3.44) found in section 3.2 applying the same free-particle approximation to the shells of the density profile. Moreover the estimation (3.74) can be confronted with the exact one recalled in section 2.1

$$\frac{t_{\text{coll, exact}}}{t_i} = \frac{9\pi}{10}\frac{1}{\delta(0,a_i)}\,,$$

in the following way:

$$\frac{t_{\text{coll, Zel'dovich}}}{t_{\text{coll, exact}}} = \frac{10}{3\pi}\left(\frac{3}{\delta(0,a_i)}\right)^{1/2}\,. \tag{3.75}$$

We can see that the two expressions are similar for small enough initial overdensities, and in particular they tend to be equal for $\delta(0,a_i) \simeq 3$.

The global evolution of the overdensity in consideration therefore is as follows: inner regions, for which the condition $\delta(r_x,a_i) > 3$ is fulfilled, directly contract; regions more external initially expand and then start to contract, at later times for more external regions. The distribution therefore becomes more peaked as time goes on until at

$$\frac{\Delta a_{\text{coll}}}{a_i} = \frac{3}{\delta(0,a_i)}$$

a singularity at the origin of the coordinate system forms. This result is identical to the one of section 3.2.

In addition to confirming the previously stated results, what the study held in this section adds to our knowledge on the evolution of a spherically symmetric CDM fluctuation is that the behaviour of a small region of the perturbation, placed initially around $r = r_i$, depends (in free-particle approximation) both on the value of the initial density contrast in the region itself $\delta(r_i,a_i)$ and on $\bar{\delta}(r_i,a_i)$, which is the initial average density contrast inside a sphere of radius r_i, centred in the centre of symmetry of the configuration.

3.4 SN solution for a Gaussian overdensity

Scope of this section is to actualize the study held till now in a quite abstract fashion, by considering a specific initial density profile which meets the requirements of section 3.1.

We take as such a profile the one depicted in *figure 3.1* and defined by the following analytical expression

$$\rho(r,\theta,\phi,t_i) = \begin{cases} \frac{M}{\left(\sqrt{2\pi}\sigma\right)^3} e^{-\frac{1}{2}\left(\frac{r}{\sigma}\right)^2} & r \le R_f(t_i) \\ \rho_f & r > R_f(t_i)\,, \end{cases} \tag{3.76}$$

where, as before, $M = (4/3)\pi R_f^3\,\rho_f$.
σ can be taken arbitrary in a range for which the overdensity is not too peaked, in order to model a realistic primordial fluctuation, and at the same time the integral of the Gaussian for $r > R_f$ is negligible, to ensure the fact that the overdensity is compensated. By orders of magnitude, a good choice could be taking $3\sigma < R_f < 4\sigma$. Indeed for $R_f = 3\sigma$, $\rho(r=0,t_i)/\rho_f \simeq 7$ and the overdensity is compensated with a relative error of 0.3%; instead for $R_f = 4\sigma$, $\rho(r=0,t_i)/\rho_f \simeq 17$ but the overdensity is compensated with a relative error of 0.006%. For $R_f < \sqrt[3]{3}\,\sqrt[6]{\pi/2}\,\sigma \simeq 1.55\sigma$, (3.76) cease to describe an overdensity which eventually collapse, and describes an underdensity in the region $r < R_f$,

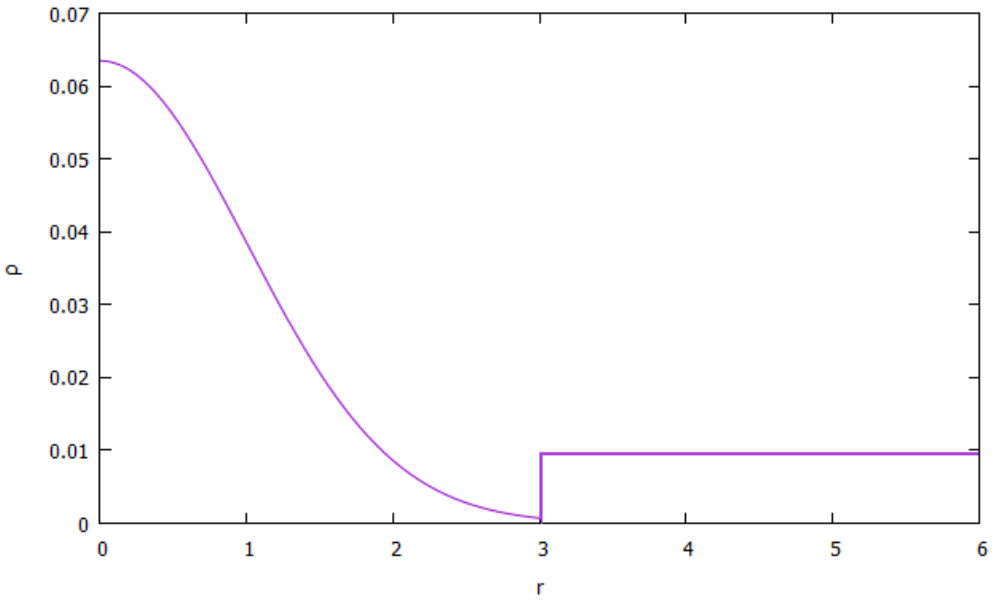

Figure 3.1: $\rho(r)$ of a spherically symmetric Gaussian compensated overdensity described by the density profile (3.76) with $M = \sigma = 1$.

which expands at a faster rate than the surroundings; in this case the perturbation is obviously not compensated.

In order to check if the overdensity described by this $\rho(r)$ is compensated, we need to calculate the following integral

$$\int_{r<R_f} \rho(\mathbf{r})\, d^3r = 4\pi \frac{M}{\left(\sqrt{2\pi}\sigma\right)^3} \int_0^{R_f} e^{-\frac{1}{2}\left(\frac{r}{\sigma}\right)^2} r^2 dr \ ; \tag{3.77}$$

in the hypothesis that the integral from R_f to ∞ was negligible, and using the fact that the integrand is even, (3.77) equals

$$\frac{M}{\sqrt{2\pi}\sigma^3} \int_{-\infty}^{+\infty} e^{-\frac{1}{2}\left(\frac{r}{\sigma}\right)^2} r^2 dr = \frac{M}{\sqrt{2\pi}\sigma^3} \sqrt{2\pi}\sigma^3 = M\,.$$

Therefore it is compensated.

The mass $m_i(r)$ enclosed by a spherical shell of radius r at $t = t_i$ reads

$$m_i(r) = \frac{M}{\sqrt{2\pi}\sigma^3} \int_0^r e^{-\frac{1}{2}\left(\frac{r'}{\sigma}\right)^2} r'^2 dr'\,. \tag{3.78}$$

Let us now check if the criterion (3.4) for the absence of shell crossing

$$\frac{m_i(r_1)}{r_1^3} > \frac{m_i(r_2)}{r_2^3} \qquad \forall\, r_1 < r_2$$

is satisfied. The first inequality is equivalent to

$$\frac{\int_0^{r_1} e^{-\frac{1}{2}\left(\frac{r'}{\sigma}\right)^2} r'^2 dr'}{r_1^3} > \frac{\int_0^{r_1} e^{-\frac{1}{2}\left(\frac{r'}{\sigma}\right)^2} r'^2 dr' + \int_{r_1}^{r_2} e^{-\frac{1}{2}\left(\frac{r'}{\sigma}\right)^2} r'^2 dr'}{r_2^3}\,.$$

Let us now take $r_2 = r_1 + dr$; with this hypothesis, neglecting powers of the differential higher than the first, we obtain

$$\frac{\int_0^{r_1} e^{-\frac{1}{2}\left(\frac{r'}{\sigma}\right)^2} r'^2 dr'}{r_1^3} > \frac{\int_0^{r_1} e^{-\frac{1}{2}\left(\frac{r'}{\sigma}\right)^2} r'^2 dr' + e^{-\frac{1}{2}\left(\frac{r}{\sigma}\right)^2} r^2 dr}{r_1^3 + 3r_1^2 dr}$$

which is satisfied if

$$e^{-\frac{1}{2}\left(\frac{r}{\sigma}\right)^2} r^2 dr < 3r_1^2 dr$$

and therefore if

$$-\frac{1}{2}\left(\frac{r}{\sigma}\right)^2 < \ln 3$$

which is satisfied in turn $\forall r$ since the left hand side is negative and the right hand one is positive.
We just demonstrated that every shell starts to collapse before and at a lower radius than the adjacent external one; this fact ensures the absence of shell crossing.

The Gaussian profile can be divided in shells, and the results of the previous sections are valid for it: an exact SN solution can be found with the exact form and procedure of section 3.1, the free-particle approximation predicts an initial expansion of the less overdense shells (i.e. the external part of the Gaussian), followed by a contraction which eventually leads to the formation of a singularity at the origin of the coordinates.

Also the global evolution of the overdensity in Zel'dovich approximation can be particularized to the density profile (3.76). The two quantities which determines the initial wavefunction $\Psi(r_x, a_i)$ in the region $r_x \leq R_f/a_i$ are

$$\delta(r_x, a_i) = \frac{\rho - \rho_f}{\rho_f} = \frac{\frac{M}{\left(\sqrt{2\pi}\sigma\right)^3} e^{-\frac{1}{2}\left(\frac{a_i r_x}{\sigma}\right)^2} - \rho_f}{\rho_f} \tag{3.79}$$

and (for the derivation from (3.58) see the appendix)

$$\Phi(r_x, a_i) = \frac{1}{a_i}\frac{r_x''^2}{6} - \frac{M}{a_i\,\rho_f\left(\sqrt{2\pi}\sigma\right)^3}\int_0^{r_x} dr_x'' \frac{1}{r_x''^2}\int_0^{r_x''} e^{-\frac{1}{2}\left(\frac{r_x'}{\sigma/a_i}\right)^2} {r_x'}^2\, dr_x' \,. \tag{3.80}$$

The Zel'dovich trajectories are

$$\begin{aligned} r_x &= \bar{q}_s - \Delta a\,\frac{1}{a_i\,q^2}\int \delta(r_x', a_i)\,{r_x'}^2\, dr_x'\Big|_{\bar{q}_s} \\ &= \bar{q}_s + \frac{1}{3}\frac{\Delta a}{a_i}\bar{q}_s - \frac{\Delta a}{a_i}\,\frac{M}{\rho_f\,\left(\sqrt{2\pi}\sigma\right)^3}\,\frac{1}{\bar{q}_s^2}\int_0^{\bar{q}_s} e^{-\frac{1}{2}\left(\frac{r_x'}{\sigma/a_i}\right)^2} {r_x'}^2\, dr_x' \,. \end{aligned} \tag{3.81}$$

Since the overdensity is compensated, with an error assumed to be negligible, a fluid element initially at $r_x = R_f/a := R_{x,f}$ should stay forever at the same comoving coordinate. In the appendix this result is explicitly found, as a consistency check.

The free-particle one is an approximation, and therefore it can be improved. In particular, in the next section we will refine the prediction of the evolution of the Gaussian distribution computed in free-particle approximation, with the use of Time Dependent Perturbation Theory (TDPT).

3.5 Time Dependent Perturbation Theory

In section 3.2 we started from a spherically symmetric density profile, we divided it in shells, we wrote for a generic j-th shell the wavefunction satisfying the Schrödinger equation for a free particle [72]

$$i\nu\frac{\partial\Psi_j}{\partial a} = -\frac{\nu^2}{2}\nabla_x^2\Psi_j \tag{3.82}$$

at initial time $t = t_i$, and we computed its temporal evolution. We moreover discovered that the velocity potential Φ which realized the free particle approximation in the j-th shell is

$$\Phi_{Z,j} = -\varphi_j := -\frac{2}{3a^3H_f^2}(V_j - V_f)\,, \tag{3.83}$$

while the corresponding exact peculiar velocity potential can be expressed by means of equation (3.21) as a function of the known, physical velocity potential (3.8); the result is

$$\Phi_j = \frac{H_j - H_f}{\dot{a}}\frac{r_x^2}{2}\,. \tag{3.84}$$

The velocity potential (3.84) is exact in the limit of shells of infinitesimal thickness. Using it, the effective potential introduced in section 2.2, which is null in the free particle approximation, would result[3]

$$\begin{aligned}\tilde{V}_j' &= \frac{3}{2a}(\Phi_j + \varphi_j) = \\ &= \frac{3}{2a^2}\left(\frac{H_j}{H_f} + \frac{1}{3}\frac{\Omega_j H_j^2}{H_f^2} - \frac{4}{3}\right)\frac{r_x^2}{2}\,.\end{aligned} \tag{3.85}$$

If there was no overdensity, $H_j = H_f$, $\Omega_j = 1$, and $\tilde{V}_j'$ would be null. As it is known in literature, from for example CMB observations, primordial density fluctuations were tiny, and therefore so was $\tilde{V}_j'$, at least in the early stages of the collapse. Hence, at least in a certain range of time, we are allowed to consider $\tilde{V}_j'$ a small perturbation respect to the null potential of last section. Since this perturbation is evidently time-dependent, we will make use of time-dependent perturbation theory (TDPT).
Let us consider the following quantity: the modulus of the ratio of the perturbed velocity potential Φ_j over the unperturbed one $-\varphi_j$

$$\begin{aligned}\mathcal{R} := \left|\frac{\Phi_j}{-\varphi_j}\right| &= \frac{H_j - H_f}{\dot{a}}\frac{r_x^2}{2}\,\frac{3a^3H_f^2}{2(V_j - V_f)} = \\ &= \frac{(H_j - H_f)\,3a^2H_f}{2G\frac{r^2}{2}(\frac{m_j}{r_j^3(a)} - \frac{M}{R_f^3(a)})}\frac{r_x^2}{2} = \\ &= \frac{3H_f(H_j - H_f)}{\Omega_j H_j^2 - H_f^2}\,;\end{aligned} \tag{3.86}$$

the last passage makes use of a calculation performed in deriving (3.85), reported in the appendix. I propose the following criterion to state whether (3.85) could be safely considered a perturbation: when the parameter $\mathcal{R}$ takes values < 1, (3.85) is a small perturbation to the free-particle case.

H_j and Ω_j are functions of the mean density inside the j-th shell. If we study shells of infinitesimal thickness, the mass of the shell itself is negligible, and therefore we can

[3] For the derivation, see the appendix.

assume it does not influence the density inside it. This fact together with the absence of shell crossing decouples the potential $\tilde{V}$ from the evolution of the Ψ describing the shell; therefore Schrödinger-Newton equations become linear, and we can use the superposition principle.

Let us start therefore finding a basis of free particle solutions in which we can write the wavefunction Ψ_j of a single shell, known which, with the piecewise solutions (3.7) (3.8), we can describe the whole Gaussian overdensity. Let us notice that the Gaussian density profile (3.76) has the property of having a negligible matter density at $r = R_f$. Therefore let us search for solutions of the free particle Schrödinger equation (3.82) in the region $r < R_f$, which go to zero at $r = R_f$. For achieving this task, let us make use of a mathematical artifice: let us consider the potential of an infinite spherical well

$$V_0(r_x) = \begin{cases} 0 & r_x \leq R_{x,f} \\ \infty & r_x > R_{x,f} \end{cases} , \tag{3.87}$$

where $R_{x,f} := R_f/a$; it is worth noting that, since the overdensity is compensated, R_f is a function of time, but $R_{x,f}$ is constant. The potential (3.87) is the free-particle one inside a sphere of radius $R_{x,f}$, and then it is infinite outside it, just to ensure that the wavefunction be null in that region. In fact we are interested in an overdensity localized at $r \leq R_f$, with the property of having negligible matter density at $r = R_f$, and we are not interested in describing the evolution of the homogeneous region at $R > R_f$. In other words this trick makes the wavefunction describing just the overdensity and not the background too.
As said, the potential V_0 (3.87) is introduced in order to find a basis for the vector space of which the wavefunction Ψ_j of a shell is an element. Therefore during its whole evolution, the shell has to be writeable as a superposition of the eigenfunctions of a Hamiltonian which contains the potential V_0. This would not be possible if a shell would expand at radii $r > R_f := aR_{x,f}$ at a certain point of its evolution. Since, in the last section, we demonstrated that the Gaussian profile satisfies the criterion (3.4), shell crossing does not occur during the whole evolution of the overdensity. This means in particular that each shell turns around at a lower radius than every outer shell, and therefore that there is not a shell whose distribution peak ever goes outside R_f.
This would be enough to justify the choice (3.87) for V_0 in the $\nu \to 0$ limit, where the thickness of the shell does not increase with time. Unfortunately for finite ν, a shell spreads in thickness of a length $\sigma(\Delta a)$ (3.43).
We can consider the shell at time coordinate Δa as included between $\mu(\Delta a) - \sigma(\Delta a)$ and $\mu(\Delta a) + \sigma(\Delta a)$, where μ is given by (3.42). This is a conservative choice, because the exponential (3.40), which appears in the expression of Ψ_j, makes the shells of overdensities focus, i.e. becoming thinner, as time flows. With our conservative convention, the maximum radius reached by a generic j-th shell is

$$r_{\mathrm{MAX}} := a_{\max} \left[\mu(\Delta a_{\max}) + \sigma(\Delta a_{\max})\right] , \tag{3.88}$$

with $\Delta a_{\max}$ the turn around time coordinate of the j-th shell (3.49). Only shells which enclose an initial overdensity $\bar{\delta}_j(a_i) < 3$ turn around, as discussed in section 3.2; let us restrict to those, which constitute the external, initially expanding part of the overdensity. Let us omit the temporal dependence of the initial mean overdensity inside the j-th shell $\bar{\delta}_j(a_i)$ in order to keep the notation readable; therefore in the following $\bar{\delta}_j := \bar{\delta}_j(a_i)$. With

this convention, for those peripheral shells, the condition (3.88) reads:

$$r_{\mathrm{MAX},j} = a_{\max}\, r_{x,i}\, \left(\frac{1}{2} + \frac{\bar{\delta}_j}{6}\right) + a_{\max}\sqrt{\nu\, \frac{a_i\,(3-\bar{\delta}_j)}{2\,\bar{\delta}_j}\, \left[\frac{1}{2} + \frac{\bar{\delta}_j}{6}\right]} =$$

$$= r_i\, \left(\frac{1}{2} + \frac{\bar{\delta}_j}{6}\right) + r_i \frac{9-\bar{\delta}_j^2}{12\,\bar{\delta}_j} + \left[\frac{a_i\,(3-\bar{\delta}_j)}{2\,\bar{\delta}_j} + a_i\right] \sqrt{\nu\, \frac{a_i\,(3-\bar{\delta}_j)}{2\,\bar{\delta}_j}\, \left[\frac{1}{2} + \frac{\bar{\delta}_j}{6}\right]}\,,$$

where it was plugged

$$\Delta a_{\max} = \frac{a_i\,(3-\bar{\delta}_j)}{2\,\bar{\delta}_j(a_i)}\,.$$

For what just said, the j-th shell does not ever overcome $aR_{x,f}$ if and only if

$$r_{\mathrm{MAX},j} < a_{\max}\, R_{x,f}$$

$$a_{\max}\, r_{x,i}\, \left(\frac{1}{2} + \frac{\bar{\delta}_j}{6}\right) + a_{\max}\sqrt{\nu\, \frac{a_i\,(3-\bar{\delta}_j)}{2\,\bar{\delta}_j(a_i)}\, \left[\frac{1}{2} + \frac{\bar{\delta}_j}{6}\right]} < a_{\max}\, R_{x,f}$$

$$\sqrt{\nu\, \frac{a_i\,(3-\bar{\delta}_j)}{2\,\bar{\delta}_j(a_i)}\, \left[\frac{1}{2} + \frac{\bar{\delta}_j}{6}\right]} < R_{x,f} - r_{x,i}\, \left(\frac{1}{2} + \frac{\bar{\delta}_j}{6}\right)$$

$$0 \leq \nu < \frac{12\,\bar{\delta}_j(a_i)}{a_i\,(9-\bar{\delta}_j^2)}\, \left[R_{x,f} - r_{x,i}\, \left(\frac{1}{2} + \frac{\bar{\delta}_j}{6}\right)\right]^2\,.$$

Since the right hand side of the last written inequality is always positive for $\bar{\delta}_j < 3$ and $r_{x,i} < R_{x,f}$, there exist small enough finite values of ν for which every shell is always confined at radii $r < a\, R_{x,f}$. Therefore the potential (3.87) is useful to find a basis of the space of states of the shells of the Gaussian profile (3.76) in Zel'dovich approximation. Let us see in detail how.

Let us define the Hamiltonian

$$\mathcal{H}_0 := T + V_0 = -\frac{\nu^2}{2}\nabla_x^2 + V_0\,, \tag{3.89}$$

where T represents the kinetic energy. The form of the term T is a 3D generalization of the free-particle kinetic term written by Short and Coles in [72].

Let us therefore search for solutions of the Schrödinger equation

$$\mathcal{H}_0\Psi = i\nu\frac{\partial\Psi}{\partial t} \tag{3.90}$$

which can be written as the product of a radial portion and an angular one [28]:

$$\Psi(r_x, \theta_x, \phi_x) = R(r_x)Y(\theta_x, \phi_x)\,.$$

As it is well known in literature (see for example [28]), for a spherically symmetric potential, with spherically symmetric boundary conditions, the angular part Y turns out to be the spherical harmonics $Y_l^m(\theta_x, \phi_x)$. Let us focus on the zero angular momentum case, therefore [28]

$$Y(\theta_x, \phi_x) = Y_0^0 = \sqrt{\frac{1}{4\pi}}\,.$$

On the other hand the equation (3.90) for R can be simplified in form by substituting $u(r_x) = r_x\, R(r_x)$ [28]:

$$-\frac{\nu^2}{2}\frac{d^2u}{dr_x^2} + \left[\bar{V} + \frac{\nu^2}{2}\frac{l(l+1)}{r_x^2}\right] u = i\nu\frac{\partial u}{\partial t}\,. \tag{3.91}$$

For zero angular momentum, in the region $r < R_f$, (3.91) becomes

$$-\frac{\nu^2}{2}\frac{d^2u}{dr_x^2} = i\nu\frac{\partial u}{\partial t}\,.$$

The operator on the left hand side does not depend on time, therefore we can separate variables and write

$$-\frac{\nu^2}{2}\frac{d^2u}{dr_x^2} = E_0\, u\,, \tag{3.92}$$

which becomes

$$\frac{d^2u}{dr_x^2} = -k^2 u$$

if we define $k := \sqrt{2E_0}/\nu$. The regular solution of this equation is

$$u(r_x) = A\sin(kr_x)\,,$$

where A ensures normalization and k can assume values only in a countable set[4] $\{k_n\}$, $n \in \mathbb{N}_0$. These values can be found by knowing that, because of the form of the potential, in the region $r_x > R_{x,f}$, $u(r_x) = 0$. Hence requiring that the solution vanishes at $R_{x,f}$ singles out the values of k for which at $r_x = R_{x,f}$ the sine has a node [28]:

$$k_n = \frac{n\pi}{R_{x,f}} \qquad n \in \mathbb{N}_0\,.$$

Finally, a basis of free particle solutions which go to zero at $r = R_f$ is given by

$$\Psi_n(r_x, \theta_x, \phi_x) = A\sqrt{\frac{1}{4\pi}}\frac{\sin(k_n r_x)}{r_x}\ ; \tag{3.93}$$

A can then be set by demanding

$$M = \int_{r_x<R_{x,f}} |\Psi_n(r_x,\theta_x,\phi_x)|^2 d^3x = A^2\frac{1}{4\pi}4\pi\int_0^{R_{x,f}} \sin^2(k_n r_x)\, dr_x = A^2\frac{1}{2}\,,$$

hence

$$A = \sqrt{2M}\,.$$

Therefore (3.93) becomes

$$\Psi_n(r_x, \theta_x, \phi_x) = \sqrt{\frac{M}{2\pi}}\frac{\sin(k_n r_x)}{r_x}\,. \tag{3.94}$$

For developing TDPT we have to consider the following Hamiltonian [34]

$$\mathcal{H} = \mathcal{H}_0(\mathbf{x}) + \mathcal{H}'(\mathbf{x}, a)\,. \tag{3.95}$$

Let us recall that the unperturbed Hamiltonian (3.89) in the region $r_x < R_{x,f}$ and for zero angular momentum reads

$$\mathcal{H}_0(r_x) = -\frac{\nu^2}{2}\frac{d^2}{dr_x^2}\,.$$

[4]With $\mathbb{N}_0$ I designate $\mathbb{N} \setminus \{0\}$.

The perturbation is

$$\mathcal{H}'(r_x,a)=\tilde{V}_j'=\frac{3}{2a^2}\left(\frac{H_j}{H_f}+\frac{1}{3}\frac{\Omega_j H_j^2}{H_f^2}-\frac{4}{3}\right)\frac{r_x^2}{2}\,,$$

where $\tilde{V}_j'$ is given by (3.85).

In terms of the discrete solutions Ψ_n (3.94), the static Schrödinger equation (3.92), reads [34]

$$\mathcal{H}_0\Psi_n=E_n\Psi_n$$

with $E_n:=k_n^2\nu^2/2$.

Because of the fact that the superposition principle is valid and that the Ψ_n form a basis of wavefunctions of free particle with the boundary condition $\Psi(R_{x,f})=0$, every density profile, and in particular the one of the j-th shell of the Gaussian (3.76), can be written as [34]

$$\Psi_j(a)=\sum c_n(a)\,\Psi_n\,e^{-iE_n a/\nu} \tag{3.96}$$

where the evolution of the coefficients is given by (the dot denotes derivation respect to the scale factor a) [34]

$$\dot{c}_n=-\frac{i}{\nu}\sum_m c_m\,H'_{nm}\,e^{i(E_n-E_m)a/\nu}\,, \tag{3.97}$$

where [34]

$$H'_{nm}:=\langle\Psi_n|\,H'\,|\Psi_m\rangle\ . \tag{3.98}$$

Let us calculate explicitly H'_{nm} for two generic n and $m\neq n$.

$$\begin{aligned}
H'_{nm}:=&\langle\Psi_n|\,H'\,|\Psi_m\rangle=\\
&=\int_{r_x<R_{x,f}}\Psi_n\,H'\,\Psi_m\,d^3x=\\
&=4\pi\frac{M}{2\pi}\int_0^{R_{x,f}}\frac{\sin(k_n r_x)}{r_x}H'(r_x,a)\frac{\sin(k_m r_x)}{r_x}r_x^2\,dr_x=\\
&=2M\int_0^{R_{x,f}}\sin(k_n r_x)\frac{3}{2a^2}\left(\frac{H_j}{H_f}+\frac{1}{3}\frac{\Omega_j H_j^2}{H_f^2}-\frac{4}{3}\right)\frac{r_x^2}{2}\sin(k_m r_x)\,dr_x=\\
&=\frac{3M}{a^2}\left(\frac{H_j}{H_f}+\frac{1}{3}\frac{\Omega_j H_j^2}{H_f^2}-\frac{4}{3}\right)\int_0^{R_{x,f}}\sin(k_n r_x)\,\sin(k_m r_x)\,\frac{r_x^2}{2}\,dr_x=\\
&=\frac{3M}{2a^2}\left(\frac{H_j}{H_f}+\frac{1}{3}\frac{\Omega_j H_j^2}{H_f^2}-\frac{4}{3}\right)\int_0^{R_{x,f}}\left\{\cos[(k_m-k_n)\,r_x]-\cos[(k_m+k_n)\,r_x]\right\}\,\frac{r_x^2}{2}\,dr_x=\\
&=\frac{3M}{2a^2}\left(\frac{H_j}{H_f}+\frac{1}{3}\frac{\Omega_j H_j^2}{H_f^2}-\frac{4}{3}\right)\left\{\int_0^{R_{x,f}}\cos[(k_m-k_n)\,r_x]\frac{r_x^2}{2}\,dr_x-\right.\\
&\quad\left.-\int_0^{R_{x,f}}\cos[(k_m+k_n)\,r_x]\,\frac{r_x^2}{2}\,dr_x\right\}=\\
&=\frac{3M}{2a^2}\left(\frac{H_j}{H_f}+\frac{1}{3}\frac{\Omega_j H_j^2}{H_f^2}-\frac{4}{3}\right)\left\{\frac{R_{x,f}}{(k_m-k_n)^2}-\frac{R_{x,f}}{(k_m+k_n)^2}\right\}=\\
&=\frac{3M}{2a^2}\left(\frac{H_j}{H_f}+\frac{1}{3}\frac{\Omega_j H_j^2}{H_f^2}-\frac{4}{3}\right)R_{x,f}\,\frac{4k_m k_n}{(k_m^2-k_n^2)^2}\,.
\end{aligned} \tag{3.99}$$

The solution of the integrals performed in the seventh step was done by parts and is reported in the appendix. For $m = n$ instead

$$H'_{nn} = \frac{3M}{2a^2}\left(\frac{H_j}{H_f} + \frac{1}{3}\frac{\Omega_j H_j^2}{H_f^2} - \frac{4}{3}\right)\left\{\int_0^{R_{x,f}} \cos[0]\,\frac{r_x^2}{2}\,dr_x - \int_0^{R_{x,f}} \cos[2k_n\,r_x]\,\frac{r_x^2}{2}\,dr_x\right\} =$$
$$= \frac{3M}{2a^2}\left(\frac{H_j}{H_f} + \frac{1}{3}\frac{\Omega_j H_j^2}{H_f^2} - \frac{4}{3}\right)\left\{\frac{R_{x,f}^3}{3} - \frac{R_{x,f}}{(2k_n)^2}\right\} =$$
$$= \frac{3M}{2a^2}\left(\frac{H_j}{H_f} + \frac{1}{3}\frac{\Omega_j H_j^2}{H_f^2} - \frac{4}{3}\right) R_{x,f}\left\{\frac{R_{x,f}^2}{3} - \frac{1}{4k_n^2}\right\}.$$

With these results and (3.97) we can compute

$$\dot{c}_n = -\frac{i}{\nu}\sum_m c_m\,H'_{nm}\,e^{i(E_n-E_m)a/\nu}$$
$$= -\frac{i}{\nu}\frac{3M}{2a^2}\left(\frac{H_j}{H_f} + \frac{1}{3}\frac{\Omega_j H_j^2}{H_f^2} - \frac{4}{3}\right) R_{x,f}\left\{\sum_{m\neq n} c_m\,\frac{4k_m k_n}{(k_m^2-k_n^2)^2}\,e^{i(E_n-E_m)a/\nu} + \right.$$
$$\left. + c_n\left(\frac{R_{x,f}^2}{3} - \frac{1}{4k_n^2}\right)\right\}. \tag{3.100}$$

It is worth noting that $|\dot{c}_n| \propto \nu^{-1}$, while in absence of perturbation, $\dot{c}_n = 0$. In general the i-th correction $\Psi^{(i)}$ computed with TDPT to the unperturbed wavefunction $\Psi^{(0)}$ has the following dependence on ν [72]

$$\Psi^{(i)} \propto \frac{1}{\nu^i}.$$

Therefore in order to have corrections smaller in modulus respect to $\Psi^{(0)}$, we cannot take the limit $\nu \to 0$, which would dump the quantum pressure term. We have to adopt a compromise, keeping ν small enough to make the effect of QPT not dominating over gravity, and large enough to make sense of the concept of perturbation theory [72]. To find the n-th coefficient, we need to integrate (3.100):

$$c_n(a) - c_{n,i} = -\frac{3Mi\,R_{x,f}}{2\nu}\left\{\sum_{m\neq n}\frac{4k_m k_n}{(k_m^2-k_n^2)^2}\int_{a_i}^{a} c_m\,\frac{1}{a'^2}\left(\frac{H_j}{H_f} + \frac{1}{3}\frac{\Omega_j H_j^2}{H_f^2} - \frac{4}{3}\right)\times\right.$$
$$\left.\times\, e^{i(E_n-E_m)a'/\nu}\,da' + \left(\frac{R_{x,f}^2}{3} - \frac{1}{4k_n^2}\right)\int_{a_i}^{a} c_n\frac{1}{a'^2}\left(\frac{H_j}{H_f} + \frac{1}{3}\frac{\Omega_j H_j^2}{H_f^2} - \frac{4}{3}\right)da'\right\}.$$

In the long timescales, for

$$a - a_i \gg \frac{E_1 - E_2}{\nu},$$

the first integral mediates to zero for every m. Therefore in this limit every $c_{n,i}$ of the unperturbed eigenfunction decomposition of the initial state is mapped in a $c_n(a)$ which satisfy

$$c_n(a) - c_{n,i} = -\frac{3Mi\,R_{x,f}}{2\nu}\left(\frac{R_{x,f}^2}{3} - \frac{1}{4k_n^2}\right)\int_{a_i}^{a} c_n\frac{1}{a'^2}\left(\frac{H_j}{H_f} + \frac{1}{3}\frac{\Omega_j H_j^2}{H_f^2} - \frac{4}{3}\right)da'. \tag{3.101}$$

In particular, for a fixed $a = a_1 \gg (E_1 - E_2)/\nu + a_i$

$$|c_n(a_1) - c_{n,i}| \propto \left|\frac{R_{x,f}^2}{3} - \frac{1}{4k_n^2}\right| = \left|\frac{R_{x,f}^2}{3} - \frac{R_{x,f}^2}{4\pi^2 n^2}\right| \propto \left|\frac{1}{3} - \frac{1}{4\pi^2 n^2}\right|. \tag{3.102}$$

The succession defined by last term is monotonously growing for $n \geq 1$.

For shorter periods of time, the first integral is non negligible, and in particular it couples more efficiently coefficients which refers to levels which differ less in energy. In particular, since energy levels scale $\propto n^2$, with $n \in \mathbb{N}$, lower energy states are coupled more efficiently to their neighbours than higher ones.

Since a shell is localized in space in the radial direction within an indetermination equal to the thickness of the shell, which we supposed to be very small, its decomposition in energy eigenfunctions (3.96) has many coefficients c_n with similar non vanishing moduli, because of Heisenberg principle. The overall effect of the time dependent perturbation introduced is the following. In the short timescales, it varies the energy spectral decomposition of the shell in a inhomogeneous way: the low-energy part of it undergoes more rapid and effective modifications than the high momentum one.
More importantly, in the long timescales that spectral decomposition varies in a way which makes the expectation value of the unperturbed energy of the shell increase. This can be seen by the proportionality (3.102): coefficients referring to higher energy states undergo greater modifications. One could argue that these modifications could lower or higher the modulus of a certain c_n in an a priori unpredictable way, but this is not true because the variation of a certain coefficient is weighted by the integral in (3.101); to better understand its behaviour, let us compute the following quantity, by means of eq. (3.101):

$$c_n(a_i + da) = c_n(a_i) - i\, F(a_i)\, c_n(a_i) \tag{3.103}$$

where

$$F(a) := \frac{3M\, R_{x,f}}{2\nu} \left(\frac{R_{x,f}^2}{3} - \frac{1}{4k_n^2} \right) \frac{1}{a^2} \left(\frac{H_j}{H_f} + \frac{1}{3} \frac{\Omega_j H_j^2}{H_f^2} - \frac{4}{3} \right) \geq 0\,.$$

Four situations can occur:

1. $\Re(c_{n,i}) > 0 \wedge \Im(c_{n,i}) < 0$,
2. $\Re(c_{n,i}) < 0 \wedge \Im(c_{n,i}) > 0$,
3. $\Re(c_{n,i}) > 0 \wedge \Im(c_{n,i}) > 0$,
4. $\Re(c_{n,i}) < 0 \wedge \Im(c_{n,i}) < 0$,

where $\Re(c)$ denotes the real part of a complex number c and $\Im(c)$ its imaginary one.
In the first two cases eq. (3.103) shows that a positive feedback sets in, and both $|\Re(c_n)|$ and $|\Im(c_n)|$ grow with time.
In the second two cases (i.e. 3. and 4.), equations (3.101) and (3.103) show that a negative feedback sets in, and initially $|\Re(c_n)|$ and $|\Im(c_n)|$ decrease with time. If they do not reach zero at the same time, when the first, between $|\Re(c_n)|$ and $|\Im(c_n)|$, change sign, the previously considered situations sets in, and they start growing in modulus. Since the equations governing the evolution of the real and the imaginary part of c_n are the same, they reach zero at the same time coordinate a if and only if $\Im(c_{n,i}) = \Re(c_{n,i})$. This condition defines a line in the complex plane, therefore it singles out a set of null measure in the space of possible $c_{n,i}$.

Therefore this demonstrates that in a large timescale every c_n of the unperturbed energy spectral decomposition of a shell grows in modulus, but with different rates: as (3.102) states, a coefficient c_n grows faster than a c_m iff $n > m$. Therefore in the limit of large a, the perturbation acts by making every shell gain momentum: the expectation value of the unperturbed energy, i. e. of momentum, increases at late times respect to the initial time

at which we start to consider the effect of the perturbation, and therefore respect to the free-particle prediction.

Moreover because of the presence of the term

$$\left(\frac{H_j}{H_f} + \frac{1}{3}\frac{\Omega_j H_j^2}{H_f^2} - \frac{4}{3}\right)$$

in (3.101), shells which enclose an higher overdensity gain momentum faster than ones enclosing slighter overdense regions, respect to the prediction of the free-particle approximation we saw in the previous section.

Chapter 4

Evolution of a spherically symmetric configuration coherent with the initial conditions of the Universe

Until now, we considered a perturbation that was arbitrary both in shape and in amplitude. In this section we will ground the study on a more realistic case: we will still consider a spherically symmetric overdensity arbitrarily shaped, but with an amplitude coherent with the initial density contrast of the Universe $\delta(\mathbf{r}) := [\rho(\mathbf{r}) - \bar{\rho}]/\bar{\rho}$ being a Gaussian random field.

4.1 Characterization of the primordial density field of the Universe

Let us use, as before, comoving coordinates $\mathbf{x} = (r_x, \theta_x, \phi_x)$ such that $\mathbf{r} = a\mathbf{x}$.

If we assume that the initial density field $\delta(\mathbf{x})$ is Gaussian [51], it is completely specified by its power spectrum [68], defined as [51]

$$P(k) = \langle |\delta_k|^2 \rangle \,, \tag{4.1}$$

where δ_k denotes the Fourier transform of $\delta(\mathbf{x})$ and the angular brackets a mean over space.

The field $\delta(\mathbf{x})$ can be smoothed by convolving it with a filter W. As a filter we can choose the following spherically symmetric top-hat window [51]

$$W(R_0; r_x) := \begin{cases} 1 & r_x \leq R_0 \\ 0 & r_x > R_0 \end{cases} ,$$

for some comoving radius R_0. With this choice, the smoothed field reads [51]

$$\begin{aligned} \delta(R_0; \mathbf{x}) &= \int W(R_0; |\mathbf{x} - \mathbf{y}|)\, \delta(\mathbf{y})\, d^3y \\ &= \sum_k \delta_k\, \hat{W}(R_0; k)\, e^{i\mathbf{k}\cdot\mathbf{x}} \,, \end{aligned} \tag{4.2}$$

where $\hat{W}(R_0; k)$ is the Fourier transform of $W(R_0; r)$.

A useful quantity characterising the overdensity field is the rms fluctuation of mass in a given smoothing window R_0 [51]:

$$\Delta^2(R_0) = \langle |\delta(R_0; \mathbf{x})|^2 \rangle = \sum_k P(k) \hat{W}^2(R_0; k) \,, \tag{4.3}$$

where in the last passage we plugged expression (4.2) for the smoothed overdensity field expressed in terms of its Fourier decomposition, and used the definition (4.1) of the power spectrum.

The Gaussian nature of the field $\delta(\mathbf{x})$ allows us to statistically characterize $\bar{\delta}(R_0)$, the mean initial overdensity of a spherical region with comoving radius R_0, defined by (2.6). This quantity has the following Gaussian one-point distribution function [52]

$$p(\bar{\delta}(R_0)) = \frac{1}{\sqrt{2\pi}\,\Delta(R_0)} \exp\left[-\frac{1}{2}\frac{\bar{\delta}^2(R_0)}{\Delta^2(R_0)}\right] . \tag{4.4}$$

In [6] (the famous BBKS paper) Bardeen et al. find that in the standard CDM model (Blumenthal et al. 1984; Davis et al. 1985) the power spectrum (4.1) of the mass density fluctuations is given by

$$P(k) = P_0 \kappa T^2(\kappa) \,, \tag{4.5}$$

with [51]

$$T(\kappa) = \frac{\ln(1+2.34\kappa)}{2.34\kappa} \left[1 + 3.89\kappa + (16.1\kappa)^2 + (5.46\kappa)^3 + (6.71\kappa)^4\right]^{-1/4} ,$$

where [24]

$$\kappa := \frac{k}{\mathrm{h}\Gamma\,\mathrm{Mpc}^{-1}} \,,$$

where in turn Γ was defined by Bardeen et al. [6] to be $\Gamma = \Omega_m \mathrm{h}$; this was later generalized by Sugiyama [74] to

$$\Gamma = \Omega_m \mathrm{h}\, e^{-\Omega_b(1+\sqrt{2\mathrm{h}}/\Omega_m)} .$$

The coefficient P_0 in (4.5) can be set normalizing the power spectrum by imposing [51] [24]

$$\Delta(8\mathrm{h}^{-1}\mathrm{Mpc}) = \sigma_8 \,,$$

where σ_8 can be estimated from observations [66] [24]. The value $R_0 = 8\mathrm{h}^{-1}\mathrm{Mpc}$ for the smoothing radius is chosen because of the observational result that the variance of counts of galaxies in spheres of this size is of order unity [18].

Recalling the following expression for the top-hat filter function in Fourier space [24]

$$\hat{W}(R_0; k) = \frac{3 j_1(kR_0)}{kR_0} \,, \tag{4.6}$$

where j_1 is the first-order spherical Bessel function, we can finally write the r.m.s. fluctuation (4.3) for the power spectrum (4.5); it reads

$$\Delta^2(R_0) = \sum_k P(k)\, \hat{W}^2(R_0; k) = \sum_k P_0 \kappa T^2(\kappa) \frac{9 j_1^2(kR_0)}{k^2 R_0^2} = \frac{9\, P_0}{R_0^2 \mathrm{h}\Gamma\,\mathrm{Mpc}^{-1}} \sum_k T^2(\kappa)\, \frac{j_1^2(kR_0)}{k} \,. \tag{4.7}$$

In order to state for which values of the smoothing radius R_0 the last written series converges, let us calculate the following quantity

$$
\begin{aligned}
l &:= \limsup_{k\to\infty} \sqrt[k]{T^2(\kappa)\,\frac{j_1^2(kR_0)}{k}} \\
&= \limsup_{k\to\infty} \sqrt[k]{\frac{\ln^2(1+2.34\kappa)}{2.34^2\kappa^2\left[1+3.89\kappa+(16.1\kappa)^2+(5.46\kappa)^3+(6.71\kappa)^4\right]^{1/2}}\left\{\sin\left(kR_0+\frac{\pi}{4}\right)\times\right.} \\
&\qquad \overline{\left.\times\left[\frac{3}{4\sqrt{2\pi}}\left(\frac{1}{kR_0}\right)^{3/2}+O\left(\left(\frac{1}{kR_0}\right)^{7/2}\right)\right]+\right.} \\
&\qquad \overline{\left.\left.+\cos\left(kR_0+\frac{\pi}{4}\right)\left[-\sqrt{\frac{2}{\pi}}\left(\frac{1}{kR_0}\right)^{1/2}+O\left(\left(\frac{1}{kR_0}\right)^{5/2}\right)\right]\right\}} = \\
&= 0\,.
\end{aligned}
$$

Being $l < 1$ regardless of the value of R_0, for the root test the series is convergent for every value of the smoothing radius.

With the theory recalled in this section, in the next one we will build a model for a primordial overdensity $\delta_i(r)$ coherent with the initial conditions of the Universe.

4.2 Specification of a model for a spherically symmetric overdensity coherent with the initial conditions of the Universe

Let us consider at an initial reference time $t = t_i$ the spherically symmetric overdensity described by the following density contrast (which is a model for (4.2))

$$
\delta_i(R_0; r_x) = \begin{cases} \frac{N}{\left(\sqrt{2\pi}\sigma\right)^3}\exp\left[-\frac{1}{2}\frac{r_x^2}{\sigma^2}\right] & r_x \le R_0 \\ 0 & r_x > R_0 \end{cases}. \tag{4.8}
$$

Then at $t = t_i$ the mean overdensity inside a sphere of comoving radius R_0 is

$$
\begin{aligned}
\bar{\delta}(R_0) &= \frac{4\pi}{V}\int_0^{R_0}\frac{N}{\left(\sqrt{2\pi}\sigma\right)^3}\,e^{-\frac{1}{2}\left(\frac{r}{\sigma}\right)^2}r^2dr = \\
&= \frac{2}{V}\frac{N}{\sqrt{2\pi}}\int_0^{R_0} e^{-\frac{1}{2}\left(\frac{r}{\sigma}\right)^2}\left(\frac{r}{\sigma}\right)^2\frac{dr}{\sigma} = \\
&= \frac{N}{V}\left[\mathrm{erf}\left(\frac{R_0}{\sqrt{2}\sigma}\right)-\frac{1}{\sqrt{2\pi}}\frac{R_0}{\sigma}\,e^{-\frac{1}{2}\left(\frac{R_0}{\sigma}\right)^2}\right].
\end{aligned} \tag{4.9}
$$

If we assume the primordial density contrast of the Universe to be a Gaussian random field, the above written quantity is distributed according to the probability distribution (4.4). It appears hence meaningful to study an overdensity as big as the square root of the variance of that distribution, as a fair model for a primordial fluctuation.
With this condition we can constrain one of the three parameters defining our density profile (4.8): N, σ and R_0.
In order to make our Gaussian profile (4.8) the most possible adherent to the initial conditions of the Universe, we could impose that at two radii the mean interior overdensity were

equal to the one placed at 1σ of its probability distribution in the primordial Universe. In formulae we could impose simultaneously

1. $\bar{\delta}(R_0) = \Delta(R_0)$, which sets the global amplitude of the fluctuation, inside the smoothing radius R_0;
2. $\bar{\delta}(R_0/2) = \Delta(R_0/2)$, which tunes how much the Gaussian has to be peaked to best model a realistic initial overdensity.

In order to find expressions for the right hand sides of these two constraints using (4.7) we must normalize the power spectrum, and thus set the value of P_0. To do so, we have to impose

$$\Delta^2(8\mathrm{h}^{-1}\mathrm{Mpc}) = \sigma_8^2 \,.$$

If we define for notational clearness R_8 as the comoving radius that in current units measures $8\mathrm{h}^{-1}$Mpc, we obtain

$$P_0 = \sigma_8^2 \, \frac{R_8^2 \mathrm{h}\Gamma \,\mathrm{Mpc}^{-1}}{9 \sum_k T^2(\kappa) \frac{j_1^2(kR_8)}{k}} \,. \tag{4.10}$$

Then using (4.9) for the left hand sides and (4.7) for the right hand ones, the two constraints read respectively

$$\frac{N}{\frac{4}{3}\pi R_0^3} \left[\mathrm{erf}\left(\frac{R_0}{\sqrt{2}\sigma}\right) - \frac{1}{\sqrt{2\pi}} \frac{R_0}{\sigma} \, e^{-\frac{1}{2}\left(\frac{R_0}{\sigma}\right)^2} \right] = \sigma_8 \frac{R_8}{R_0} \sqrt{\frac{\sum_k T^2(\kappa) \frac{j_1^2(kR_0)}{k}}{\sum_k T^2(\kappa) \frac{j_1^2(kR_8)}{k}}} \tag{4.11}$$

$$\frac{N}{\frac{\pi}{6}R_0^3} \left[\mathrm{erf}\left(\frac{R_0/2}{\sqrt{2}\sigma}\right) - \frac{1}{\sqrt{2\pi}} \frac{R_0/2}{\sigma} \, e^{-\frac{1}{2}\left(\frac{R_0/2}{\sigma}\right)^2} \right] = \sigma_8 \frac{R_8}{R_0} \sqrt{\frac{\sum_k T^2(\kappa) \frac{j_1^2(kR_0/2)}{k}}{\sum_k T^2(\kappa) \frac{j_1^2(kR_8)}{k}}} \tag{4.12}$$

For every choice of the smoothing radius R_0, the one written above is a system of two transcendental equations in two variables: N and σ. Unfortunately, being transcendental, these equations do not have closed-form solutions and even numerical methods of resolution do not converge, even for the easiest sensible choice of the smoothing radius $R_0 = R_8$.

On the other hand, the fact that our density profile at $r \leq R_0$ is determined by two parameters is incidental, since it follows from our arbitrary choice of the shape of the configuration we are studying. Imposing the two just exposed constraints it would possibly lead to the system most adherent to reality one can construct with a spherically symmetric overdensity with a Gaussian density contrast profile. Here we choose instead to pay the price of studying a model less adherent to the reality of primordial fluctuations, in order to be easy enough to allow us to make predictions on its evolution. In order to do so, let us impose

$$R_0 = 4\sigma \,, \tag{4.13}$$

an assumption whose consequences will be evaluated once the other parameters of the profile (4.8) will be set.

With this assumption, the integral

$$\frac{4\pi}{V} \int_{R_0}^{+\infty} \frac{N}{\left(\sqrt{2\pi}\sigma\right)^3} \, e^{-\frac{1}{2}\left(\frac{r}{\sigma}\right)^2} r^2 dr$$

becomes negligible and therefore the expression (4.9) simplifies in

$$\bar{\delta}(R_0) = \frac{N}{V} = \frac{3N}{4\pi R_0^3} \,. \tag{4.14}$$

Now let us impose the constraint

$$\bar{\delta}(R_0) = \Delta(R_0)\,.$$

Combining (4.14), (4.7) and (4.10), one finds that to ensure this condition the normalization must read

$$N(R_0) = \frac{4\pi}{3} R_0^2 R_8 \sigma_8 \sqrt{\frac{\sum_k T^2(\kappa)\,\frac{j_1^2(kR_0)}{k}}{\sum_k T^2(\kappa)\,\frac{j_1^2(kR_8)}{k}}}\,. \tag{4.15}$$

We should now set the smoothing radius R_0, which determines the size of the system we are describing. To do so, let us recall that what our spherically symmetric configuration, described by the profile (4.8), models are clusters of galaxies. They typically have radii ranging from ~ 1 to ~ 10 Mpc [18]. In 1958 Abell proposed a criterion of classification for galaxy clusters based on the number of galaxies with a certain magnitude, that have distances to the cluster centre smaller than the "Abell radius", which is of $1.5\mathrm{h}^{-1}$ Mpc [50]. The virialized structure of which our Milky Way is part is not strictly speaking a galaxy cluster but a group. By definition, groups are systems of galaxies smaller than clusters, although the dividing line between groups and clusters is quite arbitrary [50]. This Local Group that contains our galaxy, has a radius $R_{\mathrm{LG}} = (1.18 \pm 0.15)\,\mathrm{Mpc}$ [78]. Always in order to convey an idea of the average dimension of a galaxy cluster, in *table 4.1* are listed, for some galaxy clusters, the radii R_{200}. For each cluster, R_{200} is the clustocentric radius at which the mean interior density is 200 times the critical density $\rho_{\mathrm{crit}} := 3H^2/8\pi G$. Data are taken from [65].

Table 4.1: Radii of some galaxy clusters. From [65].

Name	R_{200} (Mpc)
Abell 85	1.80
Abell 119	1.83
Abell 660	1.36
ZwCl 1215.1+0400	1.73
Abell 1775	3.27
Abell 1795	1.44
Abell 1800	2.04
ZwCl 1518.8+0747	2.13
Abell 2061	1.63
Abell 2065	3.77
Abell 2199	1.52
Abell 2255	2.45
Coma	3.28

All these dimensions should be confronted with the radius r_{vir} at which a matter overdensity virializes, which is given by (2.12):

$$r_{\mathrm{vir}} = \frac{r_{\max}}{2} = \frac{3}{10}\frac{R_0}{\bar{\delta}(R_0)}\,. \tag{4.16}$$

Let us now make the guess $R_0 = R_8$ and see at which present-day radius it would virialize an overdensity described by our profile (4.8) with the choices (4.13) for σ, (4.15) for N, and $8\mathrm{h}^{-1}$Mpc for the comoving smoothing radius R_0 in current units. Using the Planck

2018 [66] measure of the power spectrum normalization $\sigma_8 = 0.8102 \pm 0.0060$, (4.16) predicts

$$r_{\rm vir}(R_0 = R_8) = \frac{3}{10}\frac{R_8}{\sigma_8} = (2.96 \pm 0.02)\,{\rm h}^{-1}{\rm Mpc} \simeq 4\,{\rm Mpc}\,,$$

where in the last passage it was assumed $\rm h = 0.7$. This value of $r_{\rm vir}$ happens to be slightly greater than the values mentioned above, but comparable to them. It is worth noting that R_{200} and $r_{\rm vir}(R_0)$ do not measure exactly the same quantity. We can model for concreteness the density profile of a virialized halo of dark matter as isothermal, i.e. $\rho \propto 1/r^2$. R_{200} is the radius inside which the mean density is 200 times the critical one, while $r_{\rm vir}(R_0)$ is the radius occupied by the outermost shell of the virialized overdensity, the one placed at R_0 at $t = t_i$. Therefore, for every continuous density profile, $R_{200} < r_{\rm vir}(R_0)$.

Let us hence also compute the mass M_8 which would constitute our overdensity in the case $R_0 = R_8$ (V_8 is the volume of a sphere of radius R_8):

$$\begin{aligned} M_8 &= V_8\,\bar\rho\left[\bar\delta(R_8) + 1\right] = (5.12 \times 10^6)\,{\rm Mpc\,km^2/s^2} \times \frac{\Omega_m(\sigma_8 + 1)}{G}\,{\rm h}^{-1} \\ &= (6.8 \pm 0.2) \times 10^{14}\,{\rm h}^{-1}{\rm M}_\odot\,. \end{aligned} \tag{4.17}$$

In the last passage there were substituted the numerical values $\Omega_m = 0.3153 \pm 0.0073$ and $\sigma_8 = 0.8111 \pm 0.0060$ from the Planck 2018 data release [66], $G = (6.67430 \pm 0.00015) \times 10^{-11}\,{\rm m^3 kg^{-1} s^{-2}}$ from the NIST reference on constants [75], ${\rm M}_\odot = (1.9884 \pm 0.0002) \times 10^{30}\,{\rm kg}$ from the Astronomical Almanac [76].
The value (4.17) for M_8 is perfectly plausible as mass of a cluster of galaxies, because cluster masses typically range between $\sim 10^{14}\,{\rm h}^{-1}{\rm M}_\odot$, which can be taken as critical value which separates groups (lighter) and clusters (heavier), and $\sim 10^{15}\,{\rm h}^{-1}{\rm M}_\odot$, the characteristic mass of rich clusters [50]. Curiously, $6.8 \times 10^{14}\,{\rm h}^{-1}{\rm M}_\odot$ is precisely the mass within the Abell radius of the Coma cluster[1] [18].

Therefore the guess of taking the smoothing radius equal to R_8 is motivated, in order to describe an overdensity of the LSS of the Universe. We therefore have to study the matter configuration described by the density contrast (4.8) with the following parameters (which completely specify it)

$$R_0 = R_8\,, \tag{4.18}$$

$$N = \frac{4\pi}{3}R_8^3\sigma_8\,, \tag{4.19}$$

$$\sigma = \frac{R_8}{4}\,. \tag{4.20}$$

As promised, before going on let us evaluate the consequences of our arbitrary choice of the parameter σ.

Reminiscent of the constraint we could not impose,

$$\Delta(R_8/2) = \bar\delta(R_8/2)\,,$$

let us characterize σ by looking at which mean overdensity $\bar\delta(R_8/2)$ a certain choice of σ leads to. In *figure 4.1* it is plotted the mean overdensity inside a comoving radius of $R_8/2$ versus different values of σ, once N and R_0 are set by (4.18) and (4.19).

[1] Nonetheless, the Coma cluster in its whole is more massive: within its radius $R_{200} = 1.99^{+0.21}_{-0.22}\,{\rm h}^{-1}\,{\rm Mpc}$, it has a mass of $M_{200} = 1.88^{+0.65}_{A-0.56} \times 10^{15}{\rm h}^{-1}\,{\rm M}_\odot$ [40].

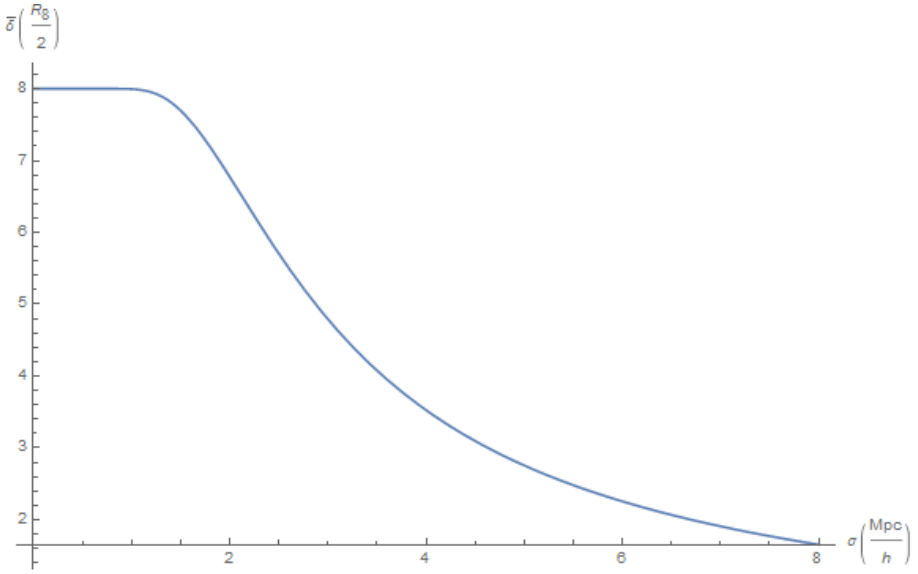

Figure 4.1: Mean overdensity inside a sphere of comoving radius $R_8/2$ as a function of different values of σ, for the density contrast profile (4.8) with N and R_0 set by respectively (4.18) and (4.19).

The rms fluctuation of density contrast in a comoving radius of $R_8/2$ prescribed by the power spectrum (4.5) is

$$\Delta(R_8/2) = 2\,\sigma_8 \sqrt{\frac{\sum_k T^2(\kappa)\,\frac{j_1^2(kR_8/2)}{k}}{\sum_k T^2(\kappa)\,\frac{j_1^2(kR_8)}{k}}} = 2.09 \pm 0.02\,.$$

This value was computed knowing that only certain terms of the series are relevant: for large k, both $T^2(k)$ and the filter function become negligible. In [24], Docters argues that an integral closely related to the series in (4.2) is mostly determined by the power spectrum within the approximate range $0.1 \leq k \leq 2$. The two series in (4.2) were evaluated by summing their first 146 terms.

Let us now call $\bar{\delta}_{\sigma_4}(r)$ the mean overdensity determined with the parameter choices (4.18), (4.19), (4.20). Then

$$\bar{\delta}_{\sigma_4}(R_8/2) = 8\left[\text{erf}\left(\sqrt{2}\right) - \frac{2}{\sqrt{2\pi}}\,e^{-2}\right] = 6.77\,.$$

We know that the quantity $\bar{\delta}(R_8)$ is distributed according to

$$p(\bar{\delta}(R_8)) = \frac{1}{\sqrt{2\pi}\,\Delta(R_8)} \exp\left[-\frac{1}{2}\frac{\bar{\delta}^2(R_8)}{\Delta^2(R_8)}\right]. \tag{4.21}$$

Therefore in a sphere of comoving radius $R_8/2$, fluctuations of the mean density contrast large at least $\bar{\delta}_{\sigma_4}(R_8/2)$ occur with a probability of 3.2σ.

The probability of having a fluctuation in an infinitesimal interval $d\delta$ around $\bar{\delta}_{\sigma_4}(R_8/2)$ is

$$p(\bar{\delta}_{\sigma_4}(R_8/2))\,d\delta = \frac{1}{\sqrt{2\pi}\,\Delta(R_8/2)} \exp\left[-\frac{1}{2}\frac{\bar{\delta}^2_{\sigma_4}(R_8/2)}{\Delta^2(R_8/2)}\right] d\delta = 0.0010\,d\delta\,. \tag{4.22}$$

Then we have finally defined our model: we will study in the following the evolution of the primordial spherically symmetric density fluctuation given by

$$\delta_i(r_x) = \begin{cases} \frac{4^3\sqrt{2}\sigma_8}{3\sqrt{\pi}} \exp\left[-\frac{1}{2}\frac{r_x^2}{(R_8/4)^2}\right] & r_x \leq R_8 \\ 0 & r_x > R_8 \end{cases} . \tag{4.23}$$

4.3 SN solution for the overdensity

The evolution of the system can be predicted, in the SN approach to CDM modelling, with a calculation analogous to the one of section 3.1. For the profile that we are here considering, (4.23), as well as for the one of section 3.1, shell crossing does not take place during its evolution, since $\delta_i(r_1) \geq \delta_i(r_2) \quad \forall\, r_1 \leq r_2$. Moreover the initial (i.e. at $a = a_i$) density profile

$$\rho_i(r_x) := \bar{\rho}(a_i)\ [1 + \delta_i(r_x)] \tag{4.24}$$

is continuous in the region $r \leq R_0$, because product of continuous functions. However the overdensity, contrarily to the case studied in section 3.1, is not compensated.

Consider then n initial comoving radii $r_{i,j}$, with $j = 1...n$, in the range $(0, R_0]$. Choose the indices such that $r_{i,j} \leq r_{i,k} \iff j < k$. Let it be m_j the mass enclosed by the shell of radius $r_{i,j}$, as it was in section 3.1. The temporal evolution $r_j(t)$ of each $r_{i,j}$ is predicted by eq. (2.3). For the considerations exposed in section 3.1, we can write the following ψ for a discretized version of the density profile (4.24)

$$\psi(r,t) = \alpha(r,t)\, e^{\frac{i}{\nu}\phi(r,t)}\,, \tag{4.25}$$

which is solution of Schrödinger-Newton equations (1.19) (1.11)

$$\begin{aligned} i\nu\frac{\partial\psi}{\partial t} &= -\frac{\nu^2}{2}\nabla^2\psi + V\psi \\ \nabla^2 V &= 4\pi G|\psi|^2 \end{aligned}$$

with

$$\alpha(r,t) = \begin{cases} \sqrt{\frac{3\Omega_1(t)H_1^2(t)}{8\pi G}} & r < r_1(t) \\ \sqrt{\frac{3\Omega_2(t)H_2^2(t)}{8\pi G}} & r_1(t) \leq r < r_2(t) \\ ... & ... \\ \sqrt{\frac{3H_f^2(t)}{8\pi G}} & r \geq r_n(t) \end{cases}$$

$$\phi(r,t) = \begin{cases} \frac{H_1(t)r^2}{2} & r < r_1(t) \\ \frac{H_2(t)r^2}{2} - \frac{G}{2}\int_0^t \left(\frac{m_1}{r_1(t)} - \frac{m_2\, r_1^2(t)}{r_2^3(t)}\right) dt' & r_1(t) \leq r < r_2(t) \\ ... & ... \\ \frac{H_f(t)r^2}{2} - \frac{G}{2}\int_0^t \left(\frac{m_1}{r_1(t)} + ... + \frac{m_n}{r_n(t)} - \frac{m_2\, r_1^2(t)}{r_2^3(t)} - \frac{m_3\, r_2^2(t)}{r_3^3(t)} - ... - \frac{M\, r_n^2(t)}{R_f^3(t)}\right) dt' & r \geq r_n(t) \end{cases}$$

$$V(r,t) = \begin{cases} Gm_1\, \frac{r^2}{2r_1^3(t)} & r \leq r_1(t) \\ Gm_2\, \frac{r^2}{2r_2^3(t)} + \frac{G}{2}\left(\frac{m_1}{r_1(t)} - \frac{m_2\, r_1^2(t)}{r_2^3(t)}\right) & r_1(t) < r \leq r_2(t) \\ ... & ... \\ GM\, \frac{r^2}{2R_f^3(t)} + \frac{G}{2}\left(\frac{m_1}{r_1(t)} + ... + \frac{m_n}{r_n(t)} - \frac{m_2\, r_1^2(t)}{r_2^3(t)} - \frac{m_3\, r_2^2(t)}{r_3^3(t)} - ... - \frac{M\, r_n^2(t)}{R_f^3(t)}\right) & r > r_n(t)\,, \end{cases}$$

where

$$H_j = \frac{a_j^3}{2Gm_j}\frac{\cos(\eta/2)}{\sin^3(\eta/2)}\,,$$
$$\Omega_j = \frac{1}{\cos^2(\eta/2)}\,,$$
$$H_f = \frac{2}{3t}\,,$$

where in turn

$$t = \frac{Gm_j}{a_j^3}(\eta - \sin\eta)\,,$$
$$a_j = \sqrt{\frac{2Gm_j}{r_{\mathrm{max},j}}}\,,$$
$$r_{\mathrm{max},j} = \frac{3r_j}{5\bar{\delta}_i(r_j)}\,.$$

In the limit $n \to \infty$ this solution describes exactly the density profile (4.24).

This solution predicts that the overdensity initially expands, reaching the turnaround radius of the outermost shell (see (2.9))

$$r_{\max} = \frac{3}{5}\frac{R_8}{\bar{\delta}_i(R_8)} = \frac{9\sqrt{2\pi}\,e^8}{640\,\sigma_8}R_8 = (1036 \pm 8)\mathrm{h}^{-1}\,\mathrm{Mpc} \tag{4.26}$$

at (see (2.8))

$$t_{\mathrm{ta}} = \frac{9\pi}{20}\frac{t_i}{\bar{\delta}_i(R_8)} = \frac{3\pi}{4}\frac{9\sqrt{2\pi}e^8}{640\,\sigma_8}\,t_i = (305 \pm 2)t_i\,.$$

Inner shells turn around earlier and at smaller radii, as it is clear from the just written equations. The first to undergo collapse is the densest innermost shell, which forms a singularity at $r = 0$ at time

$$t_{\mathrm{coll}} = 2\,t_{\mathrm{ta},1} = \frac{9\pi}{10}\frac{t_i}{\delta_i(0)} = \frac{27\pi^{3/2}}{4^3 \cdot 10\sqrt{2}\sigma_8}\,t_i = (0.205 \pm 0.002)\,t_i\,. \tag{4.27}$$

Deriving other predictions from the solution (4.25) is hard, because of its great analytical complexity. In order to simplify, and clarify, the treatment, we can use the free-particle approximation.

4.4 Zel'dovich approximation

Let us define

$$\Psi(\mathbf{x}, a) = \sqrt{1 + \delta(r_x, a)}\,e^{\frac{i}{\nu}\Phi(\mathbf{x},a)}\,,$$

where

$$\frac{d\mathbf{x}}{da} := \nabla_x\Phi\,.$$

Then the time evolution of the overdensity $\Psi(\mathbf{x}, a_i)$, where $a_i := a(t_i)$, is predicted by the Schrödinger equation (2.31) coupled to the modified Poisson equation (2.32)

$$i\nu\frac{\partial\Psi}{\partial a} = -\frac{\nu^2}{2}\nabla_x^2\Psi + \tilde{V}\psi \tag{4.28}$$
$$\nabla_x^2\left[\tilde{V} + \frac{3i\nu}{4a}\ln\left(\frac{\Psi}{\Psi^*}\right)\right] = \frac{3}{2a^2}(|\Psi|^2 - 1)\,. \tag{4.29}$$

Let us recall that in these equations (see section 2.2)

$$\tilde{V} := \frac{3}{2a}(\Phi + \varphi)\,, \qquad \varphi := \frac{2\mathcal{V}}{3a^3H^2}\,, \qquad \mathcal{V} := V - \bar{V}\,.$$

We can then impose $\tilde{V} = 0$ (free-particle approximation), and hence (4.29) becomes (2.46), which at initial time, $a = a_i$, becomes the following relation between modulus and phase of the wavefunction

$$\nabla_x^2 \Phi(\mathbf{x}, a_i) = -\frac{\delta_i(r_x)}{a_i}\,, \tag{4.30}$$

with $\delta_i(r_x)$ given by (4.23).

If we restrict to zero angular momentum configurations, which allow the existence of a solely radial velocity field, we can impose spherical symmetry on Φ, and therefore (4.30) becomes (3.58):

$$\Phi(r_x, a_i) = -\frac{(V/a_i^3)}{4\pi\, a_i} \int_0^{r_x} \frac{\bar{\delta}(r'_x, a_i)}{{r_x}'^2}\, dr'_x\,.$$

As it was done in section 3.2, the temporal evolution of the initial configuration $\Psi(r_x, a_i)$ can be computed using the free-particle propagator G via (3.29):

$$\Psi(r_x, a) = \int G(r_x, a|q, a_i)\, \Psi(q, a_i)\, dq\,,$$

where G is given by (3.30).

If we define $\Delta a := a - a_i$, we obtain

$$\begin{aligned}
\Psi(r_x, a) =& (2\pi i\nu\Delta a)^{-1/2} \int e^{\frac{i}{\nu}\frac{(r_x-q)^2}{2\Delta a}} \sqrt{1+\delta_i(q)}\, e^{\frac{i}{\nu}\Phi(q,a_i)}\, dq = \\
=& (2\pi i\nu\Delta a)^{-1/2} \left[\int_0^{R_8} e^{\frac{i}{\nu}\frac{(r_x-q)^2}{2\Delta a}} \sqrt{1 + \frac{4^3\sqrt{2}\sigma_8}{3\sqrt{\pi}} e^{-\frac{1}{2}\frac{q^2}{(R_8/4)^2}}}\, e^{\frac{i}{\nu}\Phi(q,a_i)}\, dq + \right. \\
&\left. + \int_{R_8}^{+\infty} e^{\frac{i}{\nu}\left[\frac{(r_x-q)^2}{2\Delta a} + \Phi(q,a_i)\right]}\, dq \right]\,.
\end{aligned} \tag{4.31}$$

Let us now focus on the second term, the integral between R_8 and $+\infty$. In order to compute it, let us before calculate the following limit

$$\lim_{q\to+\infty} \Phi(q, a_i) = -\frac{1}{a_i}\left[\int_0^{R_8} \frac{\int_0^{r''_x} \delta_i\, {r'_x}^2\, dr'_x}{{r''_x}^2}\, dr''_x + \frac{1}{R_8}\int_0^{R_8} \delta_i\, {r'_x}^2\, dr'_x \right] \in \mathbb{R}\,.$$

Making use of this result, it is easy to see that

$$\lim_{q\to+\infty} \frac{1}{\nu}\left[\frac{(r_x-q)^2}{2\Delta a} + \Phi(q, a_i) \right] = +\infty \tag{4.32}$$

for every (fixed) $(\nu, \Delta a, r_x) \in \mathbb{R}^3_+$.
Therefore the integrand of the second integral in the last line of (4.31) oscillates infinite times, with constant amplitude, in the domain of integration $]R_8, +\infty[$. Because of that, the integral is null and we recover

$$\Psi(r_x, a) = (2\pi i\nu\Delta a)^{-1/2} \int_0^{R_8} \sqrt{1 + \frac{4^3\sqrt{2}\sigma_8}{3\sqrt{\pi}} e^{-\frac{1}{2}\frac{q^2}{(R_8/4)^2}}}\, e^{\frac{i}{\nu}\left[\frac{(r_x-q)^2}{2\Delta a} + \Phi(q,a_i)\right]}\, dq\,. \tag{4.33}$$

This is exactly equal to expression (3.59), if one performs the substitutions

$$\frac{\rho(q,a_i)}{\rho_f(a_i)} \to [1+\delta_i(q)]\ ,$$
$$\frac{R_f}{a} \to R_8\,.$$

This allows us to recover predictions for our density profile (4.23) just re-interpreting the results found in section 3.3 for the profile (3.1). In particular, since the profile (4.23) does not give rise to shell crossing, we have to take the $\nu \to 0$ limit of $\Psi(r_x, a)$ in order to recover the Zel'dovich approximation from the free-particle one [72]. We can therefore make once again use of the stationary phase approximation, which becomes exact in this limit. The stationary points $\bar{q}_s$ of the phase are (3.60):

$$\begin{aligned} r_x &= \bar{q}_s + \Delta a\, \frac{\partial}{\partial q}\Phi(q,a_i)\bigg|_{\bar{q}_s} \\ &= \bar{q}_s - \Delta a\, \frac{1}{a_i\, q^2} \int \delta_i(r'_x)\, {r'_x}^2\, dr'_x \bigg|_{\bar{q}_s} \\ &= \begin{cases} \bar{q}_s - \Delta a\, \frac{1}{a_i\, \bar{q}_s^2} \int_0^{\bar{q}_s} \frac{4^3\sqrt{2}\sigma_8}{3\sqrt{\pi}} \exp\left[-\frac{1}{2}\frac{r_x^2}{(R_8/4)^2}\right] {r'_x}^2\, dr'_x & \bar{q}_s \le R_8 \\ \bar{q}_s - \Delta a\, \frac{1}{a_i\, \bar{q}_s^2} \int_0^{R_8} \frac{4^3\sqrt{2}\sigma_8}{3\sqrt{\pi}} \exp\left[-\frac{1}{2}\frac{r_x^2}{(R_8/4)^2}\right] {r'_x}^2\, dr'_x & \bar{q}_s > R_8 \end{cases} . \end{aligned} \tag{4.34}$$

From the study held in chapter 3 we hence know that the overdensity (4.23) can be decomposed in two parts: an internal one, for which $\bar{\delta}(r_x) \le 3$, that directly collapse, and a complementary external one which initially expands, then turns around and collapse. The initial time mean overdensity inside a sphere of comoving radius r_x is given by (4.9):

$$\bar{\delta}(r_x) = \frac{R_8^3}{r_x^3}\,\sigma_8 \left[\mathrm{erf}\left(\frac{r_x}{\sqrt{2}(R_8/4)}\right) - \frac{1}{\sqrt{2\pi}}\frac{r_x}{(R_8/4)}\, e^{-\frac{1}{2}\left(\frac{r_x}{(R_8/4)}\right)^2}\right] . \tag{4.35}$$

The just written function is a monotonous decreasing one, therefore the critical comoving radius $\tilde{r}_x$ for which

$$\bar{\delta}(\tilde{r}_x) = 3$$

is uniquely defined, and it is

$$\tilde{r}_x = (5.13 \pm 0.01)\,\mathrm{h}^{-1}\,\mathrm{Mpc}\,. \tag{4.36}$$

This value was computed with numerical methods [84] using the already mentioned Planck 2018 [66] value for σ_8; the error was computed with the formula reported in the appendix.

Zel'dovich approximation predicts moreover that regions of the overdensity (4.23) placed at a comoving radius $r_x > \tilde{r}_x$ turn around at a time coordinate given by (3.66):

$$\frac{(\Delta a)_{\mathrm{ta}}}{a_i} = \frac{3-\bar{\delta}(r_i)}{2\bar{\delta}(r_i)}\,.$$

Eventually every shell collapses into a singularity in the centre of symmetry of the configuration, at a time coordinate given by (3.67):

$$\frac{(\Delta a)_{\mathrm{coll}}}{a_i} = \frac{3}{\bar{\delta}(r_i)}\,.$$

The perturbation, globally, is described by the following density profile as a function of the scale factor a (3.72)

$$\rho(r,a) = \frac{a_i^3}{a^3} \frac{1}{\left|1 - \frac{\Delta a}{a_i}\left[\delta(a_i\bar{q}_s, a_i) - \frac{2}{3}\bar{\delta}(a_i\bar{q}_s, a_i)\right]\right|} \rho(a_i\bar{q}_s, a_i)\,. \tag{4.37}$$

As already discussed in the last chapter, the first factor accounts for the dilution of pressureless matter due to the expansion of the Universe, while the second one is due to the gravitational auto-interaction of matter.

As time goes on the density profile becomes more peaked in $r = 0$, until a caustic forms there when the denominator of the second factor of (4.37) becomes null, i.e. at (for the demonstration see section 3.3)

$$\frac{\Delta a_{\text{coll}}}{a_i} = \frac{3}{\delta(0,a_i)} = 0.217 \pm 0.002\ . \tag{4.38}$$

This estimation can be confronted with the exact one (4.27) by means of (3.75):

$$\frac{t_{\text{coll, Zel'dovich}}}{t_{\text{coll, exact}}} = \frac{10}{3\pi}\left(\frac{3}{\delta(0,a_i)}\right)^{1/2} = 0.495 \pm 0.004\,. \tag{4.39}$$

For our profile (4.8) the collapse therefore happens in Zel'dovich approximation twice as fast as predicted by the exact treatment.

In the following section we will describe the evolution of a matter distribution close to the one studied until now, but with a new element.

4.5 Perturbing the system by adding a test body

Let us now consider a test body (i.e. a mini halo) placed inside the spherical configuration which we described in this chapter. Be the mini halo small enough to not perturb sensibly the dynamics of the large-scale distribution (4.23), and in particular to left approximately untouched the average density contrast $\bar{\delta}(r)$. Then all the passages which lead to (4.37) can be repeated and the following expression for the temporal evolution of the system in Zel'dovich approximation is still valid

$$\rho(r_x,a) = \frac{a_i^3}{a^3} \frac{1}{\left|1 - \frac{\Delta a}{a_i}\left[\delta(\bar{q}_s, a_i) - \frac{2}{3}\bar{\delta}(\bar{q}_s, a_i)\right]\right|} \rho(\bar{q}_s, a_i)\,. \tag{4.40}$$

But now, $\delta(\bar{q}_s, a_i)$ presents a bump, where the test halo is initially placed, let us say at a comoving radius $r_x = r_t$ (where t stands for test). Let therefore the mini halo be modelled as point-like.

Obviously, the presence of the test halo destroys the spherical symmetry and it is no more valid that points placed on the same shell have common evolutions. But if the halo is small enough, we can come arbitrarily close to spherical symmetry. If this is the case, $\bar{\delta}(\bar{q}_s, a_i)$ is solely influenced by the large-scale matter distribution (4.23), and

$$\delta(r_t, a_i) = \alpha\, \delta_i(r_t)$$

where $\delta(r_t, a_i)$ is the perturbed density contrast, which accounts fot the presence of the test halo, $\delta_i(r_t)$ is (4.23), and $\alpha > 1$ tunes the dimension of the mini halo.

Since the turnaround time depends only on $\bar{\delta}(r)$ at the initial time, the shell at $r = r_t$ turns around as before, at a time coordinate given by (3.66). What differs, is that (4.40) predicts that the density at comoving radius r_t diverges at

$$1 - \frac{(\Delta a)_{\text{coll},\,t}}{a_i}\left[\alpha\,\delta_i(r_t) - \frac{2}{3}\bar{\delta}(r_t, a_i)\right] = 0$$

which is solved by

$$\frac{(\Delta a)_{\text{coll},\,t}}{a_i} = \frac{1}{\alpha\,\delta_i(r_t) - \frac{2}{3}\bar{\delta}(r_t, a_i)}\,. \tag{4.41}$$

We moreover know that Zel'dovich approximation is valid only until shell do not cross. Therefore we can conclude that a singularity forms at $r_x = r_t$ instead than at $r_x = 0$ if

$$\frac{(\Delta a)_{\text{coll},\,t}}{a_i} < \frac{(\Delta a)_{\text{coll}}}{a_i}$$

(where the right hand side is given by (4.38)), which means if

$$\alpha > \frac{\frac{1}{3}\delta_i(0) + \frac{2}{3}\bar{\delta}(r_t, a_i)}{\delta_i(r_t)}\,. \tag{4.42}$$

$\delta_i(0)$ is fixed and $\bar{\delta}(r, a_i)$ is a more slowly varying function of r than $\delta_i(r)$; therefore (4.42) predicts that regions closer to $r_x = 0$, where $\delta_i(r_t)$ is bigger, need a less massive mini halo placed there (i.e. a lower α) to give rise to a singularity.

4.6 Equilibrium configurations

Until now we saw, with the aid of different techniques, that a spherically symmetric primordial overdensity first of all expands, but at a slower rate than its surroundings, then its shells reach a maximum expansion, and then they "turn around" and collapse. In absence of shell crossing they continue collapsing till they form a singularity, while in a realistic case shell crossing provides the mixing necessary to make violent relaxation take place [50]. At the end of this phase the system approaches a virialized state of equilibrium. Once the system has virialized, its density and size do not change [56]. In other words, its internal evolution decouples from the expansion of the Universe. Because of that, in this phase the CDM evolution can be fairly described by SN equations in a static background (1.19), (1.20) [17]:

$$i\nu\frac{\partial\psi}{\partial t} = \left(-\frac{\nu^2}{2}\nabla^2 + V\right)\psi \tag{4.43}$$

$$\nabla^2 V = 4\pi G\,|\psi|^2\,. \tag{4.44}$$

Moroz, Penrose and Tod in [53] found solutions of this system valid once two assumptions are made:

- *spherical symmetry*: for what concerns their spatial dependence, $\rho := |\psi|^2$ and subsequently V, in a 3D spherical system of coordinates, are functions of the radial one only;
- *stationarity*: the matter distribution does not evolve, i.e. ρ does not depend on time. Consequently, neither the gravitational potential V vary in time.

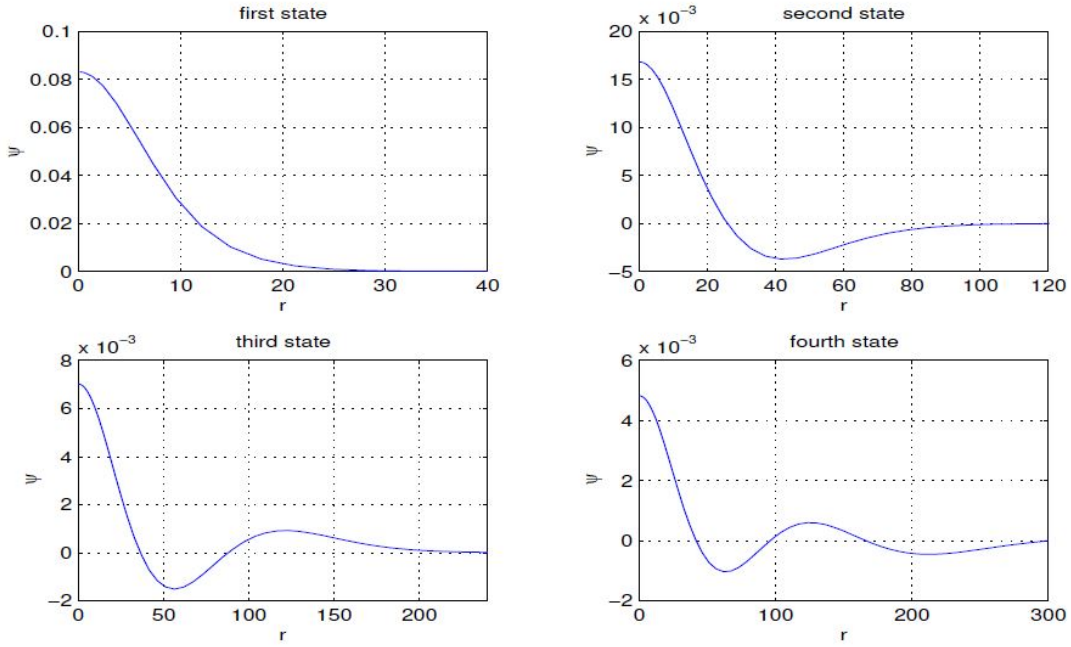

Figure 4.2: The four lowest energy solutions of Schroedinger-Newton equations. From [35].

The first assumption is true by construction for the profile we studied until now, while the second becomes valid once virialization is achieved.

The solution of Poisson equation in this hypothesis takes the form

$$V(r) = -4\pi G \frac{\int_0^r r'^2 \rho(r')\, dr'}{r}\,. \tag{4.45}$$

Since we made the assumption that the gravitational potential V doesn't vary in time, we can separate the variables of the Schrödinger equation, obtaining the static Schrödinger equation [53]

$$-\frac{\nu^2}{2}\nabla^2\psi + V\psi = E\psi \tag{4.46}$$

still coupled to the Poisson one.

Because of stationarity, $\phi(\mathbf{x}, t)$ is constant. Since therefore the phase of the wavefunction ψ (1.14) is constant too, we can make use of the global U(1) symmetry of states in Quantum Mechanics and consider ψ real without loss of generality [53].

Demanding only that ψ and V be finite and smooth everywhere, Tod and Moroz in [77] show analytically that there is a discrete family of solutions of equations (4.43) and (4.44), the *bound-state* solutions, labelled by natural numbers. The wavefunction of the nth solution has n zeros, and the wavefunctions are normalizable. The corresponding energy eigenvalues are negative, converging monotonically to zero as n increases. These solutions are the only finite and smooth $\forall r$; other solutions tend to infinity at a finite value of the coordinate r.

The explicit analytical expression for the $\psi_n(r)$ is not known, but Moroz et al. in [53] calculate them numerically. In *figure 4.2* is plotted the result for the first four eigenfunctions, normalized such that $\int |\psi|^2\, d^3x = 4\pi$. The first eigenvalues E_n in units of G^2/ν^2 are collected in the table in *figure 4.3* and plotted in *figure 4.4*. Since they are negative,

Number of zeros	Energy Eigenvalue
0	-0.16276929132192
1	-0.03079656067054
2	-0.01252610801692
3	-0.00674732963038
4	-0.00420903256689
5	-0.00287386420271
6	-0.00208619042678
7	-0.00158297244845
8	-0.00124207860434
9	-0.00100051995162
10	-0.00082314193054
11	-0.00068906850493
12	-0.00058527053127
13	-0.00050327487416
14	-0.00043737620824
15	-0.00038362194847
16	-0.00033920111442
17	-0.00030207158301
18	-0.00027072080257
19	-0.00024400868816
20	-0.00022106369652

Figure 4.3: In the first column the number of zeros n of the eigenfunction, and in the second one the corresponding energy eigenvalues in units of G^2/ν^2. From [35].

in order to use a log scale, in the y axis is shown (the logarithm of) the absolute value of the energy.
In the paper the authors actually consider a different version of SN equations, in which ν is replaced by $\hbar/m$. In that context, the parameter m represents the mass of the particle described by the wavefunction ψ, and it appears in the unit of measure of the energy eigenvalues. Definitions in the paper are different from the ones adopted here in two aspects: (4.46) is written in a way which imply that the energy eigenvalue, for a certain potential V, is defined as $E_{\mathrm{MPT}} = mE$. Moreover, the gravitational potential obeys to a Poisson equation in which in the right hand side a term m^2 more than in (4.44) appear.

These stationary solutions represent, once averaged with Husimi procedure and squared, the possible density profile to which an halo can settle down when virialized.

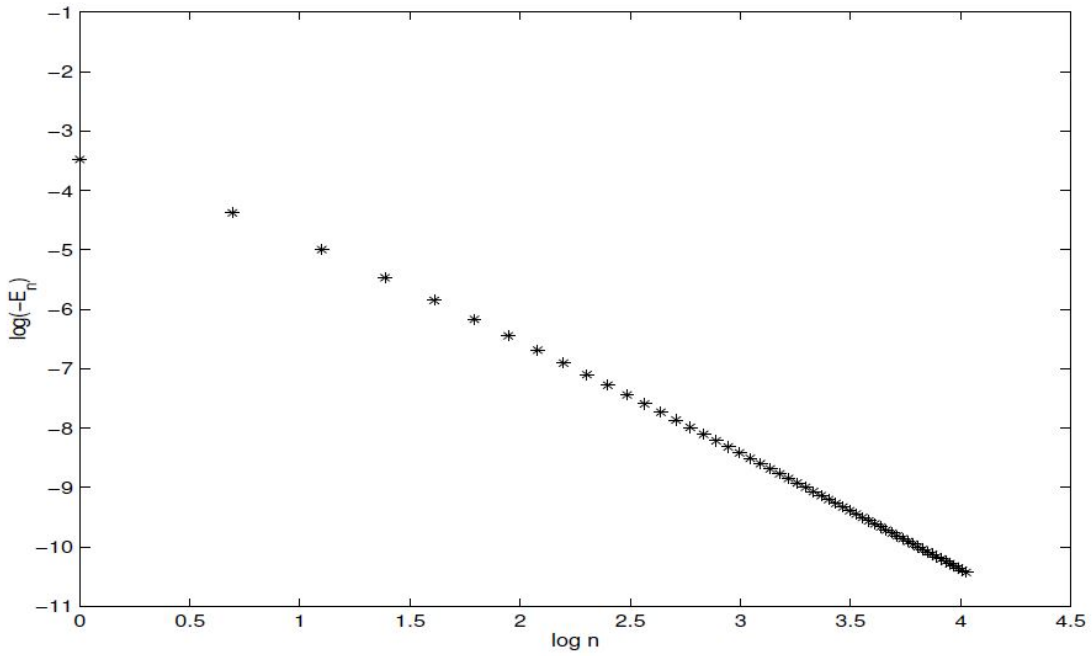

Figure 4.4: Log-log plot of the energy eigenvalues vs the number of nodes n of the corresponding eigenfunction. From [35].

Chapter 5

Top-hat SN solution in a ΛCDM background

The standard model of cosmology contemplates the existence of a non vanishing cosmological constant Λ in order to properly forecast the observed accelerated expansion of the Universe, and a number of other characteristics of its, such as age, flatness, number of galaxies at high redshift and large-scale structure, as it is resumed in [41].
It is therefore worth considering the same homogeneous overdensity of mass M studied by Johnston et al. in [38] and exposed in section 2.4, in a Universe with non null cosmological constant. This will indeed provide a more accurate description of spherical collapse in our Universe. Moreover, since we used the Johnston et al. top-hat solution to find solutions of SN equations for the overdensities treated in the previous chapter, with this generalization we can comment also on the evolution of those overdensities in a ΛCDM background.

In the paper of Johnston et al. [38] SN solutions for a flat and a closed universe with non null cosmological constant are presented, but without explicitly computing the piecewise solution of the top-hat overdensity (for which care has to be taken to match the potentials at boundaries). Here, by constructing the compensated top-hat solution and by studying the temporal evolution of the quantities appearing in it, we will see the qualitative evolution of the overdensity in a Universe with $\Lambda \neq 0$, in comparison with the one in an EdS background. Moreover, a way of generalizing a solution of SN equation in a certain background to another arbitrary background, is presented, using equations derived in [72].

In this chapter we therefore aim at finding a solution of Schrödinger-Newton equations for the overdensity depicted in *figure 2.1* in a Universe with $\Lambda \neq 0$.

5.1 Top-hat solution in terms of physical coordinates

Flat region For the flat region at $r \geq R_f$ we already know the solution from the work of Johnston et al. [38]: as demonstrated in chapter 2.4, the following expressions for the matter density and the velocity and gravitational potentials hold (I am following the same

notation adopted in chapter 2.4) [38]

$$\rho_f(t) = \frac{\Lambda c^2}{8\pi G}\,\mathrm{cosech}^2\,(\lambda t)\ , \tag{5.1}$$

$$\phi_f(r,t) = \frac{H_f r^2}{2} + \mathcal{C}(t)\,, \tag{5.2}$$

$$V_f(r,t) = \frac{\Lambda c^2}{12}\left[\coth^2(\lambda t) - 3\right] r^2 + \mathfrak{c}(t)\,, \tag{5.3}$$

where

$$\lambda := \frac{3}{2}\sqrt{\frac{\Lambda c^2}{3}}\,,$$

$$H_f(t) = \sqrt{\frac{8\pi G}{3}\rho_f(t) + \frac{\Lambda c^2}{3}}\,, \tag{5.4}$$

and $\mathcal{C}$ and $\mathfrak{c}$ are generic functions of time only. The form of the velocity potential is motivated by the fact that, as in the work by Johnston et al., the only motion of the matter present is the one due to the Hubble expansion of the Universe. From (5.1) we can deduce the temporal evolution of R_f knowing that the overdensity is compensated (i.e. $M = (4/3)\pi R_f^3 \rho_f$):

$$R_f(t) = \sqrt[3]{\frac{6GM}{\Lambda c^2}}\,\sinh^{2/3}\,(\lambda t)\ . \tag{5.5}$$

Void region Let us define the energy density associated to a certain cosmological constant Λ as follows

$$\rho_v = \frac{\Lambda c^2}{8\pi G}\,.$$

We know that in the case of an energy density which is constant in a comoving volume, like the pressureless matter one ρ_f, which scales like a^{-3}, the following equation [55]

$$\nabla_r^2 V_f = \frac{1}{a^2}\nabla_x^2 V_f = 4\pi G \rho_f \tag{5.6}$$

is solved by [55]

$$V_f = \frac{2\pi G}{3}\rho_f |\mathbf{x}|^2\,. \tag{5.7}$$

Now as ρ_f is constant in comoving coordinates, ρ_v is constant in physical ones, therefore multiplying both sides of (5.6) by a^2 and operating the substitution $\mathbf{x} \to \mathbf{r}$, the solution to

$$\nabla_r^2 V_v = 4\pi G \rho_v \tag{5.8}$$

happens to be

$$V_v = \frac{2\pi G}{3} a^2 \rho_v |\mathbf{r}|^2 = \frac{\Lambda c^2}{12} a^2 |\mathbf{r}|^2\,. \tag{5.9}$$

The matter density in the void region $R_c < r < R_f$ is null by definition, and therefore the velocity potential is undefined.

Closed region To find the SN solution valid in the region $r \leq R_c$, we will rely on the description of the temporal evolution of an homogeneous spherical overdensity in a $\Lambda \neq 0$ Universe held in [79] by Wang et al.. Let us define the following two parameters

$$x := \frac{a}{a_0}\,, \tag{5.10}$$

$$y := \frac{R_c}{R_{\max}}\,, \tag{5.11}$$

where a_0 is the value of the scale factor today and $R_{\max}$ is the radius of the overdensity at turn-around time. With these, the time evolution of the matter density in the region $r \leq R_c$, ρ_c is [79]

$$\rho_c = \frac{3}{8\pi G}\,\frac{1}{y^3}\,H_f^2(t_{\rm ta})\,\Omega_m(t_{\rm ta})\,\chi_c(t_{\rm ta})\,, \tag{5.12}$$

where $t_{\rm ta}$ is the instant of turnaround of the overdensity. In the just written expression they appear a few quantities which need to be defined and require an expression for their temporal evolution:

- H_f^2 is given by (5.4).
- $\Omega_m(t_{\rm ta})$ is the following matter energy density parameter, computed at $t_{\rm ta}$

$$\Omega := \frac{8\pi G\rho_f}{3H_f^2}\,.$$

- $\chi_c(t_{\rm ta})$ is the ratio

$$\chi_c(t_{\rm ta}) := \frac{\rho_c(t_{\rm ta})}{\rho_f(t_{\rm ta})}\,.$$

  In [79] the following approximate expression for this parameter is provided

$$\chi_c(t_{\rm ta}) = \left(\frac{3\pi}{4}\right)^2 \Omega_m^{-0.85+0.26\Omega_m}(t_{\rm ta})\,. \tag{5.13}$$

  In a calculation reported in the appendix, it is shown that using the values $\rho_c(t_{\rm ta})$ and $\rho_f(t_{\rm ta})$ valid in a Universe with $\Lambda = 0$, i.e. the ones exposed in chapter 2.4, the parameter $\chi_c(t_{\rm ta})$ takes the value $(3\pi/4)^2$ as (5.13) prescribes.

- The parameter y can be computed once we know R_c and $R_{\max}$. The latter can be computed as

$$R_{\max} = \frac{R_f(t_{\rm ta})}{\sqrt[3]{\chi_c(t_{\rm ta})}}\,,$$

  where we know the denominator from (5.13) and the numerator from (5.5) once we know $t_{\rm ta}$. Let us find $t_{\rm ta}$ and an expression for $R_c(t)$, relying on the results of Coquereaux et al. in [20].
  Let us define the following length scale [20]

$$\Lambda_c := \left(\frac{\pi}{2GM}\right)^2\,. \tag{5.14}$$

  Analytical expressions for $R_c(t)$ are different if the parameter

$$\mathcal{L} := \frac{\Lambda}{\Lambda_c} \tag{5.15}$$

takes values higher or lower than 1 [20]. Let us compute the critical mass $M_{\rm cr}$ which realizes the condition $\mathcal{L} = 1$.

$$M_{\rm cr} = \frac{\pi c^3}{2G\Lambda^{1/2}} = \frac{\pi c^4}{2GH_0\sqrt{3\Omega_\Lambda}}\,; \tag{5.16}$$

substituting the Planck 2018 values for the cosmological parameters [66]

$$H_0 = (67.36 \pm 0.54)\frac{km/s}{Mpc} \qquad \text{and} \qquad \Omega_\Lambda = 0.6847 \pm 0.0073$$

one obtains

$$M_{\rm cr} \sim 10^{23}\mathrm{M}_\odot\,. \tag{5.17}$$

If with the top-hat solution we are considering, we aim at studying a dark matter halo, M is far below this critical mass, since gravitational lensing based mensurations show that a galaxy cluster has typically a mass around $M_{\rm gc} \sim 10^{15}\mathrm{M}_\odot$ [16]. Moreover theories of structure formation in a Cold Dark Matter dominated Universe predict that massive clusters of galaxies assemble from the hierarchical merging of lower mass subhalos [64]. Therefore in the hypothesis of describing a CDM halo, we can safely restrict to the $\mathcal{L} < 1$ case.

Let us define the reduced blackbody temperature T in the following way [20]

$$R_c(\tau) = \frac{1}{\Lambda_c^{1/2}T(\tau)}\,, \tag{5.18}$$

where τ is the conformal time defined by $d\tau = dt/R_c$. In terms of this variable the we can define the following parameter too [20]

$$H_c(\tau) = \frac{\dot{R}_c}{R_c} = -\Lambda_c^{1/2}\frac{dT}{d\tau}\,. \tag{5.19}$$

In the $\mathcal{L} < 1$ case, neglecting radiation pressure, [20] gives the following expression for the reduced blackbody temperature

$$T(\tau) = 6\left(\wp(\tau; \frac{1}{12}, \frac{1-2\mathcal{L}}{6^3}) + \frac{1}{12}\right)\,, \tag{5.20}$$

where $\wp$ denotes Weierstrass p-function, defined as [71]

$$\wp(z; g_2, g_3) = \frac{1}{z^2} + \sum_{g\in\Gamma\setminus\{0\}}\left(\frac{1}{(z-g)^2} - \frac{1}{g^2}\right)\,, \tag{5.21}$$

with $\Gamma = 2g_1\mathbb{Z} + 2g_2\mathbb{Z}$. The behaviour of $T(\tau)$ is shown by *figure 5.1.* We can notice it is periodic and it ranges from a minimum, T_N, to infinity (the period P and T_N can be both calculated, for details see [20]). Referring to (5.18), we can see that this means that $R_c(\tau)$ is periodic too, and limited. It grows from $R_c(0) = 0$ to a maximum

$$R_{\rm max} = \frac{1}{\Lambda_c^{1/2}T_N}\,,$$

then it turns around and decreases until $R_c(P) = 0$.

In order to confront this result for the temporal evolution of R_c with the ones of quantities of the other regions, it is necessary to relate conformal and physical time.

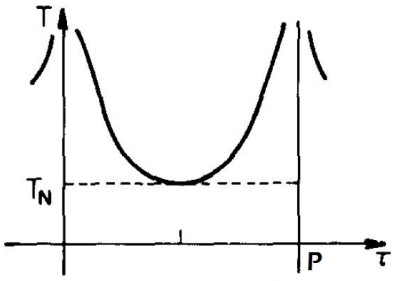

Figure 5.1: Graph of the reduced blackbody temperature T of a closed Universe with non vanishing cosmological constant versus conformal time τ (in the case $\mathcal{L} < 1$). Adapted from [20].

Integrating the definition of the former, we obtain

$$\int dt = \int R_c(\tau)\, d\tau \tag{5.22}$$

$$t = \frac{1}{\Lambda_c^{1/2}} \int \frac{1}{T(\tau)}\, d\tau \tag{5.23}$$

$$t = \frac{2}{\Lambda_c^{1/2}} \int \frac{1}{\left(12\wp(\tau; \frac{1}{12}, \frac{1-2\mathcal{L}}{6^3}) + 1\right)}\, d\tau\,, \tag{5.24}$$

where all the integrals should be considered between the instant of Big Bang and a generic time t or τ.

We have therefore an expression for $R_c(t)$, (5.18,) and $t_{\rm ta} = t(P)$.

In [38] the following expression for $\alpha_c := \sqrt{\rho_c}$, equivalent to (5.12), is proposed:

$$\alpha_c = \text{constant} \times \exp\left(-\frac{3}{2}\int H_c dt\right)\,.$$

Knowing $H_c(\tau)$, (5.19), and $t(\tau)$, (5.24), we can write the velocity potential valid in the $r \leq R_c$ in analogy with the one for $r \geq R_f$ [38]:

$$\phi_c = \frac{1}{2} H_c r^2 + \mathcal{K}(t)\,, \tag{5.25}$$

with $\mathcal{K}$ generic.

Now that we know ϕ_c , we can calculate the gravitational potential V_c by means of Bernoulli equation (1.13) in the following way: let us write $\mathcal{K}(t)$ in the form

$$\phi_c = \frac{H_c r^2}{2} - \int_0^t \kappa(t')\, dt'\,.$$

Then Bernoulli equation [19]

$$\frac{\partial \phi_c}{\partial t} + \frac{1}{2}(\nabla \phi_c)^2 = -V_c$$

becomes

$$\frac{r^2}{2}\left(\frac{\ddot{R}_c}{R_c} - H_c^2\right) - \kappa = -\frac{1}{2} H_c^2 r^2 - V_c\,,$$

and

$$\frac{r^2}{2}\left(\frac{\ddot{R}_c}{R_c}\right) - \kappa = -V_c\,, \tag{5.26}$$

and hence, using Friedmann equations,

$$V_c(r,t) = \left[\frac{4\pi G}{3}\left(\rho_c + 3\frac{P_\Lambda}{c^2}\right)\right]\frac{r^2}{2} + \kappa(t)\,. \tag{5.27}$$

P_Λ is the pressure due to the effect of the cosmological constant, which obeys the following equation of state

$$P_\Lambda = -\rho_v = -\frac{\Lambda c^2}{8\pi G}\,. \tag{5.28}$$

Johnston et al. write equation (5.26) in terms of the deceleration parameter, defined as $q = -\ddot{R}_c R_c/\dot{R_c}^2$ and thus find [38]

$$V_c(r,t) = \frac{1}{2}qH^2r^2 + \kappa\,. \tag{5.29}$$

In the $\Lambda \neq 0$ case, for arbitrary spatial curvature the deceleration parameter reads [38]

$$q = \left(\frac{1}{2}\Omega_c - \Omega_\Lambda\right)\,,$$

where [38]

$$\Omega_c := \frac{8\pi G\rho_c}{3H_c^2}\,, \qquad\qquad \Omega_\Lambda = \frac{\Lambda c^2}{3H^2}.$$

The two expressions (5.27) and (5.29) are equivalent.

Piecewise SN solution for the top-hat We are now ready to write the modulus of the wavefunction solution of SN equations for a top-hat overdensity as the one in *figure 2.1* in presence of cosmological constant:

$$\alpha = \begin{cases} \sqrt{\rho_c} & r \leq R_c(t) \\ 0 & R_c(t) < r < R_f(t) \\ \sqrt{\rho_f} & r \geq R_f(t)\,. \end{cases} \tag{5.30}$$

Let us now consider its phase, therefore the velocity potential ϕ. We need to determine the constants of time only $\mathcal{C}$ in (5.2) and $\mathcal{K}$ in (5.25). They can be set by imposing Bernoulli equation at the discontinuities R_c and R_f. The result is as follows

$$\phi = \begin{cases} \frac{H_c r^2}{2} + \int_0^t \left[-\frac{\Lambda c^2}{12}a^2R_c^2 + \frac{4\pi G}{3}\rho_c\frac{R_c^2}{2}\right]dt' & r \leq R_c(t) \\ \text{undefined} & R_c(t) < r < R_f(t) \\ \frac{H_f r^2}{2} + \int_0^t \frac{\Lambda c^2}{12}\left[-a^2 + \coth^2(\lambda t') - 3\right]R_f^2\,dt' & r \geq R_f(t)\,. \end{cases} \tag{5.31}$$

Meanwhile to set the constants $\mathfrak{c}(t)$ and $\kappa(t)$ present respectively in the expression found for V_f and for V_c we have to impose continuity of the gravitational potential, and Bernoulli equation to relate $\mathfrak{c}(t)$ and $\kappa(t)$ with $\mathcal{C}$ and $\mathcal{K}$ of the velocity potentials; the result is as follows

$$\mathfrak{c}(t) = \frac{\Lambda c^2}{12}\left[a^2 - \coth^2(\lambda t) + 3\right]R_f^2\,, \tag{5.32}$$

$$\kappa(t) = \frac{\Lambda c^2}{12} a^2 R_c^2 - \frac{2\pi G}{3} \rho_c R_c^2 \,. \tag{5.33}$$

The scale factor $a(t)$ has to be proportional to $R_f(t)$, but we can set freely the proportionality constant. If we set

$$a := \frac{R_f}{\sqrt[3]{\frac{6GM}{\Lambda c^2}}} \,, \tag{5.34}$$

$\mathfrak{c}$ takes a simpler form:

$$\mathfrak{c}(t) = \frac{\Lambda c^2}{12} \left[\sinh^{4/3}(\lambda t) - \coth^2(\lambda t) + 3 \right] R_f^2 \,. \tag{5.35}$$

Therefore, the Newtonian potential of a homogeneous compensated spherically symmetric overdensity in a ΛCDM background is

$$V = \begin{cases} \frac{2\pi G}{3} \rho_c r^2 + \kappa(t) & r \leq R_c \\ \frac{\Lambda c^2}{12} a^2 r^2 & R_c < r < R_f \\ \frac{\Lambda c^2}{12} \left[\coth^2(\lambda t) - 3 \right] r^2 + \mathfrak{c}(t) & r \geq R_f \,. \end{cases} \tag{5.36}$$

Because of discontinuities of the first derivative at both boundaries, this potential is not C^1 as the one in [38]; it is only C^0.

The explicit expression of ρ_c as a function of time can't be found analytically, from the quantities we defined above. In the following we propose therefore an alternative path, which leads to the same solution.

5.2 Schrödinger-Newton equations in a generic background

In section 2.2 we considered how to write SN equations in an Einstein-de Sitter (EdS) Universe (i.e. spatially flat with vanishing cosmological constant). In this section, we will resume the generalization of SN equations to Universes with generic density parameter Ω and cosmological constant Λ, done by Short and Coles in [72].

Writing the Newtonian dynamical equations governing the evolution of fluctuations δ in a fluid of collisionless self-gravitating CDM in an expanding Universe, one can show (see [2]) that, to first order in Eulerian PT, δ grow according to $\delta = D\delta_i$ where δ_i is the density contrast at some initial time t_i and the linear growth factor $D = D(t)$ is the growing mode solution of [14]

$$\ddot{D} + 2H\dot{D} - 4\pi G\bar{\rho} D = 0 \tag{5.37}$$

normalized so that $D_i = D(t_i) = 1$.

The dependence of D on t is in general quite complicated [14] (as previously mentioned, in the Einstein-de Sitter case $D(t) \propto a(t)$ [14]), nonetheless using the linear growth factor as time coordinate has the advantage of keeping the generalization to an arbitrary Universe of CDM fluid equations (1.9), (1.13) and (1.11) in a simple form: defining [72]

$$\mathbf{w} = \frac{d\mathbf{x}}{dD} \tag{5.38}$$

we find [72]

$$\frac{\partial \chi}{\partial D} + \nabla_x \cdot (\chi \mathbf{w}) = 0 \,, \tag{5.39}$$

$$\frac{\partial \mathbf{w}}{\partial D} + (\mathbf{w}\cdot\nabla_x)\mathbf{w} + \frac{3\bar{\Omega}}{2f^2 D}\mathbf{w} = -\nabla_x \Theta\,, \tag{5.40}$$

$$\nabla_x^2 \Theta = \frac{3\bar{\Omega}}{2f^2 D^2}\delta\,; \tag{5.41}$$

where [72]

$$f_g := \frac{d\ln D}{d\ln a} = \frac{\dot{D}}{HD} \tag{5.42}$$

is called growth index [79] and [72]

$$\Theta := \frac{\mathcal{V}}{a^2\dot{D}^2}\,, \tag{5.43}$$

where $\mathcal{V}$ is the peculiar gravitational potential and $\bar{\Omega}$ is as usual

$$\bar{\Omega} := \frac{8\pi G\bar{\rho}}{3H^2}\,. \tag{5.44}$$

Assuming an irrotational velocity field we can define the velocity potential once again as [72]

$$\mathbf{u} := \nabla_x \Phi\,. \tag{5.45}$$

With that we can integrate (5.40) obtaining Bernoulli equation [72]

$$-\frac{\partial \Phi}{\partial D} - \frac{1}{2}|\nabla_x \Phi|^2 = \tilde{V}\,, \tag{5.46}$$

where, as in the flat case, the effective potential $\tilde{V}$ depends on both the modified peculiar gravitational potential Θ and the velocity potential Φ [72]:

$$\tilde{V} = \Theta + \frac{3\bar{\Omega}}{2f^2 D}\Phi\,. \tag{5.47}$$

We possess now all the ingredients to perform the Madelung transformation [72]

$$\psi := \sqrt{\chi}\, e^{i\Phi/\nu} \tag{5.48}$$

which leads to the following Schrödinger-Poisson system [72]

$$i\nu\frac{\partial \psi}{\partial D} = -\frac{\nu^2}{2}\nabla_x^2\psi + (\tilde{V} + Q)\,\psi \tag{5.49}$$

$$\nabla_x^2\left[\tilde{V} - \frac{3\bar{\Omega}}{2f^2 D}\nu\arg(\psi)\right] = \frac{3\bar{\Omega}}{2f_g^2 D^2}(|\psi|^2 - 1)\,. \tag{5.50}$$

5.3 Top-hat solution in terms of comoving adapted coordinates

We can perform the generalization of the solution found by Johnston et al. to a Universe in which the cosmological constant is not null by using the above written equations. Let us use as background the matter density, velocity and gravitational potential of the flat region (ρ_f, ϕ_f, V_f).

In order to find the temporal variable $D(t)$, let us define the following parameter [41]

$$\lambda_0 := \frac{\Lambda}{3H_0^2}\,; \tag{5.51}$$

present observations suggest $\lambda_0 \simeq 0.8$.

Health (1977) showed that the growing mode $D(t)$, which obeys equation (5.37), is [41]

$$\delta \propto H_0^{-2} X^{1/2} x^{-1} \int_0^x X^{-3/2} dx\,, \tag{5.52}$$

where x is given by (5.10) and $X := 1 + \Omega_0(a^{-1} - 1) + \lambda_0(a^2 - 1)$. For a derivation of the exact $D(t)$ see the appendix, let us here recall some approximate expressions for the growth index (5.42) (knowing it determines also $D(t)$).

Wang et al. in [79] propose the following approximation

$$f_g = \Omega_m^\alpha(s)\,, \tag{5.53}$$

where, once set the following equation of state for dark energy

$$p_\Lambda = w\rho_\Lambda\,, \tag{5.54}$$

α is given by

$$\alpha = \frac{3}{5 - \frac{w}{1-w}} + \frac{3}{125}\frac{(1-w)(1-\frac{3}{2}w)}{\left(1-\frac{6}{5}w\right)^3}(1-\Omega_m) + o(1-\Omega_m)\,, \tag{5.55}$$

and therefore for ΛCDM ($w = -1$) $\alpha \simeq 6/11 \simeq 0.55$.

Lahav et al. in [41] improve the approximation with the following expression, valid in the range $-5 \leq \lambda \leq 5$, $0.03 \leq \Omega \leq 2$

$$f_g(x) \simeq \Omega^{0.6}(x) + \frac{1}{70}\lambda(x)\left(1 + \frac{1}{2}\Omega(x)\right)\,, \tag{5.56}$$

with $\lambda(x) := \Lambda/[3H^2(x)]$; the mean error in this approximation is 2 per cent (with a maximum error of 33 per cent in the low-Ω_0 case) [41]. Let us set $D(t)$ by (5.56).

Let us now concentrate on the region at $r < R_c(t)$. There the Newtonian potential V_c satisfies

$$\nabla_r^2 V_c = 4\pi G\rho_c = 4\pi G(\rho_f + \rho_v + \Delta\rho_c)\,, \tag{5.57}$$

where ρ_f is the matter density in the region $r > R_f$ and ρ_v is the energy density of the void, i.e. of dark energy; therefore the background energy density in the $r > R_f$ region is $\bar{\rho} = \rho_f + \rho_v$. We know from section 2.2 that the solution to the following equation

$$\nabla_r^2 \bar{V} = 4\pi G\bar{\rho} \tag{5.58}$$

is given by eq. (2.49)

$$\bar{V} = \frac{\Lambda c^2}{12}\left[\coth^2(\lambda t) - 3\right] r^2\,, \tag{5.59}$$

where

$$\lambda := \frac{3}{2}\sqrt{\frac{\Lambda c^2}{3}}\,. \tag{5.60}$$

The peculiar gravitational potential $\mathcal{V}_c$ in the region $r < R_c$, defined by

$$V_c = \bar{V} + \mathcal{V}_c \,, \tag{5.61}$$

obeys the following Poisson equation

$$\nabla_x^2 \mathcal{V}_c = 4\pi G a^2 (\rho_c - \bar{\rho}) = 4\pi G a^2 \bar{\rho} \delta_c \,. \tag{5.62}$$

With $\mathcal{V}_c$ we can find Θ of last section and with that the effective potential $\tilde{V}$

$$\Theta := \frac{\mathcal{V}_c}{a^2 \dot{D}^2} \qquad\qquad \tilde{V} = \Theta + \frac{3\bar{\Omega}}{2f^2 D} \Phi \,.$$

Defining

$$\psi := \sqrt{\frac{\rho_c}{\bar{\rho}}}\, e^{i\Phi/\nu} \tag{5.63}$$

the SN equations governing the evolution of the region $r < R_c$ become (5.49) and (5.50).

But also the $\Lambda = 0$ case studied by Johnston et al. can be described by the same equations, once

- we use as time variable the EdS growing mode solution of (5.37) $D(t) \propto a_{\Lambda=0}(t)$; an explicit expression for $a_{\Lambda=0}(t)$ is (2.68);
- we define the effective potential $V_{\Lambda=0}$ as

$$V_{\Lambda=0} = \frac{\mathcal{V}_{\Lambda=0}}{a_{\Lambda=0}^2 \dot{a}_{\Lambda=0}^2} + \frac{3}{2a_{\Lambda=0}} \Phi_{\Lambda=0} \,, \tag{5.64}$$

  where $\mathcal{V}_{\Lambda=0}$ is given by the potential in (2.79) valid for $r < R_c$ minus the one valid for $r > R_f$, and $\Phi_{\Lambda=0}$ is given by equation (3.20), which gives

$$\Phi_{\Lambda=0}(\phi_{\Lambda=0}) = \frac{1}{a_{\Lambda=0}^2 \dot{a}_{\Lambda=0}} \phi_{\Lambda=0} - \frac{1}{a_{\Lambda=0}} \frac{r_x^2}{2} \,; \tag{5.65}$$

- we define

$$\psi_{\Lambda=0} := \sqrt{\frac{\rho_{c,\Lambda=0}}{\rho_{f,\Lambda=0}}}\, e^{\frac{i}{\nu}\Phi_{\Lambda=0}} \,. \tag{5.66}$$

Therefore, knowing that the Johnston et al. one, with this formalism, is a solution of (5.49) and (5.50), we can exploit the formal equality of equations with and without cosmological constant, and find the solution in presence of dark energy just interpreting differently (i.e. in the light of a different background), the quantities appearing in the $\Lambda = 0$ case. Starting therefore with the expression for $\psi_{\Lambda=0}$ known from Johnston et al., we must interpret $V_{\Lambda=0}$ as V, $\psi_{\Lambda=0}$ as ψ and the time variable as $D(t)$, i.e.:

$$V_{\Lambda=0} = \frac{\mathcal{V}_c}{a^2 \dot{D}^2} + \frac{3\Omega_f}{2f^2 D} \Phi \,, \tag{5.67}$$

$$\sqrt{\frac{\rho_{c,\Lambda=0}}{\rho_{f,\Lambda=0}}}\, e^{\frac{i}{\nu}\Phi_{\Lambda=0}} = \sqrt{\frac{\rho_c}{\bar{\rho}}}\, e^{i\Phi/\nu} \,, \tag{5.68}$$

where $\rho_{f,\Lambda=0}(t)$ is given by (2.47) and

$$\Omega_f := \frac{8\pi G \rho_f}{3H_f^2} \,. \tag{5.69}$$

Therefore these two equations, together with the Poisson one for the peculiar gravitational potential (5.62), form a system of three coupled equations in three unknowns: ρ_c, Φ, $\mathcal{V}_c$.

The path followed until now is completely general: it allows, knowing a solution of SN equations in a certain background, to find its equivalent in another background, defined by its energy density, velocity and gravitational potential.

Solving equation (5.67) for the gravitational potential in the overdense region, one obtains

$$V_c = \frac{GMa^2\dot{D}^2}{a^2_{\Lambda=0}\dot{a}^2_{\Lambda=0}}\left(\frac{a^2_{\Lambda=0}r_x^2}{2R^3_{c,\Lambda=0}} - \frac{a^2_{\Lambda=0}r_x^2}{2R^3_{f,\Lambda=0}} + \frac{3}{4R_{c,\Lambda=0}} + \frac{3}{4R_{f,\Lambda=0}}\right) + \frac{3a^2\dot{D}^2}{2a_{\Lambda=0}}\left(\frac{H_{c,\Lambda=0}r_x^2}{2\dot{a}_{\Lambda=0}} - \frac{r_x^2}{2a_{\Lambda=0}}\right) + \\ - \frac{3\Omega_f a^2\dot{D}^2}{2f^2D}\left(\frac{H_c r_x^2}{2\dot{a}} - \frac{r_x^2}{2a}\right) + \frac{\Lambda c^2}{12}\left[\coth^2(\lambda t) - 3\right] r^2 + c(t) \quad (5.70)$$

with $c(t)$ (for continuity):

$$c(t) = \frac{2\pi G}{3}a^2\rho_v R_c^2 - \frac{a^2\dot{D}^2 GM}{a^2_{\Lambda=0}\dot{a}^2_{\Lambda=0}}\left(\frac{1}{2R_{c,\Lambda=0}} - \frac{R^2_{c,\Lambda=0}}{2R^3_{f,\Lambda=0}} + \frac{3}{4R_{c,\Lambda=0}} + \frac{3}{4R_{f,\Lambda=0}}\right) + \\ - \left[\frac{3}{2a_{\Lambda=0}}\left(\frac{H_{c,\Lambda=0}R_c^2}{2\dot{a}_{\Lambda=0}} - \frac{R_c^2}{2a_{\Lambda=0}}\right) - \frac{3\Omega_f}{2f^2D}\left(\frac{H_c R_c^2}{2\dot{a}} - \frac{R_c^2}{2a}\right)\right]\dot{D}^2 - \frac{\Lambda c^2}{12}\left[\coth^2(\lambda t) - 3\right] R_c^2 \,. \quad (5.71)$$

With this potential one can solve Schrödinger equation (5.49) for ρ_c. Then $\phi_c = (1/2)H_c r^2$, where the Hubble function can be easily computed with Friedmann equations knowing ρ_c.

The analytical complexity of the solution has, in any case, increased respect to the $\Lambda = 0$ case of chapter 2.4. What however has not changed is its qualitative behaviour for an overdensity with $M < M_{\rm cr} \sim 10^{23}\mathrm{M}_\odot$ (with $M_{\rm cr}$ precisely given by (5.16)): the overdense region is expected to expand, with a slower rate than the void one, until it reaches a maximum radius and then starts to collapse finally giving rise to a singularity. The qualitative behaviour of the overdensity studied in chapters 3 and 4 in an Einstein de Sitter background would be therefore the same in a ΛCDM one.

Chapter 6

Conclusions

In this thesis the collapse of spherically symmetric CDM overdensities has been studied using techniques which are signature of quantum mechanics.

This has been possible thanks to the wave-mechanical approach to the study of collisionless self-gravitating matter exposed in chapter 1. The justification of this approach lays in the mathematical equivalence of a system of coupled Schrödinger and Poisson equations, which takes the name of Schrödinger-Newton equations, and a slightly modified version of the equations describing a fluid: continuity and Bernoulli ones.

In the second chapter we recalled some theory which has been used to treat the evolution of spherically symmetric overdensities in the following chapters. In particular they have been of capital importance the *free-particle approximation* proposed by Short and Coles in [72] and the solution of Schrödinger-Newton equations for a matter distribution similar to a top-hat overdensity, found by Johnston et al. in [38].

In chapter 3 this solution has been used to build a root of Schrödinger-Newton equations for an overdensity which satisfies two requirements: being spherically symmetric and having a density profile which ensures absence of shell crossing during its evolution. The principle used to find this solution is that such an overdensity can be decomposed in an arbitrary number of shells, which, because of Birkhoff theorem, are not influenced by matter outside the shell itself. Their evolution is driven instead by the matter inside them, in a way that makes possible to describe them in terms of the solution found by Johnston et al..
The path integral representation of quantum mechanics has then been used to find the temporal evolution of a generic one of these shells in the free-particle approximation. Zel'dovich approximation and a slightly modified version of the adhesion one are recovered imposing different conditions on the results of the free-particle approximation.
Zel'dovich approximation has moreover been used to compute the temporal evolution of a spherically symmetric density profile that avoids shell crossing, without dividing it in shells, and making use, this time, of the stationary phase approximation.
The results found until there have then been applied to a specific density profile which meets the requirements of spherical symmetry and no shell crossing.
For that profile, seen that the free-particle one is an approximation, it has been refined with the use of time dependent perturbation theory.
Some differences are present in the predictions of different approximations, but it is generally true that the evolution of the overdensity computed with every technique is a collapse towards a singularity in the origin of the coordinates.
In particular, the free-particle approximation already forecasts the formation of this singularity; TDPT tells us that, for the specific profile for the evolution of which TDPT

were used, the collapse predicted by the approximation is slower than the actual one, a description of which would be obtained solving Schrödinger-Newton equations without approximations: to first order in perturbation theory, shells gain momentum as time flows, because of the potential which constitutes the perturbation, respect to the prediction of the free-particle approximation alone.

In chapter 4, it is studied an overdensity coherent with the initial conditions of the Universe, after the end of inflation. For this system it is once again found a shell-by-shell SN exact solution, the results of free-particle approximation are derived and it is briefly discussed the effect of such an overdensity on a small test halo which occupy a position internal to the overdensity itself. Unsurprisingly, this overdensity too ends up in a singularity.

Despite the fact that the final formation of a singularity is a common prediction of every technique, it is not the destiny of a real primordial overdensity of our Universe. Indeed it is a correct prediction for the density profile studied, but the latter is a very idealized system: a spherically symmetric one, tailored to avoid shell crossing. A realistic matter distribution evolves as calculations performed in this thesis predict, until a process called violent relaxation sets in. It is described in section 2.1 and it drives the system to a final virilized state of equilibrium instead that to a singularity. Once again this equilibrium configuration can be described by a wavefunction obeying Schrödinger-Newton equations: the countably infinite possible final-state wavefunctions are presented in section 4.6.

Finally in chapter 5, relying once again on the work of Johnston et al. [38], it is found a solution for the matter distribution considered in their paper, but in a Universe with non null cosmological constant. That solution was expressed both in terms of physical coordinates, to have a more transparent description, and in the adapted comoving coordinates proposed in [72], to draw a general procedure to embed a solution in a background different from the one in which it was conceived.

Appendix

A.1 The cosmological theory of Empedocles

Empedocles was a Greek philosopher born in Akragas (Agrigento) between 484 and 481 b.C. and dead there when he was almost sixty [1]. He has been also a politician, a physician, a thaumaturge and a scientist [1]. We posses fragments of two of his poems: *On nature*, cosmological, and *Purifications*, which is theological.

In *On nature* Empedocles presents the cycle which he believes the Universe undergoes. He believes in the existence of a material content of the Universe which is never created nor destroyed, but just transformed in different kinds of aggregation of the "four roots": earth, water, air and fire. What drives this transformations are two forces: one cohesive, which is love, and one which tends to detach things one from the other, which is hate. The cosmic cycle starts with the Universe in a state of pure dominance of cohesion, in which the matter is all stuck together and no life can form, then hate starts to disaggregate the roots, and our present Universe lays in a phase in which love and hate coexist compelling, and make life possible. Eventually hate will dominate and the Universe will be in a state of chaos, from which love will start to act again, until it gradually becomes dominant and closes the circle in the initial state, giving rise to a never ending process [1].

I find that interesting because such a description have some common traits with the evolution of a closed Universe with low enough cosmological constant: it expands until it reaches a turning point and then contracts back to a singularity which can lead to a "Big Bounce": a new expansion, establishing a cycle. Obviously the idea of expansion is absent in the writings of Empedocles, and also the fundamental idea of the impossibility of destroying or creating matter is erroneous, since the presence of expansion makes the Universe not invariant under time translations and therefore Noether theorem cannot be used to ensure energy conservation in the Universe; indeed, even at this very moment, some dark energy creates and some energy of radiation fades away.

A.2 Johnston et al. SN solution checked at its discontinuities

As previously shown, the wavefunctions and gravitational potentials found by Johnston et al. in [38] for each piece of the system studied, correctly satisfy Schrödinger and Poisson equations. The global discontinuous wavefunction on the contrary has been explicitly checked to satisfy at the boundaries only continuity equation in the paper [38]. The following calculation checks its validity as solution of the Schrödinger equation with quantum pressure term (1.16) with the appropriate gravitational potential (2.79) on the boundaries R_c and R_f.

I will restrict to an infinitesimal neighbourhood of the discontinuities of the solution (2.73). I expect only the quantum potential to be relevant there, since I expect V, being C^1, to vary slowly enough to be approximable by a constant in a small enough neighbourhood of a point, and thus being irrelevant in such a range. This negligibility will be analytically justified in the following.

Let us recall the form of the Schrödinger equation equivalent to the hydrodynamical treatment of CDM [19]:

$$i\nu\frac{\partial\psi}{\partial t} = -\frac{\nu^2}{2}\nabla^2\psi + (V+Q)\psi \ , \tag{1}$$

where [19]

$$Q = \frac{\nu^2}{2}\frac{\nabla^2|\psi|}{|\psi|} \, . \tag{2}$$

Let us concentrate on the neighbourhood of a discontinuity; let us consider R_c for concreteness, but the reasoning can be repeated almost identical for R_f.
In such a range [38]

$$|\psi| = \sqrt{\frac{3\Omega H_c^2}{8\pi G}}\left[1 - \mathrm{H}(r-R_c)\right] \ , \tag{3}$$

where H is the Heaviside step function.
Let us define for notational convenience

$$f(t) := \sqrt{\frac{3\Omega H_c^2}{8\pi G}} \, . \tag{4}$$

Because of spherical symmetry, the Laplacian takes the form (2.72) [38]:

$$\nabla^2 = \frac{\partial^2}{\partial r^2} + \frac{2}{r}\frac{\partial}{\partial r} \, .$$

It is consequently useful to compute the following quantities

$$\frac{\partial|\psi|}{\partial r} = -f\,\delta(r-R_c)$$
$$\frac{\partial^2|\psi|}{\partial r^2} = -f\,\delta'(r-R_c)$$

in order to find an expression for the quantum potential:

$$Q = -\frac{\nu^2}{2}\frac{\delta'(r-R_c) + \frac{2}{r}\delta(r-R_c)}{1-\mathrm{H}(r-R_c)} \, . \tag{5}$$

Computing the time partial derivative of ψ and plugging the expressions for the Laplacian (2.72) and for the quantum potential (5) in (1) we obtain

$$-\frac{\nu^2}{2}\left[\frac{\partial^2\psi}{\partial r^2}+\frac{2}{r}\frac{\partial\psi}{\partial r}\right]+V\psi-\frac{\nu^2}{2}\frac{\delta'(r-R_c)+\frac{2}{r}\delta(r-R_c)}{1-\mathrm{H}(r-R_c)}\psi=$$
$$=i\nu\left\{e^{\frac{i}{2\nu}H_c r^2}\left(\dot f+f\frac{i}{2\nu}r^2\dot H_c\right)[1-\mathrm{H}(r-R_c)]+f\,e^{\frac{i}{2\nu}H_c r^2}\delta(r-R_c)\dot R_c\right\}.$$

In order to make sense of the Dirac deltas we need to integrate in dr, and since we already know ψ is a solution in each of the three regions separated by R_c and R_f, let us integrate from $R_c(t)-\epsilon$ to $R_c(t)+\epsilon$, where the solution has not been checked yet. Indicating $\partial\psi/\partial r$ as ψ' for notational convenience we obtain

$$-\frac{\nu^2}{2}\left[\psi'(R_c+\epsilon)-\psi'(R_c-\epsilon)+\int_{R_c-\epsilon}^{R_c+\epsilon}\frac{2}{r}\psi'\,dr\right]+\int_{R_c-\epsilon}^{R_c+\epsilon}V\psi\,dr+$$
$$-\frac{\nu^2}{2}\int_{R_c-\epsilon}^{R_c+\epsilon}\frac{\delta'(r-R_c)+\frac{2}{r}\delta(r-R_c)}{1-\mathrm{H}(r-R_c)}\psi\,dr=$$
$$i\nu\int_{R_c-\epsilon}^{R_c+\epsilon}e^{\frac{i}{2\nu}H_c r^2}\left(\dot f+f\frac{i}{2\nu}r^2\dot H_c\right)[1-\mathrm{H}(r-R_c)]\,dr+i\nu\int_{R_c-\epsilon}^{R_c+\epsilon}f\,e^{\frac{i}{2\nu}H_c r^2}\delta(r-R_c)\dot R_c\,dr\,. \tag{6}$$

Using integration by parts the second term can be expressed as

$$\int_{R_c-\epsilon}^{R_c+\epsilon}\frac{2}{r}\psi'\,dr=\left(\frac{2}{r}\psi\right]_{R_c-\epsilon}^{R_c+\epsilon}+\int_{R_c-\epsilon}^{R_c+\epsilon}\frac{2}{r^2}\psi\,dr\,. \tag{7}$$

Moreover, let us recall a result found in [33] using again integration by parts: for a generic quantity $g(r)$

$$\int_{R_c-\epsilon}^{R_c+\epsilon}\delta'(r-R_c)g(r)\,dr=-\int_{R_c-\epsilon}^{R_c+\epsilon}\delta(r-R_c)g'(r)\,dr=-\bar{g'}(R_c)\,, \tag{8}$$

where the bar over last g denotes an average, defined even for discontinuous g, as follows [33]

$$\bar g\,(R_c):=\frac{[g(R_c^+)+g(R_c^-)]}{2}\,, \tag{9}$$

where in turn I introduced the following shortage

$$g\left(R_c^+\right):=\lim_{r\to R_c^+}g(r)$$
$$g\left(R_c^-\right):=\lim_{r\to R_c^-}g(r)\,.$$

Let us now take the $\epsilon\to 0$ limit of equation (6). All the integrals of limited functions go to zero, since the measure of the space of parameters in which we are integrating tends to zero. In particular it goes to zero the second term of the right hand side of expression (7), the third term of (6) and the first integral on the right hand side of the same equation. We are left with

$$\psi'\left(R_c^+\right)-\psi'\left(R_c^-\right)+2\left[\frac{\psi\left(R_c^+\right)-\psi\left(R_c^-\right)}{R_c}\right]-\overline{\left(\frac{\psi}{1-\mathrm{H}}\right)'}(R_c)+$$
$$+\frac{2}{R_c}\overline{\left(\frac{\psi}{1-\mathrm{H}}\right)}(R_c)=-\frac{2i}{\nu}\psi\left(R_c^-\right)\dot R_c\,. \tag{10}$$

Let us calculate

$$\overline{\left(\frac{\psi}{1-\mathrm{H}}\right)'}(R_c) = \overline{\frac{\psi'}{1-\mathrm{H}}}(R_c) + \overline{\psi\frac{\delta}{1-\mathrm{H}}}(R_c)\,, \tag{11}$$

where it has been used $(1-\mathrm{H})^2 = 1-\mathrm{H}$.

In order to compute the first term of the right hand side we recall a definition of the Heaviside step function $\mathrm{H}(x)$ [83]

$$\mathrm{H}(x) = \lim_{t\to 0}\left[\frac{1}{2} + \frac{1}{\pi}\tan^{-1}\left(\frac{x}{t}\right)\right]. \tag{12}$$

With this we can compute the following two limits

$$\begin{aligned}
\lim_{r\to R_c^-}\frac{\psi'(r)}{1-\mathrm{H}(r-R_c)} &= \lim_{r\to R_c^-}\lim_{t\to 0}\frac{\psi'(r)}{1-\left[\frac{1}{2}+\frac{1}{\pi}\tan^{-1}\left(\frac{r-R_c}{t}\right)\right]} = \lim_{t\to 0}\frac{\psi'(R_c^-)}{1-\frac{1}{2}} = 2\,\psi'(R_c^-)\,,\\
\lim_{r\to R_c^+}\frac{\psi'(r)}{1-\mathrm{H}(r-R_c)} &= \lim_{r\to R_c^+}\lim_{t\to 0}\frac{\psi'(r)}{1-\left[\frac{1}{2}+\frac{1}{\pi}\tan^{-1}\left(\frac{r-R_c}{t}\right)\right]} = \lim_{t\to 0}\frac{0}{\frac{1}{2}} = 0\,.
\end{aligned}$$

Thus using formula (9) we can compute

$$\overline{\frac{\psi'}{1-\mathrm{H}}}(R_c) = \frac{2\,\psi'\left(R_c^-\right)+0}{2} = \psi'\left(R_c^-\right). \tag{13}$$

In order to compute the second term on the right hand side of (11) we need to evaluate

$$\begin{aligned}
\lim_{r\to R_c^-}\left[\psi(r)\frac{\delta(r-R_c)}{1-\mathrm{H}(r-R_c)}\right] &= 0\,,\\
\lim_{r\to R_c^+}\left[\psi(r)\frac{\delta(r-R_c)}{1-\mathrm{H}(r-R_c)}\right] &= 0\,.
\end{aligned}$$

Therefore

$$\overline{\psi\frac{\delta}{1-\mathrm{H}}}(R_c) = 0\,. \tag{14}$$

Thus we finally obtain, from (10),

$$-\psi'\left(R_c^-\right) - 2\left[\frac{\psi\left(R_c^-\right)}{R_c}\right] - \psi'\left(R_c^-\right) + 2\frac{\psi\left(R_c^-\right)}{R_c} + \frac{2i}{\nu}\psi\left(R_c^-\right)\dot{R}_c = 0\,; \tag{15}$$

or, by simplifying,

$$2\,\psi'\left(R_c^-\right) - \frac{2i\dot{R}_c}{\nu}\psi\left(R_c^-\right) = 0\,.$$

Plugging in this the following expression for the derivative of ψ

$$\psi'\left(R_c^-\right) = \frac{i}{\nu}\psi\left(R_c^-\right)H_cR_c$$

one obtains the following identity

$$\frac{2i}{\nu}\dot{R}_c\psi\left(R_c^-\right) - \frac{2i}{\nu}\dot{R}_c\psi\left(R_c^-\right) = 0\,. \tag{16}$$

This confirms the validity of the solution at its discontinuity at R_c.

Let us repeat the reasoning at $r = R_f$, in order to check if solutions are well behaved at that discontinuity too. In a neighbourhood of that point [38]

$$|\psi| = \sqrt{\frac{3H_f^2}{8\pi G}}\,[\mathrm{H}(r - R_f)] := \tilde{f}(t)\,[\mathrm{H}(r - R_f)]\,. \tag{17}$$

Thus

$$\frac{\partial|\psi|}{\partial r} = \tilde{f}\,\delta(r - R_f)\,,$$
$$\frac{\partial^2|\psi|}{\partial r^2} = \tilde{f}\,\delta'(r - R_f)\,,$$

and so the quantum potential becomes

$$Q = \frac{\nu^2}{2}\frac{\delta'(r - R_f) + \frac{2}{r}\delta(r - R_f)}{\mathrm{H}(r - R_f)}\,. \tag{18}$$

Computing the time partial derivative of ψ and plugging the expressions for the Laplacian (2.72) and for the quantum potential (18) in (1) we obtain

$$-\frac{\nu^2}{2}\left[\frac{\partial^2\psi}{\partial r^2} + \frac{2}{r}\frac{\partial\psi}{\partial r}\right] + V\psi + \frac{\nu^2}{2}\frac{\delta'(r - R_f) + \frac{2}{r}\delta(r - R_f)}{\mathrm{H}(r - R_f)}\psi =$$
$$i\nu\left\{e^{\frac{i}{2\nu}H_f r^2}\left(\dot{f} + f\frac{i}{2\nu}r^2\dot{H}_f\right)\mathrm{H}(r - R_f) - f\,e^{\frac{i}{2\nu}H_f r^2}\delta(r - R_f)\dot{R}_f\right\}\,. \tag{19}$$

Let us now once again integrate in dr from $R_f(t) - \epsilon$ to $R_f(t) + \epsilon$. Indicating $\partial\psi/\partial r$ as ψ', as before, we obtain

$$-\frac{\nu^2}{2}\left[\psi'(R_f + \epsilon) - \psi'(R_f - \epsilon) + \int_{R_f-\epsilon}^{R_f+\epsilon}\frac{2}{r}\psi'\,dr\right] + \int_{R_f-\epsilon}^{R_f+\epsilon} V\psi\,dr +$$
$$+\frac{\nu^2}{2}\int_{R_f-\epsilon}^{R_f+\epsilon}\frac{\delta'(r - R_f) + \frac{2}{r}\delta(r - R_f)}{\mathrm{H}(r - R_f)}\psi\,dr =$$
$$i\nu\int_{R_f-\epsilon}^{R_f+\epsilon} e^{\frac{i}{2\nu}H_f r^2}\left(\dot{f} + f\frac{i}{2\nu}r^2\dot{H}_f\right)\psi\,\mathrm{H}(r - R_f)\,dr - i\nu\int_{R_f-\epsilon}^{R_f+\epsilon} f\,e^{\frac{i}{2\nu}H_f r^2}\delta(r - R_f)\dot{R}_f\,dr\,. \tag{20}$$

The second term once again turns out to be

$$\int_{R_f-\epsilon}^{R_f+\epsilon}\frac{2}{r}\psi'\,dr = \left(\frac{2}{r}\psi\right]_{R_f-\epsilon}^{R_f+\epsilon} + \int_{R_f-\epsilon}^{R_f+\epsilon}\frac{2}{r^2}\psi\,dr\,. \tag{21}$$

Let us now take the $\epsilon \to 0$ limit of equation (20), obtaining

$$-\left\{\psi'\left(R_f^+\right) - \psi'\left(R_f^-\right) + 2\left[\frac{\psi\left(R_f^+\right) - \psi\left(R_f^-\right)}{R_f}\right]\right\} - \overline{\left(\frac{\psi}{\mathrm{H}}\right)'}(R_f) +$$
$$+\frac{2}{R_f}\overline{\left(\frac{\psi}{\mathrm{H}}\right)}(R_f) = -\frac{2i}{\nu}\psi\left(R_f^+\right)\dot{R}_f\,. \tag{22}$$

Calculating

$$\overline{\left(\frac{\psi}{\mathrm{H}}\right)'}(R_f) = \overline{\left(\frac{\psi'}{\mathrm{H}}\right)}(R_f) - \overline{\left(\psi\frac{\delta}{\mathrm{H}}\right)}(R_f) = \overline{\left(\frac{\psi'}{\mathrm{H}}\right)}(R_f) - \overline{\left(\frac{\psi}{\mathrm{H}}\right)}(R_f)$$

and repeating the same reasoning for the limits at R_c we finally obtain

$$-\psi'\left(R_f^+\right) - 2\left[\frac{\psi\left(R_f^+\right)}{R_f}\right] - \psi'\left(R_f^+\right) + 2\frac{\psi\left(R_f^+\right)}{R_f} + \frac{2i}{\nu}\psi\left(R_f^+\right)\dot{R}_f = 0\,. \tag{23}$$

We are thus left with

$$-2\,\psi'\left(R_f^+\right) + \frac{2i}{\nu}\dot{R}_f\psi\left(R_f^+\right) = 0\,; \tag{24}$$

plugging in this the following expression for the derivative of ψ

$$\psi'\left(R_f^+\right) = \frac{i}{\nu}\psi\left(R_f^+\right)H_f R_f\,, \tag{25}$$

one obtains, as for $r = R_c$,

$$-\frac{2i}{\nu}\dot{R}_f\psi\left(R_f^+\right) + \frac{2i}{\nu}\dot{R}_f\psi\left(R_f^+\right) = 0\,. \tag{26}$$

What we have just shown is that the wavefunction for a top-hat proposed in [38] is solution of the Schrödinger equation with quantum pressure term even at the discontinuities.

A.3 Calculations

Chapter 3

Section 2.2: Schrödinger-Newton equations in a spatially flat expanding background

Derivation of the formula (2.19) for continuity in an Einstein de Sitter background

$$
\begin{aligned}
\frac{\rho\dot{\bar{\rho}}}{\bar{\rho}} + \frac{\partial\chi}{\partial a}\dot{a}\bar{\rho} - H(\mathbf{r}\cdot\nabla_r\rho) + \bar{\rho}\dot{a}\left[\nabla_r\cdot(\chi\mathbf{x}) + \nabla_r\cdot(\chi a\nabla_x\Phi)\right] &= 0 \\
\frac{\chi}{\dot{a}}\dot{\bar{\rho}} + \frac{\partial\chi}{\partial a}\bar{\rho} - \frac{1}{a}(\mathbf{r}\cdot\nabla_r\rho) + \bar{\rho}\nabla_r\cdot(\chi\mathbf{x}) + \bar{\rho}a\nabla_r\cdot(\chi\nabla_x\Phi) &= 0 \\
-a^{-1}H^{-1}\chi 3H\bar{\rho} + \frac{\partial\chi}{\partial a}\bar{\rho} - (\mathbf{x}\cdot\nabla_r\rho) + \nabla_r\cdot(\rho\mathbf{x}) + \bar{\rho}a\nabla_r\cdot(\chi\nabla_x\Phi) &= 0 \\
-3\frac{\rho}{a} + \frac{\partial\chi}{\partial a}\bar{\rho} - (\mathbf{x}\cdot\nabla_r\rho) + \nabla_r\rho\cdot\mathbf{x} + \rho\frac{1}{a}\nabla_x\cdot\mathbf{x} + \bar{\rho}a\nabla_r\cdot(\chi\nabla_x\Phi) &= 0 \\
-3\frac{\rho}{a} + \frac{\partial\chi}{\partial a}\bar{\rho} + \rho\frac{1}{a}3 + \bar{\rho}\nabla_x\cdot(\chi\nabla_x\Phi) &= 0 \\
\frac{\partial\chi}{\partial a} + \nabla_x\cdot(\chi\nabla_x\Phi) &= 0 \qquad (27)
\end{aligned}
$$

In the second passage I used Friedmann equations.

Section 3.2: Evolution of the shells of the overdensity in the free-particle approximation

Let us define here, for notational convenience,

$$B_j(a) := -\frac{\bar{\delta}_j(a)}{6a}\,.$$

Derivation of expression (3.34) Now let us start from expression (3.33) and complete the square:

$$
\begin{aligned}
\Psi_j(r_x,a) &= \delta r_{x,i}\,\frac{\sqrt{\chi_j(a_i)}}{\sqrt{2\pi i\nu\Delta a}}\,e^{\frac{i}{2}\left[\frac{(r_x-r_{x,i})^2+2\,\Delta a\,B_j(a_i)\,r_{x,i}^2}{\nu\Delta a}\right]} = \\
&= \delta r_{x,i}\,\frac{\sqrt{\chi_j(a_i)}}{\sqrt{2\pi i\nu\Delta a}}\,e^{\frac{i}{2}\left[\frac{(2\,\Delta a\,B_j(a_i)+1)\,r_{x,i}^2+r_x^2-2r_xr_{x,i}}{\nu\Delta a}\right]} = \\
&= \delta r_{x,i}\,\frac{\sqrt{\chi_j(a_i)}}{\sqrt{2\pi i\nu\Delta a}}\,e^{\frac{i}{2\,\nu\Delta a}\left[\left(\sqrt{2\,\Delta a\,B_j(a_i)+1}\,r_{x,i}-\frac{1}{\sqrt{2\,\Delta a\,B_j(a_i)+1}}r_x\right)^2+\frac{2\,\Delta a\,B_j(a_i)}{2\,\Delta a\,B_j(a_i)+1}r_x^2\right]} = \\
&= \delta r_{x,i}\,\frac{\sqrt{\chi_j(a_i)}}{\sqrt{2\pi i\nu\Delta a}}\,e^{\frac{i}{2\,\nu\Delta a}\left(\sqrt{2\,\Delta a\,B_j(a_i)+1}\,r_{x,i}-\frac{1}{\sqrt{2\,\Delta a\,B_j(a_i)+1}}r_x\right)^2}\,e^{\frac{i}{\nu}\frac{B_j(a_i)}{2\,\Delta a\,B_j(a_i)+1}r_x^2} = \\
&= \delta r_{x,i}\,\frac{\sqrt{\chi_j(a_i)}}{\sqrt{2\pi i\nu\Delta a}}\,e^{\frac{i}{2\,\nu\Delta a}\left(\frac{r_x-[2\,\Delta a\,B_j(a_i)+1]r_{x,i}}{\sqrt{2\,\Delta a\,B_j(a_i)+1}}\right)^2}\,e^{\frac{i}{\nu}\frac{B_j(a_i)}{2\,\Delta a\,B_j(a_i)+1}r_x^2}\,,
\end{aligned}
$$

which is

$$\Psi_j(r_x, a) = \delta r_{x,i} \, \frac{\sqrt{\chi_j(a_i)}}{\sqrt{2\pi i \nu \Delta a}} \, e^{\frac{i}{\nu} \frac{B_j(a_i)}{2\,\Delta a\, B_j(a_i)+1} r_x^2} e^{\frac{i}{2}\left(\frac{r_x-\mu}{\sigma}\right)^2}$$

if one defines

$$\begin{aligned}
\mu(r_{x,i}, \Delta a) &= r_{x,i}\,(1 + 2\Delta a\, B_j(a_i))\,, \\
\sigma(\Delta a) &= \sqrt{\nu[\Delta a + 2(\Delta a)^2\, B_j(a_i)]}\,.
\end{aligned}$$

Derivation of the deformation tensor (3.46) Let us, just for this calculation, simplify the notation and call (x, y, z) the Cartesian comoving coordinates $\mathbf{x}$ and (r, θ, ϕ) the spherical comoving coordinates, which are called (r_x, θ_x, ϕ_x) in the rest of the thesis.
We will make use of Cartesian partial derivatives in spherical coordinates [30]:

$$\begin{aligned}
\frac{\partial}{\partial x} &= \frac{\partial r}{\partial x}\frac{\partial}{\partial r} + \frac{\partial \theta}{\partial x}\frac{\partial}{\partial \theta} + \frac{\partial \phi}{\partial x}\frac{\partial}{\partial \phi} \\
&= \sin\theta\cos\phi\frac{\partial}{\partial r} + \frac{1}{r}\cos\theta\cos\phi\frac{\partial}{\partial \theta} - \frac{\sin\phi}{r\sin\theta}\frac{\partial}{\partial \phi} \\
\frac{\partial}{\partial y} &= \sin\theta\sin\phi\frac{\partial}{\partial r} + \frac{1}{r}\cos\theta\sin\phi\frac{\partial}{\partial \theta} + \frac{\cos\phi}{r\sin\theta}\frac{\partial}{\partial \phi} \\
\frac{\partial}{\partial z} &= \cos\theta\frac{\partial}{\partial r} - \frac{1}{r}\sin\theta\frac{\partial}{\partial \theta}\,.
\end{aligned}$$

The deformation tensor of the j-th shell is defined as [67]

$$d_{kl} = \frac{\partial^2 \Phi_j}{\partial q_k \partial q_l}\,,$$

where q_k and q_l are Cartesian coordinates and

$$\Phi_j = -\frac{3\Omega_j H_j^2 - 8\pi G\rho_f}{48\pi G a\,\rho_f}(a_i)\, r^2 := B_j(a_i)\, r^2\,. \tag{28}$$

Therefore

$$\begin{aligned}
d_{kl} &:= \frac{\partial^2 \Phi_j}{\partial q_k \partial q_l} \\
&:= \frac{\partial}{\partial q_k}\left(\tfrac{\partial \Phi_j}{\partial x},\quad \tfrac{\partial \Phi_j}{\partial y},\quad \tfrac{\partial \Phi_j}{\partial z}\right) = \\
&= 2B_j(a_i)\frac{\partial}{\partial q_k} r\left(\sin\theta\cos\phi,\quad \sin\theta\sin\phi,\quad \cos\theta\right) = \\
&= 2B_j(a_i) \times \begin{pmatrix} a_{11}, & a_{12}, & a_{13} \\ a_{21}, & a_{22}, & a_{23} \\ a_{31}, & a_{32}, & a_{33} \end{pmatrix}\,,
\end{aligned} \tag{29}$$

where

$$
\begin{aligned}
a_{11} &= \sin^2\theta\cos^2\phi + \frac{\sin^2\phi}{r\sin\theta}r\sin\theta + \frac{\cos\theta\cos\phi}{r}r\cos\theta\cos\phi \\
a_{12} &= \cos\phi\sin^2\theta\sin\phi - \frac{\sin\phi}{r\sin\theta}r\sin\theta\cos\phi + \frac{\cos\phi\cos\theta}{r}r\sin\phi\cos\theta \\
a_{13} &= \cos\phi\sin\theta\cos\theta + \cos\phi\cos\theta\,(-\sin\theta) \\
a_{21} &= \sin^2\theta\cos\phi\sin\phi + \cos\phi(-\sin\phi) + \sin\phi\cos\theta\cos\phi \\
a_{22} &= \sin^2\theta\sin^2\phi + \cos^2\phi + \sin^2\phi\cos^2\theta \\
a_{23} &= \sin\phi\sin\theta\cos\theta + \sin\phi\cos\theta(-\sin\theta) \\
a_{31} &= \cos\theta\cos\phi\sin\theta - \sin\theta\cos\phi\cos\theta \\
a_{32} &= \cos\theta\sin\phi\sin\theta - \sin\theta\sin\phi\cos\theta \\
a_{33} &= \cos^2\theta + \sin^2\theta\,.
\end{aligned}
$$

Using trigonometric identities, (29) reads

$$
d_{kl} = 2B_j(a_i)\,\mathbb{I}_{3\times3}\,, \tag{30}
$$

where $\mathbb{I}_{3\times3}$ is the three-dimensional identity matrix.

The three invariant of the deformation tensor, defined in section 2.3 then read

$$
I_1 = 6\,B_j\,, \qquad I_2 = 12\,B_j^2\,, \qquad I_3 = 8\,B_j^3\,.
$$

Therefore the fractional difference (2.40) between the density predicted by the free-particle approximation and the exact one is

$$
\tilde{\delta} = -12a^2B_j^2 + 16a^3B_j^3\,.
$$

Section 3.5: Time Dependent Perturbation Theory

Derivation of the formula (3.85) for the exact effective potential of the Gaussian overdensity (3.76)

$$
\begin{aligned}
V &:= \frac{3}{2a}(\Phi+\varphi) = \\
&= \frac{3}{2a}\left[\frac{1}{a^2\dot{a}}\left(\phi_j - H_f\frac{r^2}{2}\right) + \frac{2}{3a^3H_f^2}(V_j - V_f)\right] = \\
&= \frac{3}{2a}\left[\frac{H_j - H_f}{a^2\frac{\dot{a}}{a}a}\frac{r^2}{2} + \frac{2}{3a^3H_f^2}\,G\left(\frac{m_j}{r_j^3(a)} - \frac{M}{R_f^3(a)}\right)\frac{r^2}{2}\right] = \\
&= \frac{3}{2a^4H_f}\left[(H_j - H_f) + \frac{2G}{3H_f}\frac{4\pi}{3}\,(\rho_j - \rho_f)\right]\frac{r^2}{2} = \\
&= \frac{3}{2a^4H_f}\left[H_j - H_f + \frac{\Omega_jH_j^2 - H_f^2}{3H_f}\right]\frac{r^2}{2} = \\
&= \frac{3}{2a^2}\left[\frac{H_j}{H_f} + \frac{1}{3}\frac{\Omega_jH_j^2}{H_f^2} - \frac{4}{3}\right]\frac{r_x^2}{2}
\end{aligned}
$$

where in the first passage I used formulae (3.21) and (2.26), in the second one (3.8) and (3.9), and in the fourth I used Friedmann equations and the definition of density parameter Ω.

Solution of the integrals appearing in (3.99)

$$
\begin{aligned}
&\int_0^{R_{x,f}} \cos[(k_m + k_n)\, r_x]\, \frac{r_x^2}{2}\, dr_x = \\
&= \left. \frac{r_x^2 \sin[(k_m + k_n)\, r_x]}{2\,(k_m + k_n)} \right|_0^{R_{x,f}} - \int_0^{R_{x,f}} \frac{\sin[(k_m + k_n)\, r_x]}{(k_m + k_n)}\, r_x\, dr_x = \\
&= -\frac{1}{(k_m + k_n)} \int_0^{R_{x,f}} \sin[(k_m + k_n)\, r_x]\, r_x\, dr_x = \\
&= -\frac{1}{(k_m + k_n)} \left[-\left. \frac{r \cos[(k_m + k_n)\, r_x]}{(k_m + k_n)} \right|_0^{R_{x,f}} + \int_0^{R_{x,f}} \cos[(k_m + k_n)\, r_x]\, dr_x \right] \\
&= \frac{R_{x,f}}{(k_m + k_n)^2}
\end{aligned}
$$

The other one is completely analogous.

Section 3.3: Global evolution

Derivation of the turnaround time coordinate of a fluid element, of the Gaussian overdensity, initially at r_i (3.66) Let us recall the following expression for the radial coordinate of a fluid element at generic time coordinate a

$$
r(r_i, a) = \frac{\Delta a + a_i}{a_i} r_i - (\Delta a + a_i) \Delta a\, \frac{1}{a_i^2 r_i^2} \int_0^{r_i} \delta(r', a_i)\, r'^2\, dr' \tag{31}
$$

In order to determine the turnaround time coordinate $(\Delta a)_{\rm ta}$ of the fluid element described by 31, let us impose

$$
\frac{dr}{dt}(r_i, \Delta a) = 0\,, \tag{32}
$$

which can be written as

$$
\frac{\partial r}{\partial(\Delta a)}(r_i, \Delta a)\, \frac{d(\Delta a)}{dt} = 0\,.
$$

Since $d(\Delta a)/dt \neq 0$ and making use of (31), this is equivalent to

$$
\begin{aligned}
\frac{\partial r}{\partial(\Delta a)}(r_i, \Delta a) &= 0 \\
\frac{r_i}{a_i} - (2\Delta a + a_i) \frac{r_i}{3 a_i^2} \frac{4\pi}{\frac{4\pi}{3} r_i^3} \int_0^{r_i} \delta(r', a_i)\, r'^2\, dr' &= 0 \\
3 - (2\Delta a + a_i) \frac{1}{a_i} \bar{\delta}(r_i) &= 0 \\
\frac{(\Delta a)_{\rm ta}}{a_i} &= \frac{3 - \bar{\delta}(r_i)}{2\bar{\delta}(r_i)}
\end{aligned}
$$

Derivation of the time coordinate of collapse (3.67) of a fluid element initially at r_i

$$
\begin{aligned}
r(r_i, a) &= 0 \\
\frac{\Delta a + a_i}{a_i} r_i - (\Delta a + a_i)\Delta a \, \frac{1}{a_i^2 r_i^2} \int_0^{r_i} \delta(r', a_i)\, r'^2 \, dr' &= 0 \\
\frac{\Delta a + a_i}{a_i} r_i - (\Delta a + a_i)\Delta a \, \frac{r_i}{3a_i^2} \bar{\delta}(r_i) &= 0 \\
-\frac{r_i}{3a_i^2} \bar{\delta}(r_i)\, (\Delta a)^2 + \left[\frac{r_i}{a_i} - \frac{r_i}{3a_i} \bar{\delta}(r_i) \right] \Delta a + r_i &= 0 \,.
\end{aligned}
$$

The solutions are therefore

$$
\frac{(\Delta a)_{\rm coll}}{a_i} = \left\{ -1, \, \frac{3}{\bar{\delta}(r_i)} \right\} .
$$

Section 3.4: SN solution for a Gaussian overdensity

Derivation of the formula (3.80)

$$
\begin{aligned}
\Phi(r_x, a_i) &= -\frac{1}{a_i} \int \frac{1}{r_x''^2} \int \frac{1}{\rho_f} \left(\frac{M}{\left(\sqrt{2\pi}\sigma\right)^3} e^{-\frac{1}{2}\left(\frac{a_i\, r'_x}{\sigma}\right)^2} - \rho_f \right) r_x'^{\,2} \, dr'_x \, dr''_x \\
&= -\frac{1}{a_i} \frac{1}{\rho_f} \int dr''_x \, \frac{1}{r_x''^2} \left(-\rho_f \frac{r_x''^3}{3} + \int \frac{M}{\left(\sqrt{2\pi}\sigma\right)^3} e^{-\frac{1}{2}\left(\frac{r'_x}{\sigma/a_i}\right)^2} r_x'^{\,2} \, dr'_x \right) \\
&= -\frac{1}{a_i} \frac{1}{\rho_f} \left\{ -\rho_f \frac{r_x''^2}{6} + \frac{M}{\left(\sqrt{2\pi}\sigma\right)^3} \int dr''_x \, \frac{1}{r_x''^2} \int e^{-\frac{1}{2}\left(\frac{r'_x}{\sigma/a_i}\right)^2} r_x'^{\,2} \, dr'_x \right\} \\
&= \frac{1}{a_i} \frac{r_x''^2}{6} - \frac{M}{a_i\, \rho_f \left(\sqrt{2\pi}\sigma\right)^3} \int_0^{r_x} dr''_x \, \frac{1}{r_x''^2} \int_0^{r''_x} e^{-\frac{1}{2}\left(\frac{r'_x}{\sigma/a_i}\right)^2} r_x'^{\,2} \, dr'_x
\end{aligned}
\tag{33}
$$

Derivation of the formula (3.81)

$$
\begin{aligned}
r_x &= \bar{q}_s - \Delta a \, \frac{1}{a_i\, q^2} \int \delta(r'_x, a_i)\, r_x'^{\,2} \, dr'_x \Big|_{\bar{q}_s} \\
&= \bar{q}_s - \Delta a \, \frac{1}{a_i\, q^2} \int \frac{1}{\rho_f} \left(\frac{M}{\left(\sqrt{2\pi}\sigma\right)^3} e^{-\frac{1}{2}\left(\frac{r'_x}{\sigma/a_i}\right)^2} - \rho_f \right) r_x'^{\,2} \, dr'_x \Big|_{\bar{q}_s} \\
&= \bar{q}_s - \Delta a \, \frac{1}{a_i\, \bar{q}_s^2} \int_0^{\bar{q}_s} \left(\frac{M}{\rho_f \, \left(\sqrt{2\pi}\sigma\right)^3} e^{-\frac{1}{2}\left(\frac{r'_x}{\sigma/a_i}\right)^2} - 1 \right) r_x'^{\,2} \, dr'_x \\
&= \bar{q}_s + \Delta a \, \frac{1}{a_i\, \bar{q}_s^2} \frac{\bar{q}_s^3}{3} - \Delta a \, \frac{1}{a_i\, \bar{q}_s^2} \int_0^{\bar{q}_s} \frac{M}{\rho_f \, \left(\sqrt{2\pi}\sigma\right)^3} e^{-\frac{1}{2}\left(\frac{r'_x}{\sigma/a_i}\right)^2} r_x'^{\,2} \, dr'_x \\
&= \bar{q}_s + \frac{1}{3} \frac{\Delta a}{a_i} \bar{q}_s - \frac{\Delta a}{a_i} \, \frac{M}{\rho_f \, \left(\sqrt{2\pi}\sigma\right)^3} \, \frac{1}{\bar{q}_s^2} \int_0^{\bar{q}_s} e^{-\frac{1}{2}\left(\frac{r'_x}{\sigma/a_i}\right)^2} r_x'^{\,2} \, dr'_x
\end{aligned}
\tag{34}
$$

Consistency check Since the overdensity is compensated, with an error assumed to be negligible, a fluid element initially at $r_x = R_f/a := R_{x,f}$ should stay forever at the same comoving coordinate. Let us find this result:

$$\begin{aligned} r_x(R_{x,f},\,\Delta a) &= R_{x,f} + \frac{1}{3}\frac{\Delta a}{a_i}R_{x,f} - \frac{\Delta a}{a_i}\,\frac{M}{\rho_f\,\left(\sqrt{2\pi}\sigma\right)^3}\,\frac{1}{2R_{x,f}^2}\int_{-R_{x,f}}^{R_{x,f}} e^{-\frac{1}{2}\left(\frac{r'_x}{\sigma/a_i}\right)^2}\,{r'_x}^2\,dr'_x \simeq \\ &\simeq R_{x,f} + \frac{1}{3}\frac{\Delta a}{a_i}R_{x,f} - \frac{\Delta a}{a_i}\,\frac{M}{\rho_f\,\left(\sqrt{2\pi}\sigma\right)^3}\,\frac{1}{2R_{x,f}^2}\sqrt{2\pi}\frac{\sigma^3}{a_i^3} = \\ &= R_{x,f} + \frac{1}{3}\frac{\Delta a}{a_i}R_{x,f} - \frac{\Delta a}{3\,a_i}\,\frac{M}{\frac{4\pi}{3}\,\rho_f}\,\frac{R_{x,f}}{a_i^3 R_{x,f}^3} \\ &= R_{x,f} + \frac{1}{3}\frac{\Delta a}{a_i}R_{x,f} - \frac{1}{3}\frac{\Delta a}{a_i}\,R_{x,f} \\ &= R_{x,f}\,. \end{aligned} \tag{35}$$

Chapter 4

Formula for the error of the critical radius (4.36) Let us call σ_b the error associated of a certain quantity b. Then

$$\begin{aligned} \sigma_{\tilde{r}_x} &= \left|\frac{\partial r_x}{\partial \sigma_8}\right| \times\, \sigma_{\sigma_8} = \\ &= \frac{8192\,\exp(\tilde{r}_x^2/8)\sqrt{\pi}\,\tilde{r}_x\,\mathrm{erf}[\tilde{r}_x/(2\sqrt{2})]}{-4096\sqrt{2}\sigma_8\tilde{r}_x + 4\sqrt{2}\tilde{r}_x^4 - \sqrt{2}\tilde{r}_x^6 + 24576\sigma_8\exp(\tilde{r}_x^2/8)\sqrt{\pi}\mathrm{erf}[x/(2\sqrt{2})]} \,\times\, \sigma_{\sigma_8} = \\ &= 0.013\,\mathrm{h}^{-1}\mathrm{Mpc}\,, \end{aligned}$$

where in the last passage it was used the Planck 2018 value for σ_8 and its error.

Chapter 5

Calculation of the parameter χ_c at turnaround time (5.13) in a $\Lambda = 0$ Universe

$$\chi_c(t_{\mathrm{ta}}) := \frac{\rho_c(t_{\mathrm{ta}})}{\rho_f(t_{\mathrm{ta}})} = \frac{\frac{M}{\frac{4}{3}\pi R_{\mathrm{max}}^3}}{\frac{M}{\frac{4}{3}\pi R_f^3(t_{\mathrm{ta}})}} = \frac{R_f^3(t_{\mathrm{ta}})}{R_{\mathrm{max}}^3} = \frac{\frac{9GM}{2}t_{\mathrm{ta}}^2}{R_{\mathrm{max}}^3} = \frac{\frac{9GM}{2}\frac{(GM\pi)^2}{\left(\frac{2GM}{R_{\mathrm{max}}}\right)^3}}{R_{\mathrm{max}}^3} = \frac{9\pi^2}{2^4}$$

The first passage is just the definition of the parameter, in the fourth one I used eq. (2.68), in the next one I deduced the value of η_{max} from the expression of R_c as a function of η (2.61), then I substituted it in the expression for $t(\eta)$ (3.13) in order to finally find the expression for t_{ta} written above.

Exact expressions for $D(t)$ in a ΛCDM cosmology In a model with non vanishing cosmological constant the following Friedmann equation holds [58]

$$\frac{\ddot{a}}{a} = -\frac{4\pi G}{3}\rho + \frac{\Lambda}{3}\,. \tag{36}$$

Therefore it exists an inflection point at

$$\rho_e = \frac{\Lambda}{4\pi G}\,. \tag{37}$$

If we call a_e the scale factor at the inflexion, we can define the following dimensionless quantities [58]

$$x := \frac{a}{a_e} \qquad\qquad 1 - \epsilon = \frac{kc^2}{\Lambda a_e^2} \tag{38}$$

with k the curvature parameter appearing in Robertson-Walker metric (1.1).

In terms of the above defined quantities, the solutions of eq. 5.37 in a Universe with $\Lambda \neq 0$ take the form (see [58])

$$D_2(x) = \frac{[x^3 - 3(1-\epsilon)x + 2]^{1/2}}{x^{3/2}} \tag{39}$$

$$D_1(x) = D_2(x) \int x^{3/2} \left[x^3 - 3(1-\epsilon)x + 2\right]^{-3/2} dx\,. \tag{40}$$

If moreover such a Universe is flat, as the background we want to consider, $k = 0$ by definition and hence

$$D_2(x) = \sqrt{\frac{x^3+2}{x^3}}\,. \tag{41}$$

This solution is monotonously decreasing from $\lim_{a\to 0^+} D_2(x) = +\infty$ to $\lim_{a\to+\infty} D_2(x) = 1$, therefore it is the decreasing one. The other one reads

$$D_1(x) = \sqrt{\frac{x^3+2}{x^3}} \int \left(\frac{x}{x^3+2}\right)^{3/2} dx = \frac{x\sqrt{x^3+2}}{5\sqrt{2}}\, {}_2F_1\left(\frac{5}{6}, \frac{3}{2}; \frac{11}{6}; -\frac{x^3}{2}\right), \tag{42}$$

where ${}_2F_1(a, b; c; z)$ is the Gauss hypergeometric function defined as [11]

$${}_2F_1(a,b;c;z) = 1 + \frac{ab}{1!c}z + \frac{a(a+1)b(b+1)}{2!c(c+1)}z^2 + ... = \sum_{n=0}^{\infty} \frac{(a)_n (b)_n}{(c)_n} \frac{z^n}{n!}\,. \tag{43}$$

A Gauss hypergeometric function with $c > b > 0$ and $a > 0$, as the one in (42), is "completely monotonic" [49], i.e. it possesses derivatives ${}_2F_1^{(n)}(z)$ for all $n = 0, 1, 2, ...$ and they satisfy [49]

$$(-1)^n {}_2F_1^{(n)}(z) \geq 0\,. \tag{44}$$

Therefore, its first derivative is never positive, and hence

$${}_2F_1\left(\frac{5}{6}, \frac{3}{2}; \frac{11}{6}; -\frac{x^3}{2}\right)$$

is monotonously non decreasing (because of the change of sign of the argument). Since the product of two non decreasing functions is non decreasing, $D_1(x)$ defined by (42) is the growing solution.

Bibliography

[1] N. Abbagnano, G. Fornero, *La ricerca del pensiero*, vol. 1A, Pearson Italia, Milano-Torino, 2012

[2] Abel et al., *Measurement of the Permanent Electric Dipole Moment of the Neutron*, Phys. Rev. Lett. 124 (2020)

[3] S. Arnouts, N. Malavasi and the VIPERS Collaboration, *A slice through the Universe* (2016) `https://www.eso.org/public/videos/ann16086a`

[4] E. R. Arriola, J. Soler, *Asymptotic Behaviour for the 3-D Schrödinger-Poisson System in the Attractive Case with Positive Energy*, Applied Mathematics Letters 12 (1999) 1-6

[5] M. Bahrami, A.Großardt, S. Donadi, A. Bassi, *The Schrödinger–Newton equation and its foundations*, New Journal of Physics 16 (2014)

[6] J. M. Bardeen, J. R. Bond, N. Kaiser, A. S. Szalay, *The statistics of peaks of Gaussian random fields*, The Astrophysical Journal, 304:15-61 (1986)

[7] B. Berenji, J. Gaskins, M. Meyer, *Constraints on Axions and Axionlike Particles from Fermi Large Area Telescope Observations of Neutron Stars*, Physical Review D, January 2016, arXiv:1602.00091v1

[8] Bernardeau, Colombi, Gaztañaga, Scoccimarro, *Physics Reports* 367 (2002) 1-248

[9] D. H. Bernstein, E. Giladi, K. R. W. Jones, *Eigenstates of the gravitational Schrödinger equation*, Modern Physics Letters A, Vol. 13, No. 29 (1998) 2327-2336

[10] E. Bertschinger, *Self-similar secondary infall and accretion in an Einstein-de Sitter Universe*, The Astrophysical Journal Supplement Series, 58: 39-66 (1985)

[11] F. Beukers, *Gauss' hypergeometric function*, `https://xxyyzz.cc/beukers\%20hypergeometric\%20functions.pdf`

[12] N. Bleistein, R. Handelsman, *Asymptotic Expansions of Integrals*, Dover Publications Inc., New York (1975, 1986) p. 219-223

[13] S. Bose, A. Mazumdar, G.W. Morley, H. Ulbricht, M. Toroš, M. Paternostro, A.A. Geraci, P.F. Barker, M.S. Kim, G. Milburn, *Spin entanglement witness for quantum gravity*, Phys. Rev. Lett. 119(24) (2017) 240401, arXiv:1707.06050

[14] P. Catelan, F. Lucchin, S. Matarrese, L. Moscardini, *Eulerian perturbation theory in non-flat universes: second-order approximation*, Mon. Not. R.Astron. Soc. 276, 39-56 (1995)

[15] M. Christodoulou, C. Rovelli, *On the possibility of laboratory evidence for quantum superposition of geometries*, Physics Letters B 792 (2019) 64–68

[16] D. Coe, N. Benitez, T. Broadhurst, L. A. Moustakas, *A high-resolution mass map of galaxy cluster substructure: LensPerfect analysis of A1689*, The astrophysical journal, 723:1678–1702 (2010 November 10)

[17] P. Coles, *The wave-mechanics of large-scale structure*, arXiv:astro-ph/0209576v1 (27 Sep 2002)

[18] P. Coles, F. Lucchin, *Cosmology*, 2nd edition, John Wiley and sons, LTD, Chichester (2002)

[19] P. Coles, K. Spencer, *A wave-mechanical approach to cosmic structure formation*, Mon. Not. R. Astron. Soc., (2003), 342, 176–184

[20] R. Coquereaux, A. Grossmann, *Analytic Discussion of Spatially Closed Friedman Universes with Cosmological Constant and Radiation Pressure*, Annals of physics 143, 296-356 (1982)

[21] G. Davies, L. M. Widrow, *Test-bed simulations of collisionless self-gravitationg systems using the schrödinger method*, The Astrophysical Journal, 485: 484-495 (1997 August 20)

[22] F. D'Eramo, *AstroParticle Physics*, notes for the master degree in Physics (2019)

[23] L. Diósi, *Gravitation and quantummechanical localization of macroobjects*, Phys. Lett. A 105 199–202 (1984)

[24] W. Docters, S. Zaroubi, *Determining the cosmological parameters Ω_m and σ_8 from peculiar velocity and density-contrast data* (2008)

[25] D. J. D. Earn, J. A. Sellwood, *the optimal n-body method for stability of galaxies*, The Astrophysical Journal 9504047 (14 Apr 95)

[26] M. Eliade, *Trattato di storia delle religioni.* Torino, Boringhieri, p.113.

[27] J.-P. Ernenwein, *Lecture notes for his course on Astroparticles, held at Aix-Marseille University for the master M2 in Fundamental Physics, academic year 2019/2020*

[28] L. Fortunato, *Appunti di fisica nucleare*, Rotomail Italia (2018)

[29] M. Garny, T. Konstandin, *Gravitational collapse in the Schrödinger-Poisson system*, JCAP 01 (2018) 009

[30] S. Gasiorowicz, *Quantum Physics*, 3rd edition, John Wiley and sons Inc., Hoboken NJ (2003) p. W30

[31] M. Giannotti, L.D. Duffy, R. Nita *New constraints for heavy axion-like particles from supernovae*, JCAP 01 (2011) 015, arXiv:1009.5714

[32] D. Giulini, A. Großardt, *Gravitationally induced inhibitions of dispersion according to the Schrödinger–Newton equation*, Class. Quantum Grav. 28 195026 (2011)

[33] D. J. Griffiths, *Boundary conditions at the derivative of a delta function* J. Phys. A: Math. Gen. 26 2265 (1993)

[34] D. J. Griffiths, *Introduzione alla Meccanica Quantistica*, Casa editrice ambrosiana, Rozzano (MI) (2005)

[35] R. Harrison, *A numerical study of the Schrödinger-Newton equations*, thesis submitted for the degree of Doctor of Philosophy, Oxford (2001)

[36] D. Horns, L. Maccione, M. Meyer, A. Mirizzi, D. Montanino, M. Roncadelli, *Hardening of TeV gamma spectrum of active galactic nuclei in galaxy clusters by conversions of photons into axionlike particles*, Physical Review D 86, 075024, 17 October 2012

[37] T. Ishiyama, *Supercomputer simulation of large scale structures in the Universe*, `https://www.youtube.com/watch?v=nHvcqV92oqY`

[38] R. Johnston, A. N. Lasenby, M. P. Hobson, *Cosmological fluid dynamics in the Schrödinger formalism*, Mon. Not. R. Astron. Soc. 402, 2491–2502 (2010)

[39] D. Kaiser, *The Sacred, Spherical Cows of Physics*, `http://nautil.us/issue/13/symmetry/the-sacred-spherical-cows-of-physics`

[40] J. M. Kubo et al., *The Mass of the Coma Cluster from Weak Lensing in the Sloan Digital Sky Survey*, ApJ 671 1466 (2007)

[41] O. Lahav, P. B. Lilje, J. R. Primack, M. J. Rees, *Dynamical effects of the cosmological constant* Mon. Not. R. astr. Soc. (1991) 251, 128-136

[42] O. Lahav, Y. Suto, *Measuring our universe from galaxy redshift surveys*, Living Reviews in Relativity 7 (2004) 1-81, arXiv:astro-ph/0310642

[43] E. Madelung, *Quantum Theory in Hydrodynamical Form* , Zeit. f. Phys., (1927), 40, 322

[44] R. Mandelbaum, U. Seljak, R. J. Cool, M. Blanton, C. M. Hirata, J. Brinkmann, *Density profiles of galaxy groups and clusters from SDSS galaxy–galaxy weak lensing*, Monthly Notices of the Royal Astronomical Society, Volume 372, Issue 2, Pages 758–776 (2006)

[45] J. E. Marsden, A. Tromba, *Vector Calculus*, W H Freeman and Co; 6th edition (2011)

[46] D. J. E. Marsh, *Axions and ALPs: a very short introduction*, 8 Dec 2017, arXiv:1712.03018v1

[47] C. Marletto, V. Vedral, *Gravitationally induced entanglement between two massive particles is sufficient evidence of quantum effects in gravity*, Phys. Rev. Lett. 119(24) (2017) 240402, arXiv:1804.11315

[48] S. Matarrese, *Notes on gravitational instability*, Lectures given at Scuola Normale Superiore, Pisa, between 2002 and 2005 (december 2006)

[49] K.S. Miller and S.G. Samko, *Completely monotonic functions*, Integral Transforms and Special Functions, Vol. 12, No. 4 (2001) 389-402

[50] H. Mo, F. van den Bosch, S. White, *Galaxy formation and evolution*, Cambridge University Press, Cambridge (2010)

[51] H. J. Mo, S. D. M. White, *An analytic model for the gravitational clustering of dark matter haloes*, MNRAS submitted, arXiv:astro-ph/9412088 (1994)

[52] H. J. Mo, S. D. M. White, *An analytic model for the gravitational clustering of dark matter haloes*, MNRAS submitted, astro-ph/9512127 (1995)

[53] I. M. Moroz, R. Penrose, P. Tod, *Spherically-symmetric solutions of the Schrödinger-Newton equations*, Class. Quantum Grav., (1998), 15 2733

[54] D. Nadali, A. Polcaro, *The sky from the high terrace: study on the orientation of the Ziqqurat in ancient Mesopotamia*, Mediterranean Archaeology and Archaeometry, Vol. 16, No 4, pp. 103-108 (2016)

[55] U. Natale, *Note di cosmologia*, UNIPD (2017). Notes of the course in cosmology held by prof. S. Matarrese in the academic year 2016-2017 at the University of Padua.

[56] T. Padmanabhan, *Structure Formation in the Universe*, Cambridge University Press, The Edinburgh Building, Cambridge CB2 8RU, UK (1993)

[57] A. Payez, C. Evoli, T. Fischer, M. Giannotti, A. Mirizzi, A. Ringwald, *Revisiting the SN1987A gamma-ray limit on ultralight axion-like particles*, JCAP 1502 (2015) 006, arXiv:1410.3747v2

[58] P. J. E. Peebles , *The Large-scale Structure of the Universe*, Princeton University Press (1980)

[59] R. Penrose, *On Gravity's Role in Quantum State Reduction*, General Relativity and Gravitation, Vol. 28, No. 5, 581–600 (1996)

[60] J. Peñarrubia, Y. Ma, M. G. Walker, and A. McConnachie, *A dynamical model of the local cosmic expansion*, MNRAS 443, 2204–2222 (2014)

[61] A. Perez, *Notes on the path integral representation of quantum mechanics*, Marseille (2019)

[62] *Perseus Digital Library*, `http://www.perseus.tufts.edu`

[63] M. E. Peskin, D. V. Schroeder, *An introduction to Quantum Field Theory*, CRC press, Boca Raton (2018)

[64] P. Peter, J.P. Uzan, *Primordial Cosmology*, Oxford University Press, 2005

[65] K. A. Pimbblet, S. J. Penny, R. L. Davies, *How typical is the Coma cluster?*, MNRAS 438, 3049–3057 (2014)

[66] Planck Collaboration, *Planck 2018 results. I. Overview and the cosmological legacy of Planck*, arXiv:1807.06205v2 [astro-ph.CO], 3 Dicembre 2019

[67] V. Sahni, P. Coles, *Approximation Methods for Non–linear Gravitational Clustering* Phys.Rept. 262 (1995) 1-135, arXiv:astro-ph/9505005v1 2 May 1995

[68] C. Schimd, *Lecture notes for the course on Primordial Cosmology held in Aix-Marseille University, for the master M2 in Fundamental Physics, in the academic year 20219/2020*

[69] A.E. Schulz, W. Dehnen, G. Jungman and S. Tremaine, *Gravitational Collapse in One Dimension*, Mon. Not. Roy. Astron. Soc. 431 (2013) 49 [arXiv:1206.0299]

[70] *SDSS*, `https://www.sdss.org`

[71] A. Sebbar, A. Sebbar, *Equivariant functions and integrals of elliptic functions*, Geom Dedicata DOI 10.1007/s10711-011-9688-7 (2011)

[72] C. J. Short, P. Coles, *Gravitational instability via the Schrödinger equation*, JCAP12(2006)012

[73] V. Springel, S. D. M. White, A. Jenkins, C. S. Frenk, N. Yoshida, L. Gao, J. Navarro, R. Thacker, D. Croton, J. Helly, J. A. Peacock, S. Cole, P. Thomas, H. Couchman, A. Evrard, J. Colberg, F. Pearce, *Simulating the joint evolution of quasars, galaxies and their large-scale distribution*, Nature 435:629-636 (2005), arXiv:astro-ph/0504097

[74] N. Sugiyama, *Cosmic background anistropies in cold dark matter cosmology*, Astrophysical Journal Supplement v.100, p.281, arXiv:astro-ph/9412025 (1995)

[75] *The NIST reference on constants, units and uncertainty*, https://www.nist.gov/pml

[76] *The Astronomical Almanac*, http://asa.hmnao.com

[77] P. Tod, I. M Moroz, *An analytical approach to the Schrödinger–Newton equations*, Nonlinearity 12 201 (1999)

[78] S. van den Bergh, *The local group of galaxies*, Astronomy and Astrophysics Review v.9 (1999)

[79] L. Wang, P. J. Steinhardt, *Cluster Abundance Constraints on Quintessence Models*, Astrophys.J. 508: 483-490 (1998) arXiv: astro-ph/9804015

[80] N. Wheeler, *Dirac delta function identities*, Reed College Physics Department, November 1997

[81] L. M. Widrow, N. Kaiser, *Using the Schrödinger equation to simulate collisionless matter*, The Astrophysical Journal, 416: L71-L74 (1993)

[82] Wolfram Research, *The wolfram functions site*, https://functions.wolfram.com/GeneralizedFunctions/DiracDelta/09/0005/

[83] Wolfram Research, *Wolfram MathWorld*, https://mathworld.wolfram.com/HeavisideStepFunction.html

[84] https://www.wolframalpha.com

[85] R. Wong, *Asymptotic Approximations of Integrals*, Academic Press, First edition (1989) p. 76-77

[86] Y. Xu, H. J. Newberg, J. L. Carlin, C. Liu, L. Deng, J. Li, R. Schönrich, B. Yanny, *Rings and Radial Waves in the Disk of the Milky Way*, arXiv:1503.00257, [astro-ph.GA] (2015)

[87] Y. B. Zel'dovich, *Gravitational instability: an approximate theory for large density perturbations*, Astronomy and Astrophysics 5 (1970) 84-89

Ai miei genitori ed Edoardo.